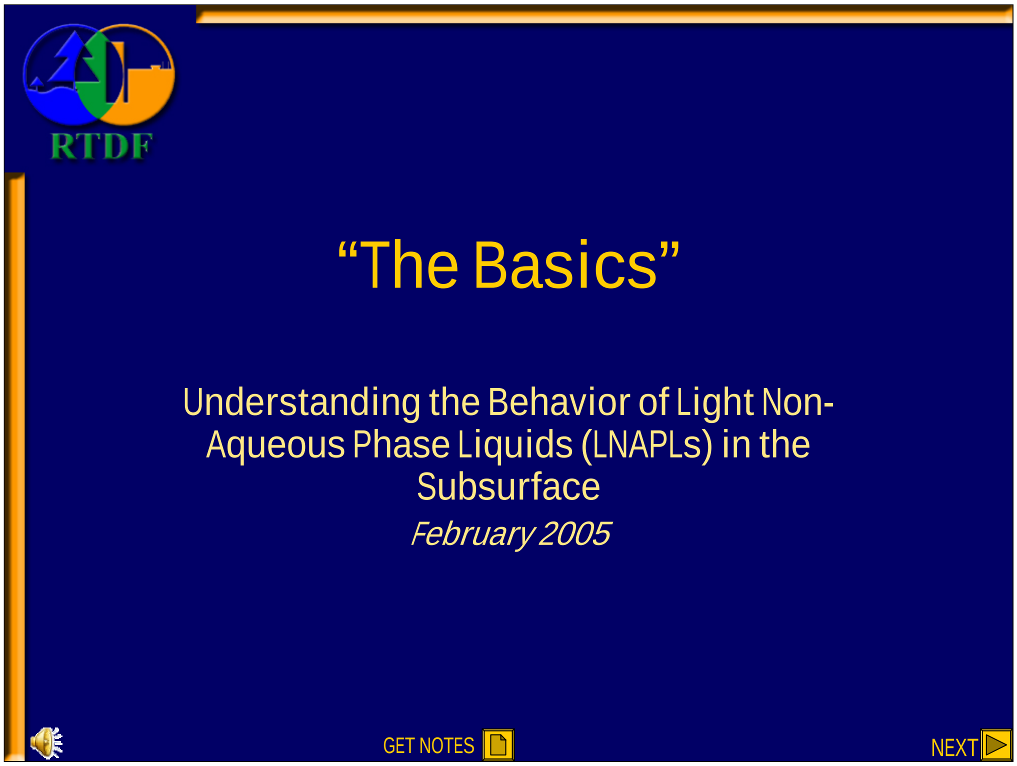

Welcome. The Remediation Technologies Development Forum (RTDF) **Non-Aqueous Phase Liquid (NAPL) Cleanup Alliance** has prepared this course on **light non-aqueous phase liquids, or LNAPLs**, and their impacts in the subsurface. The Alliance is a public-private partnership supported by the U.S. Environmental Protection Agency’s (EPA) Technology Innovation and Field Services Division. Its members include representatives of the petroleum industry, consultants, and state and federal government agencies. This training is the result of a collaborative effort involving all Alliance members. Its concept and content have evolved over several years, building upon efforts by many, including individual researchers, members of the **American Petroleum Institute** (API), and EPA’s Region 4 Innovative Training Workgroup. Initial drafts of the course content were reviewed by Alliance members, EPA scientists, and state government officials who deal with remediation of LNAPL sites. This final version incorporates their advice and comments.

This course provides a basic description of the behavior of LNAPLs (specifically, petroleum hydrocarbon liquids) in the subsurface. It helps explain what many have observed in the field for years: As LNAPLs are removed from the subsurface, LNAPLs remaining are increasingly difficult to recover.

The training presents the technical concepts involved in LNAPL behavior, discusses the application of these concepts to real world situations, and explores how heterogeneity and other factors affect LNAPL behavior and complicate recovery.

This training will be particularly useful to: Regulators who evaluate work plans and recommend LNAPL remedial strategies; hydrogeologists who make quantitative predictions about LNAPL volume, migration, and recovery to support these recommendations; and anyone who needs basic information about the nature of petroleum hydrocarbons in the subsurface.

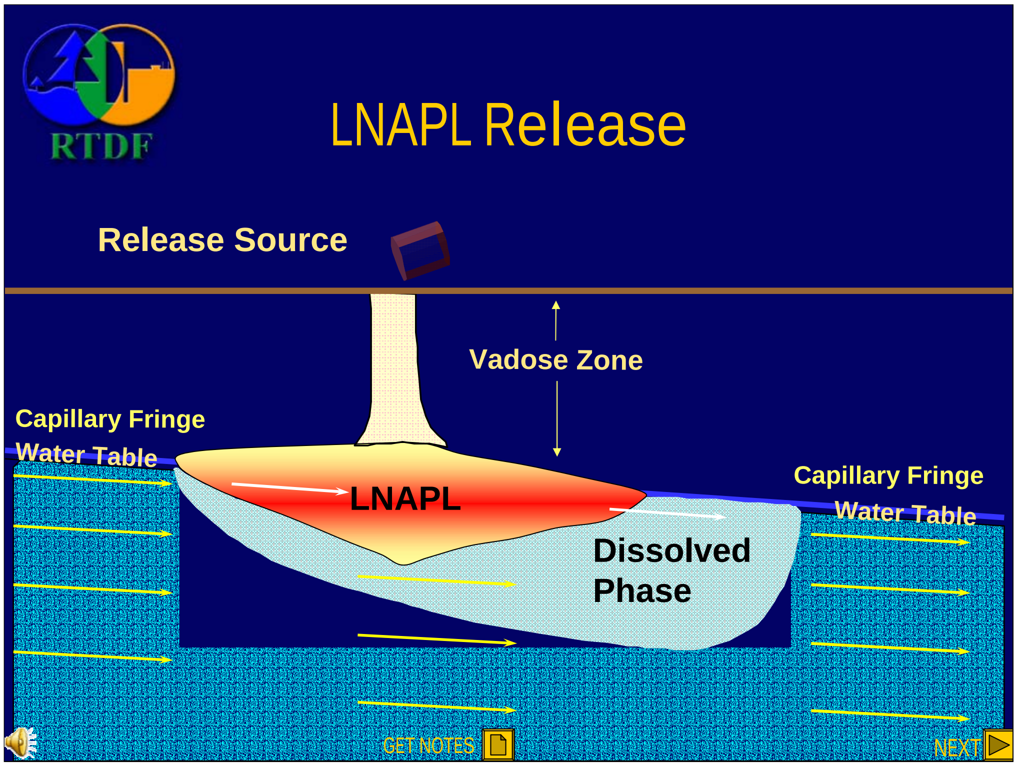

Petroleum hydrocarbons can be released to the subsurface through spills and leaking pipelines, underground storage tanks, and above ground storage tanks. Released liquids migrate downward, primarily by gravity, through the **vadose zone**, the unsaturated or partially saturated subsurface media above the **water table**. The unconsolidated porous media in the vadose zone consist of both solid material and voids, called pore spaces. These pore spaces are filled primarily with air and small amounts of water. The bottom part of the vadose zone is called the **capillary fringe** and is partially saturated with water pulled upward by capillary forces from the underlying **saturated zone**. Water pressure in the saturated zone is greater than atmospheric pressure, and water generally fills the pore space. Water in this zone is called groundwater.

As LNAPL migrates through the vadose zone toward the capillary fringe, it displaces air, but generally not water, from the pore spaces. The LNAPL-filled pores drain slowly and can leave behind LNAPL globules trapped by capillary forces. If only a small volume of LNAPL is released, it may become entirely trapped in the vadose zone. If a greater volume is released, the LNAPL may migrate completely through the unsaturated zone and accumulate in a zone that is loosely constrained by the water table.

When LNAPL reaches the capillary fringe, it begins to displace water in the pore spaces. The amount of water displaced and the resulting volume of LNAPL in the soil is a primary focus of this training. At the end of the training, you will be able to determine the volume of LNAPL in the capillary fringe at and below the water table.

It is known that LNAPL in the water table acts as a long-term source for the dissolved plume. While dissolution will not be addressed in this course, it should be noted that model results of dissolution from the LNAPL source show that maximizing hydraulic LNAPL recovery to the extent practical is not likely to reduce the risk at a site. In certain, circumstances, it may reduce the life of the risk, but the reduced longevity may not have practical significance.

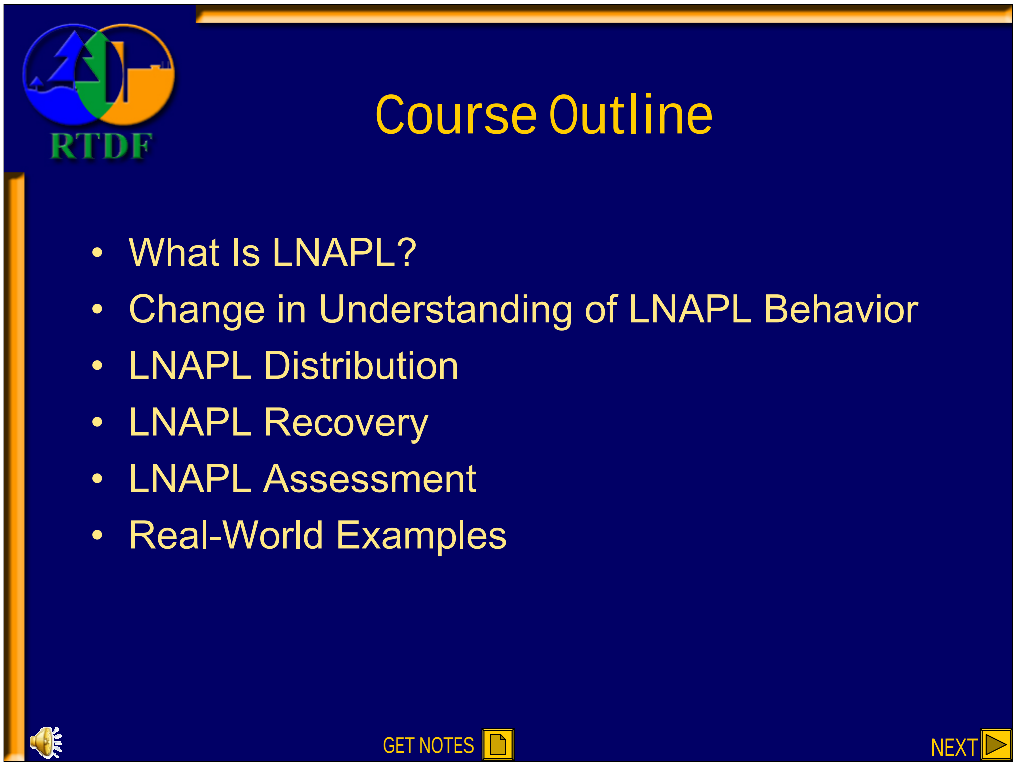

In this course, you will learn basic information about LNAPL (specifically, petroleum hydrocarbon liquid) and how it behaves in the subsurface.

We will begin by defining important terms to provide a foundation for our focus on LNAPL. You will learn how our understanding of the behavior of LNAPL in the subsurface has changed over the years. We will also explore how **aquifer** properties—like **porosity**, **saturation**, and **capillary pressure**—affect LNAPL distribution. As you progress through the course, you will learn how fluid properties—like **viscosity**, **density**, and **interfacial and surface tension**—affect LNAPL **distribution** and recovery. LNAPL distribution and its saturation determine its **conductivity**, which, in turn, influences its **migration** and potential **hydraulic recovery**.

We also will introduce methods of predicting and evaluating LNAPL recovery, briefly discuss some assessment methods and techniques, and look at core photos taken from actual LNAPL plumes.

Finally, we will present five case studies to illustrate how the basic concepts you've learned have been applied in the real world.

(**NOTE:** ***While the terms "subsurface," "solid media," and "porous media" are used in this course for technical accuracy, the term "soil" is often used in place of these terms in the field, for simplicity's sake***.)

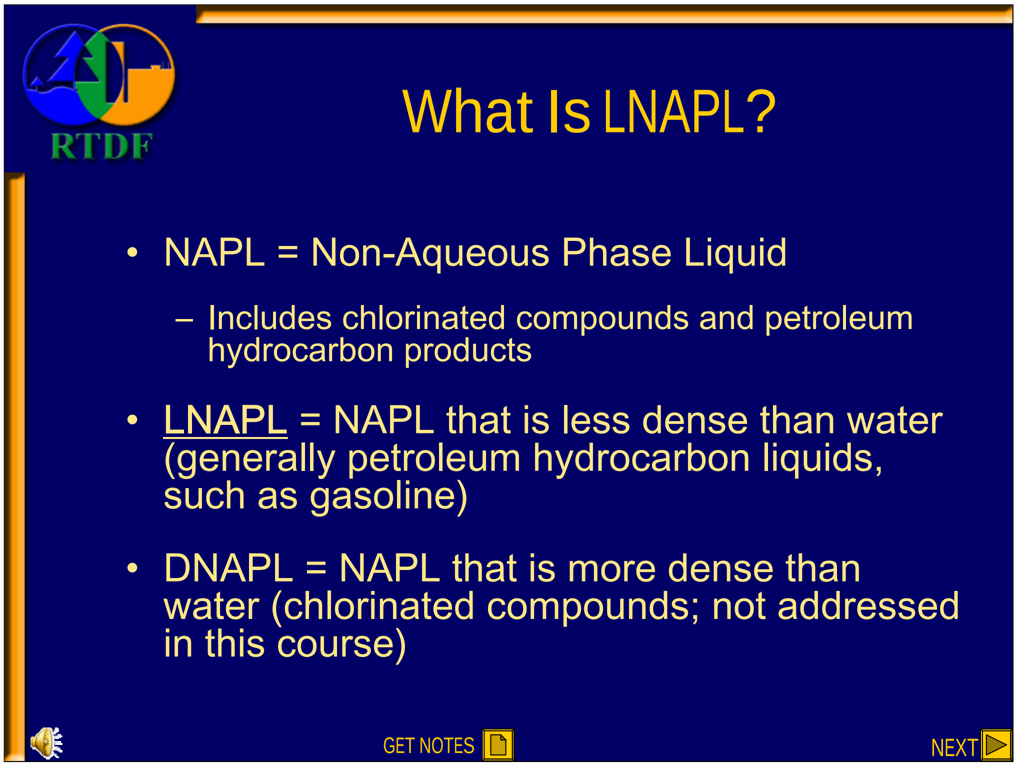

To understand LNAPLs, we first must define **NAPLs, non-aqueous phase liquids**. NAPLs are contaminants that remain undiluted as the original bulk liquid in the subsurface. They do not mix with water but form a separate phase. Chlorinated compounds and petroleum hydrocarbons are examples of NAPLs.

LNAPLs, or light non-aqueous phase liquids, are less dense than water. They do not mix but co-exist with water in the pore spaces in the aquifer. Gasoline, diesel, motor oils, and similar materials are examples of LNAPLs.

Dense non-aqueous phase liquids, or DNAPLs, are more dense than water and generally include halogenated compounds. DNAPLs are not addressed in this training. However, many of the properties that govern the flow of LNAPLs apply to DNAPLs as well. The large density difference between the two governs the differences in their subsurface behavior.

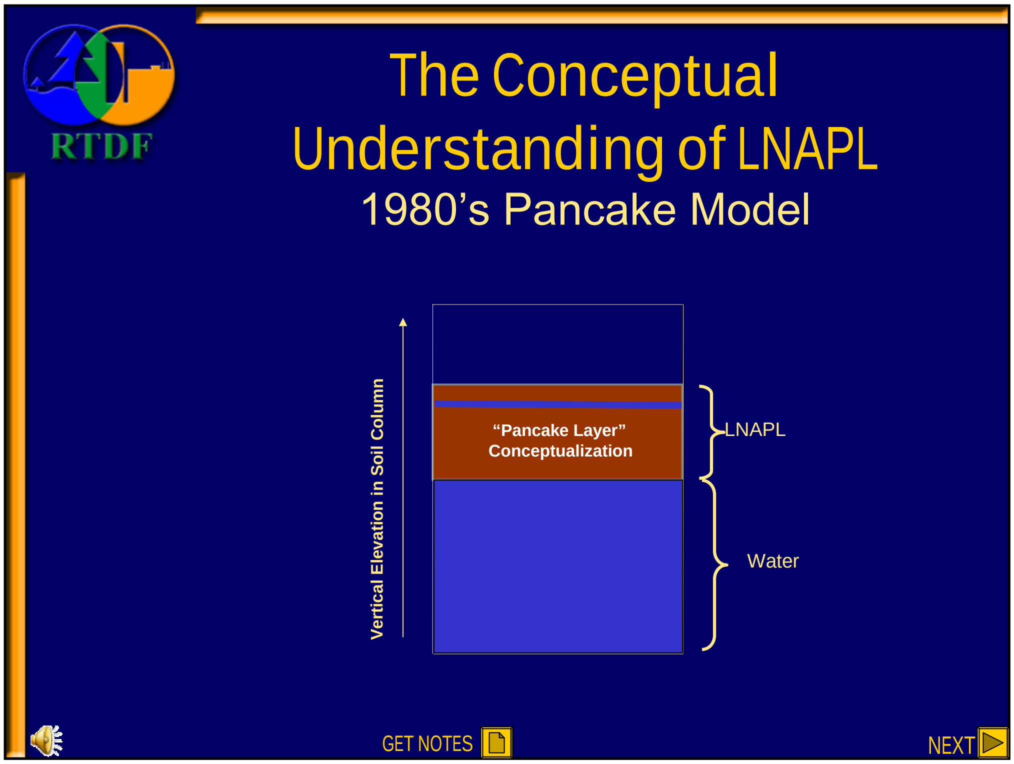

For most of the last 20 years, groundwater scientists and engineers approached the evaluation and recovery of LNAPL with a conceptual model in which LNAPL floated on the water table like a pancake, displacing nearly all of the water and the air in the pore space of the aquifer. In this model, the result was a uniformly high saturation of LNAPL on the water table.

Although many people recognized that there was a difference between the thickness of LNAPL measured in a monitoring well and the actual thickness in the aquifer, the tools needed to understand this relationship and how it varied with the type of LNAPL and aquifer had yet to be developed. People believed that, when petroleum hydrocarbon was observed in the well, it was spreading. They also believed that LNAPL moved up and down with a fluctuating water table, always riding on the top of the water table.

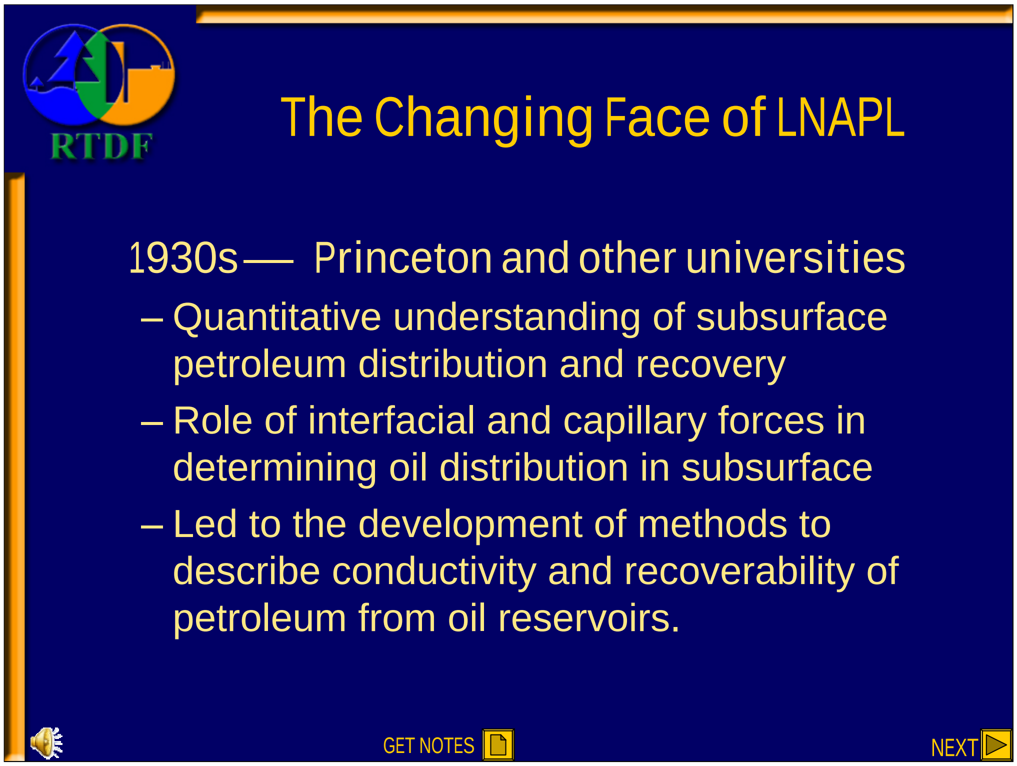

The quantitative understanding of petroleum distribution in subsurface media and its recovery was developed in the 1930s at Princeton and other universities. This understanding established the role of interfacial and capillary forces in determining the distribution of oil in subsurface media. It also led to the development of methods for describing the conductivity and recoverability of petroleum from oil reservoirs.

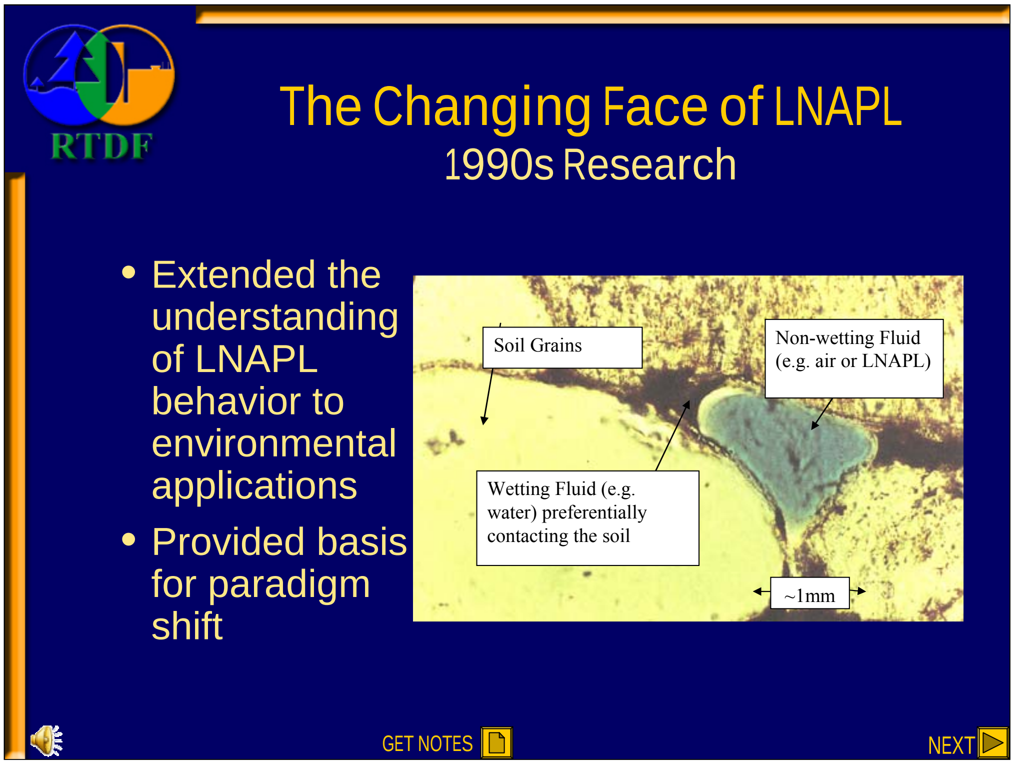

Independent research by **Farr and McWhorter** and **Lenhard and Parker** in 1990 extended the understanding of LNAPL behavior developed for oil reservoirs in the 30s to environmental applications of hydrocarbon spills and leaks. This research was the basis of a paradigm shift that occurred in the 1990s. The conceptual model resulting from the later research is shown in this slide. Unlike in the old "pancake model," we now understand that LNAPL is not continuous in the subsurface media matrix.

Why did it take so long for this new paradigm to be widely adopted? It took several years to come to an understanding of the concept and to collect the field data to support the theory.

Since the 1990s, simpler models have been developed. These models, combined with data gathered in the field, have helped to pull together a picture that can be applied to everyday situations.

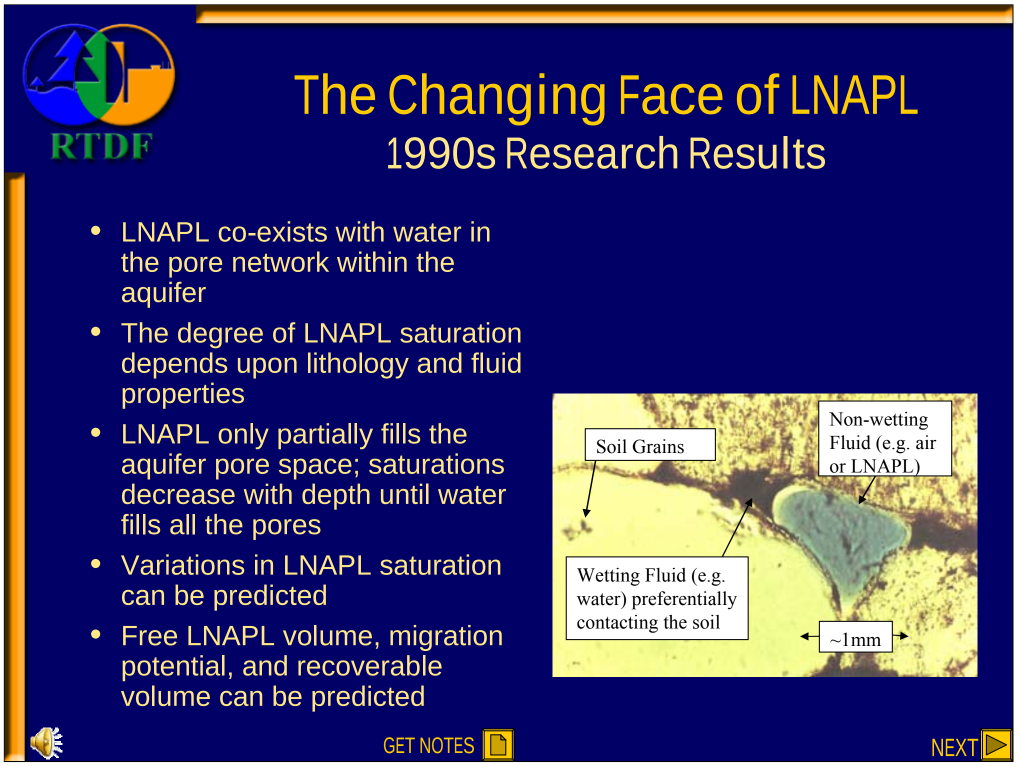

We now understand that LNAPL **co-exists with water in the pore network within the aquifer**. It does not float on the water table.

The degree of LNAPL saturation depends on the history, **lithology**, capillary parameters, and fluid properties of the site and the volume of LNAPL released. LNAPL only partially fills the aquifer pore space, and saturation decreases with depth until water fills all the pores.

The variation with depth of LNAPL saturation in the subsurface can be predicted when the properties of the subsurface media and fluid are known, and the apparent LNAPL thickness in the well is measured. This is accomplished by using the theories of Farr and McWhorter, and Lenhard and Parker. If sufficient measurements are taken across an LNAPL plume, the total volume of free LNAPL, its migration potential, and the recoverable volume also can be predicted. **Spreadsheets (API Publication 4729)** to perform these calculations have been made available by Randy Charbeneau for the API.

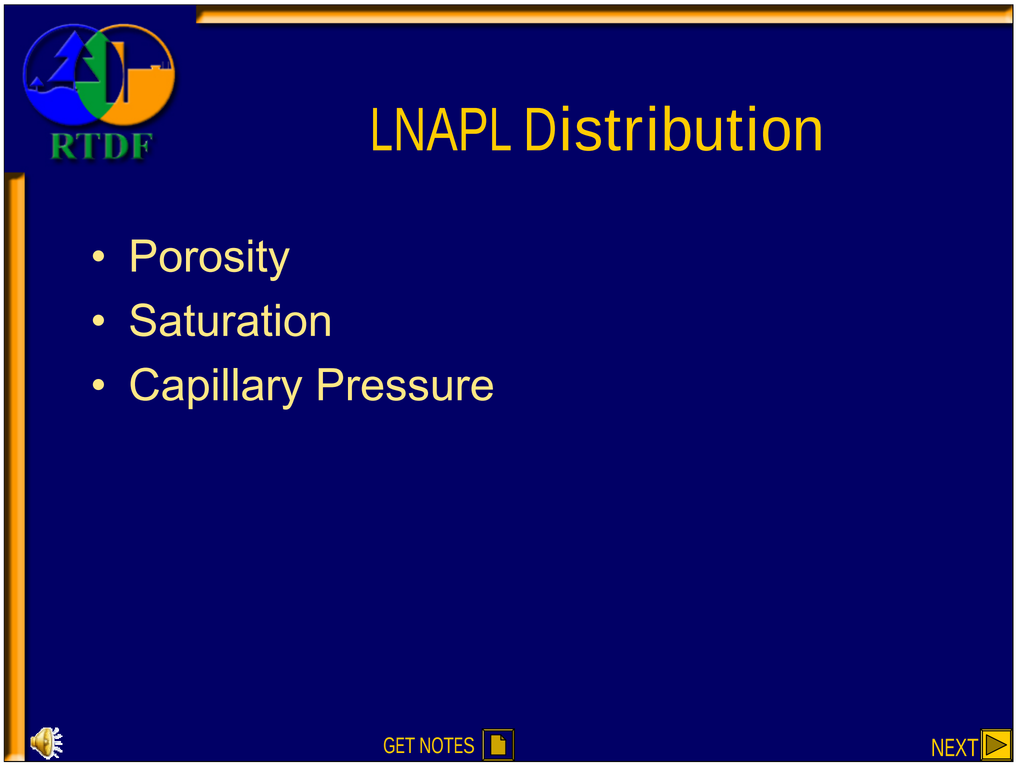

Let's move on to discuss the aquifer properties that affect LNAPL, air, and water distribution in the subsurface. Understanding how air and water interact in the subsurface will help you determine how much LNAPL exists and how much of it can be recovered.

First, we will review the basic concepts of porosity and saturation. Then, we will discuss capillary pressure, the factor that governs the interaction of water and air in the subsurface.

(**NOTE:** ***While the terms "subsurface" and "porous media" are used in this course for technical accuracy, the term "soil" is often used instead of these more technical terms in the field, for simplicity's sake***.)

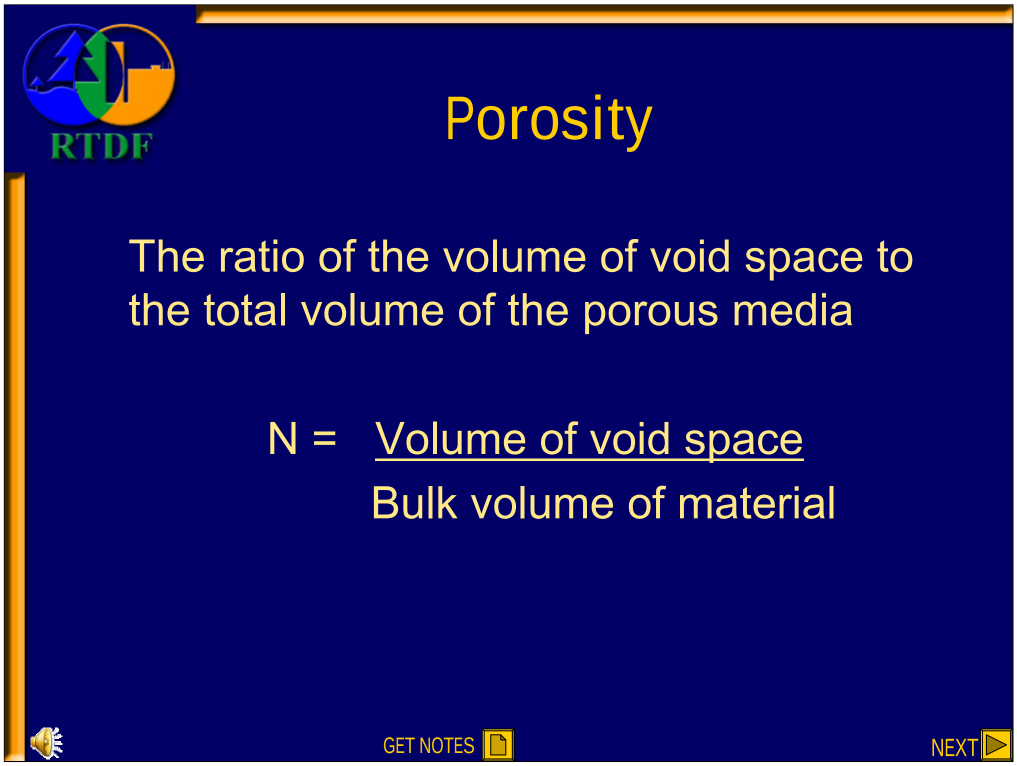

Total porosity is the ratio of the volume of void space to the total volume of the media. In other words, porosity is the fraction of the total volume that is occupied by pore space. Total porosity depends on many factors, including particle size and shape, particle size distribution, and packing of particles. Clays generally have a high total porosity (40-70%), while coarse-grained media, like sand and gravel, have a lower total porosity (25-50%). Total porosity accounts for all pore space, even pore space where the water molecules are held very tightly in place by either capillary or other polar or molecular forces.

The total porosity is typically called the primary porosity. Often in clays, small fractures, wormholes, or root borings may develop. The void space created by these features is often called secondary porosity. Secondary porosity typically has very low capillary pressure, and, while it generally constitutes a very small percentage of the total porosity, it can significantly influence the flow of fluids through the clay.

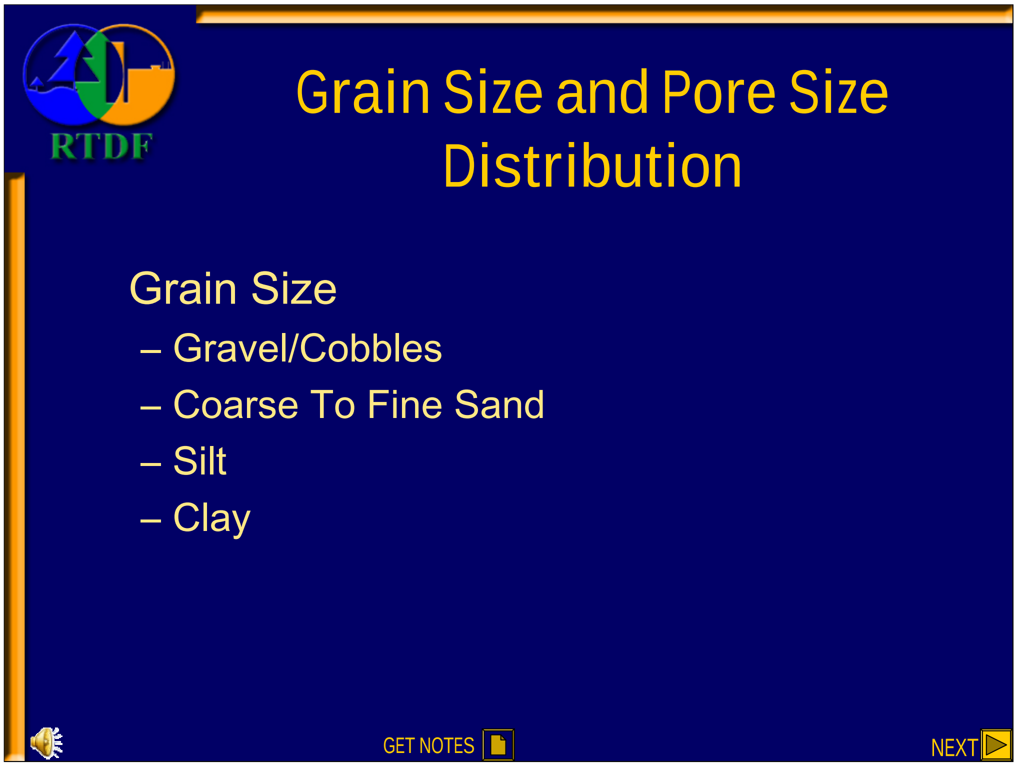

Grain size is one of the most important properties describing porous media. Grain sizes include gravel, cobbles, coarse to fine sand, silt, clay, or a combination of these sizes (e.g., silty sand or clayey silt). Gravels have relatively large pores and a narrow distribution of pore sizes (the pores are generally uniform in size). Silts and clays have very small pores but may have a broad distribution of pore sizes (the pores are not uniform in size). Sands are somewhere in between.

Often in clays, you will find a very small fraction of macro-pores. While macro-pores comprise a very small volume of pore space, fluids can travel rather quickly through them.

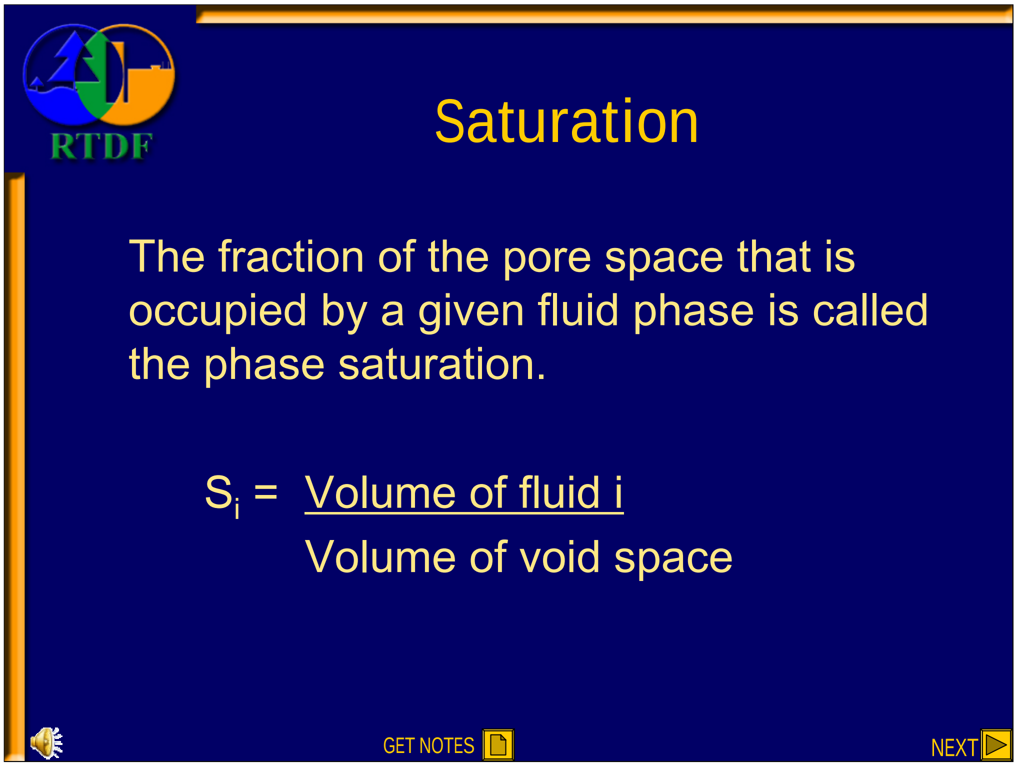

The pore space can be filled by different fluids (air, water, or LNAPL) that are not miscible (do not mix) with each other. The fraction of the pore space that is occupied by a given fluid phase is called the saturation. Saturation is either represented as a fraction or a percent. The sum of the fluid saturations should total 1, or 100%.

Below the water table and in the absence of LNAPL, the water saturation is nearly one (1), and the air saturation is nearly zero (0). As you move from the saturated zone to the capillary fringe, the water saturation decreases from 1 to a value that represents the amount of water that is held within the medium by capillary forces.

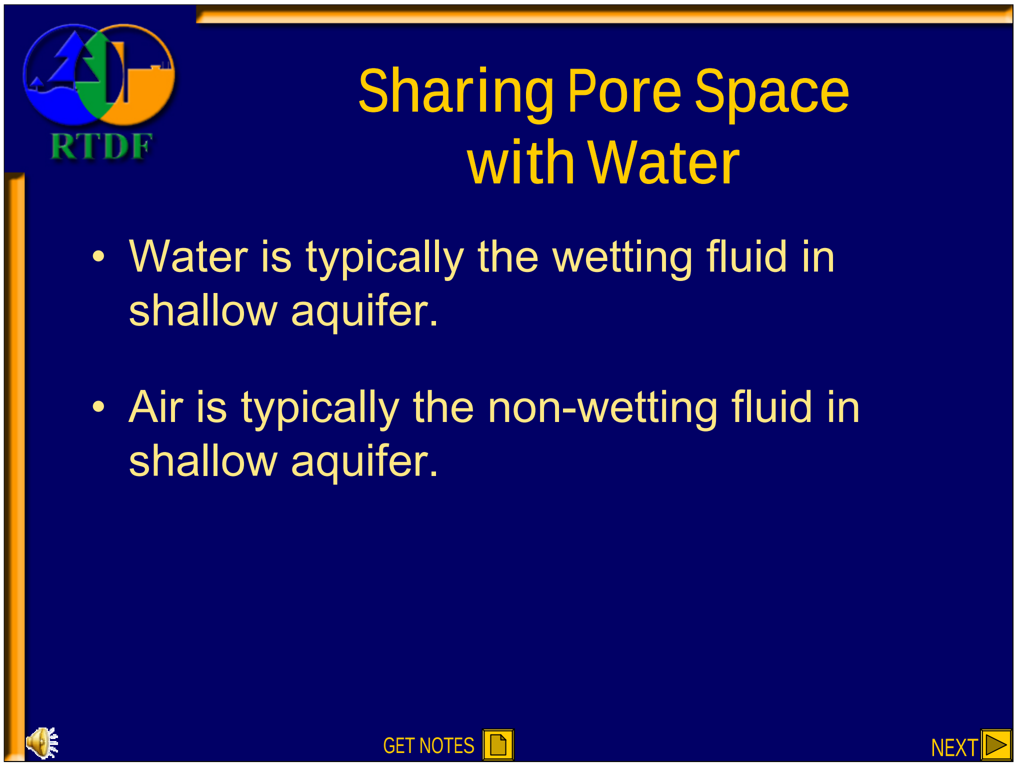

Typically in the subsurface, water preferentially "wets," or adheres to, the solid media surface and occupies the smaller pores. It is called the wetting phase and wets the surface of the solid media in preference to air. Air is called the non-wetting phase.

The implications of this relationship can be illustrated by a simple capillary rise experiment described on the next slide. Monitoring wells installed in unconfined aquifers exhibit the same behavior but on a larger scale than is represented in such an experiment.

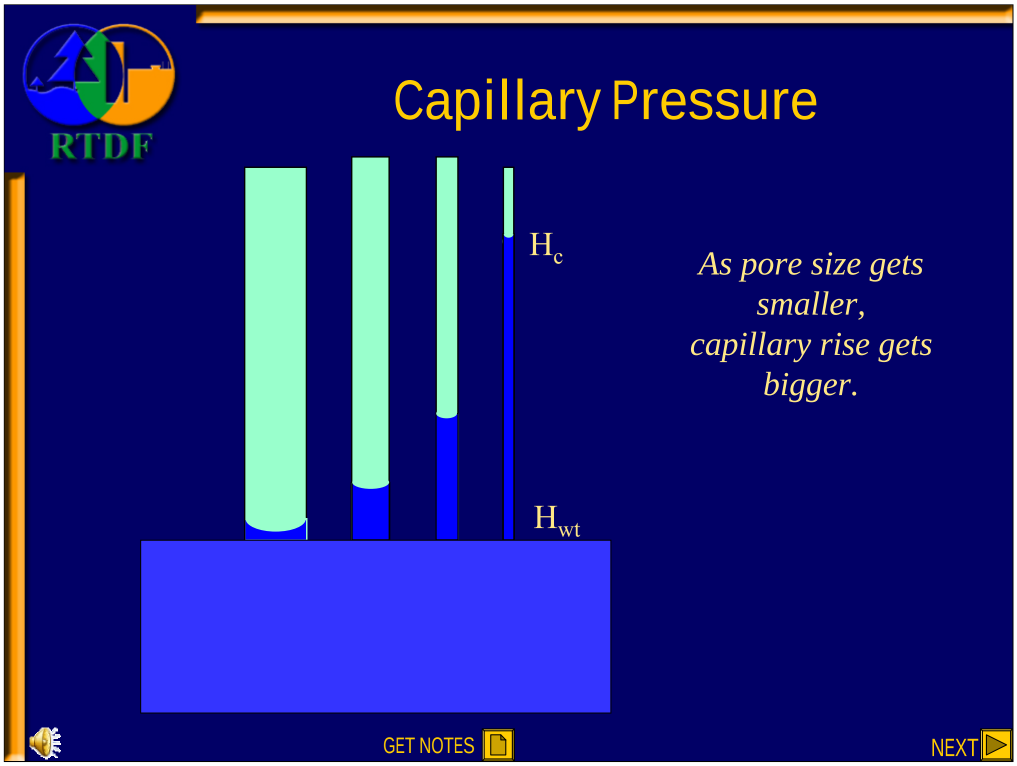

Capillary pressure is defined as the pressure in the non-wetting phase minus the pressure in the wetting phase.

When tubes of different diameters are placed in a dish containing water, the water will rise in each tube in relation to the surface tension between the air and the water, the contact angle (the angle between the surface of the water and surface of the tube), and the radius of the tube. As pore size gets smaller (reflected in the smaller-diameter tubes above), the capillary rise gets bigger—meaning that the capillary pressure is higher.

When water wets the surface of the tube, the cosine of the contact angle is unity. The capillary rise is balanced by the pressure from the height of the column of water. You can view this another way as well. In porous media, the smallest pores will take in the water first and hold it the tightest.

It takes significant pressure to get the water out of the smallest pores. This is why coarse sands and gravels have a relatively small capillary fringe, while silts and clay have a large capillary fringe (and hence, stay moist).

NOTE: Capillary pressure is often referred to as capillary suction pressure, because the wetting phase is "sucked" up the tube. The terms are interchangeable.

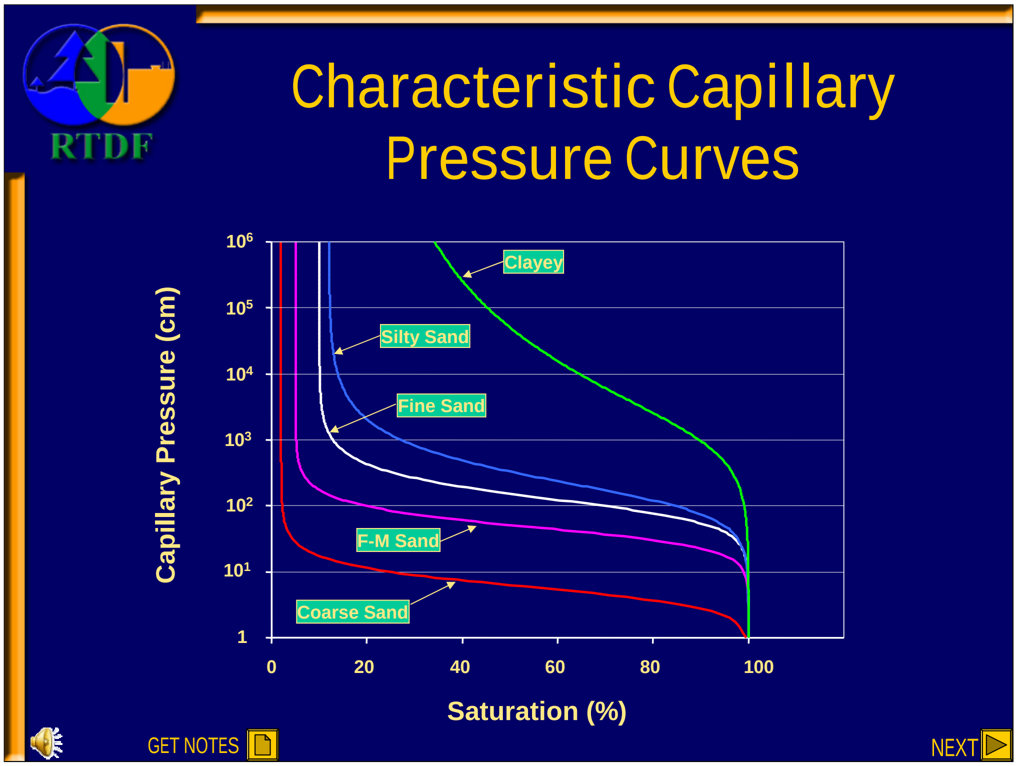

Capillary pressure curves typically are measured using the wetting and non-wetting phases we have just described.

This slide depicts ideal capillary pressure curves for different grain sizes. The X axis is water saturation. It ranges from 0, indicating that the pore space is completely filled with air, to 100 percent, indicating that the pore space is completely filled with water.

The Y axis is the capillary pressure (or capillary suction pressure). This is related to the height of the water in the tube, as described in the capillary rise experiment. Smaller tubes exhibit greater capillary pressure, which results in a greater height of water.

These capillary pressure curves illustrate two things:

First, note that the capillary pressure in the coarse sand is much lower than the capillary pressure in the clay. This indicates that the pore sizes in the sand are larger than in the clay, which is consistent with the capillary rise experiment discussed on the previous slide.

Second, the coarse sand curve is very flat over a wide range of water saturations. This indicates that the pore size distribution is uniformly large.

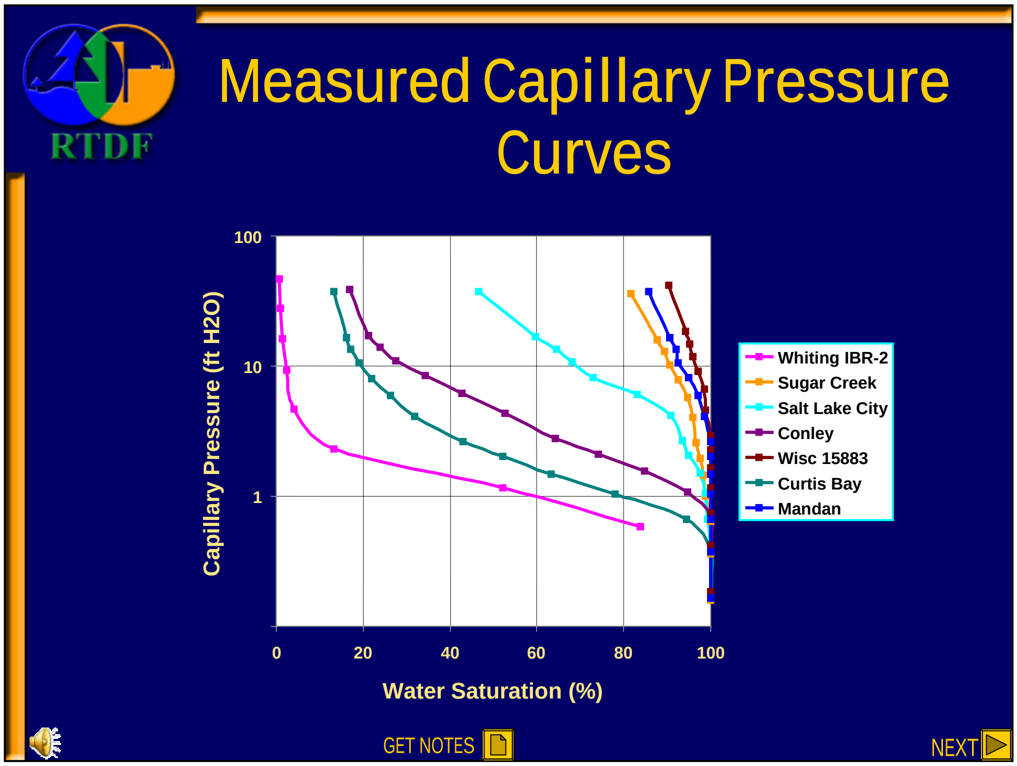

These are actual, measured capillary pressure curves for a series of porous media throughout the United States.

The Whiting IBR-2 soil (shown in red) is a sand; the Wisconsin 15883 soil (shown in purple) is a silt or clay. The Whiting IBR-2 soil has a lower capillary pressure and flatter curve, because it has larger pores and more uniform pore size than silts and clays, which have smaller pore sizes and wider pore-size distributions.

Because of the smaller pore sizes, silts and clays hold water more tightly and exhibit a higher capillary pressure than sands.

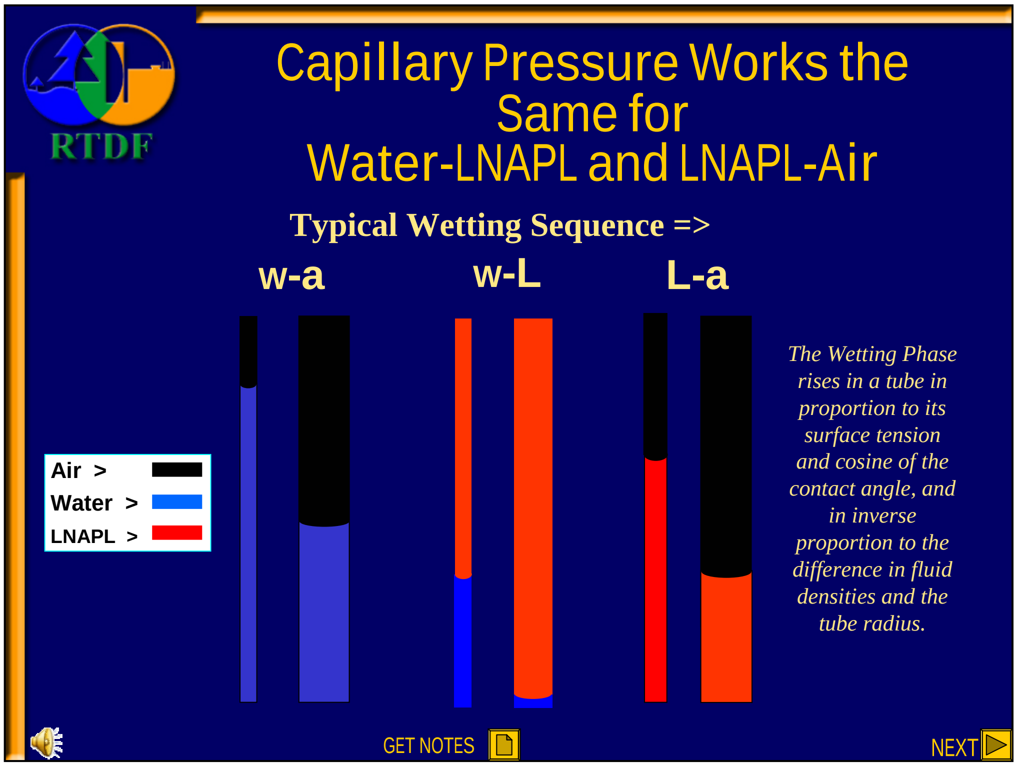

Capillary pressure works the same for water-LNAPL and LNAPL-air systems. However, there are different interfacial and density factors to consider, because the fluid combinations are changed. This slide shows that the height of the rise is proportional to the interfacial or surface tension between the fluids and the cosine of the contact angle, which is unity for a strongly wetting fluid (like pure water on clean glass). However, the height of the rise is inversely proportional to the tube radius and the density difference of the two fluids.

Typically, water wets the porous media in preference to air and LNAPL. LNAPL only wets the porous media in preference to air. In the following, we assume that the wetting fluid has a contact angle of 90 degrees (cosine 90 = 1).

As you recall, in the water-air system, water is the wetting fluid, and it rises in the tube. The extent of the rise is a balance between the capillary suction pressure and the tendency for gravity to pull it down.

In a water-LNAPL system, water is again the wetting phase. It rises higher in the smaller tube but not as high as in the water-air case, because the LNAPL density is greater than the air density, and the interfacial tension of water-LNAPL is likely to be lower than the surface tension of water-air.

In an LNAPL-air system, the LNAPL rises higher in the tubes than in the water-LNAPL system, because air is less dense than water or LNAPL. However, the LNAPL does not rise as high as the water in the water-air system, because the surface tension is less than that of water-air.

Typically then, if a capillary pressure curve is measured with one set of fluids, it can be made applicable to another set of fluids if the fluid densities and the surface or interfacial tensions are known.

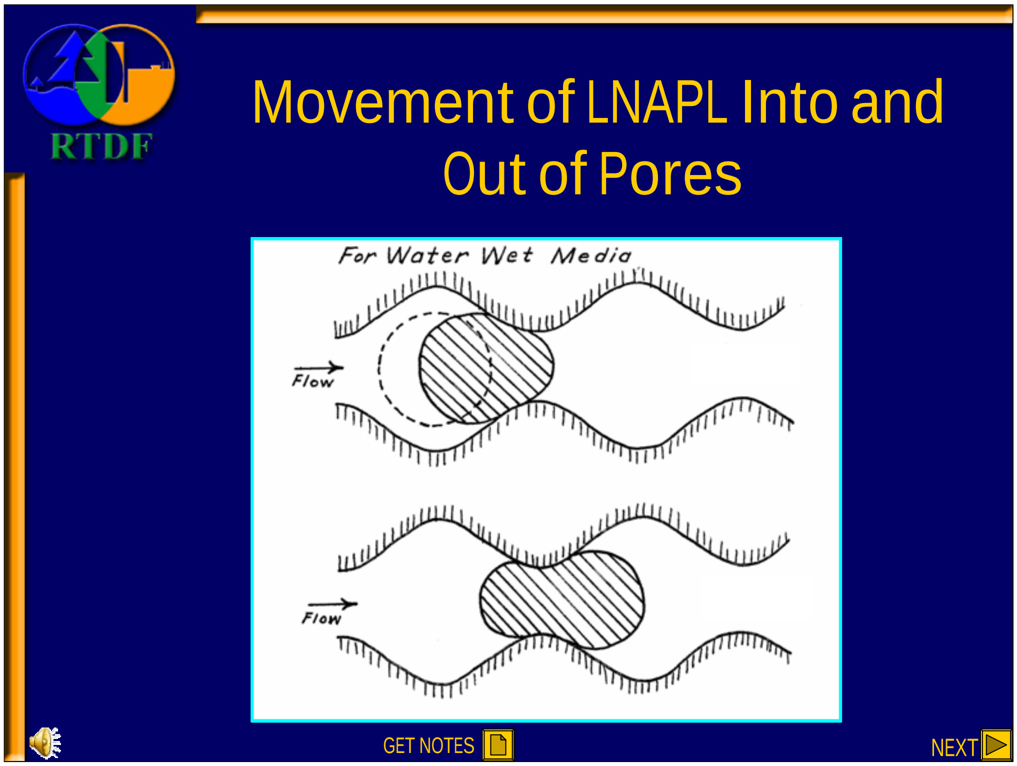

It takes pressure for LNAPL to move into or out of pores. To move in or out of these pores, a droplet may encounter pore throats that are smaller than the droplet size. Sufficient pressure must be exerted to deform the droplet enough for it to move through the pore throat. The situation is illustrated in this slide.

In the upper figure, the pressure gradient is too low to deform the LNAPL droplet and allow it to move through the pore throat. In the lower figure, the pressure is sufficient to deform the droplet and make it mobile. In this scenario, the LNAPL is recoverable.

Difficulty in overcoming the pressure gradient is the reason why LNAPL fills the large pores first in a water-wet soil. It is also why some LNAPL is trapped in the pores during recovery and cannot be removed using hydraulic recovery methods, such as pump-and-treat.

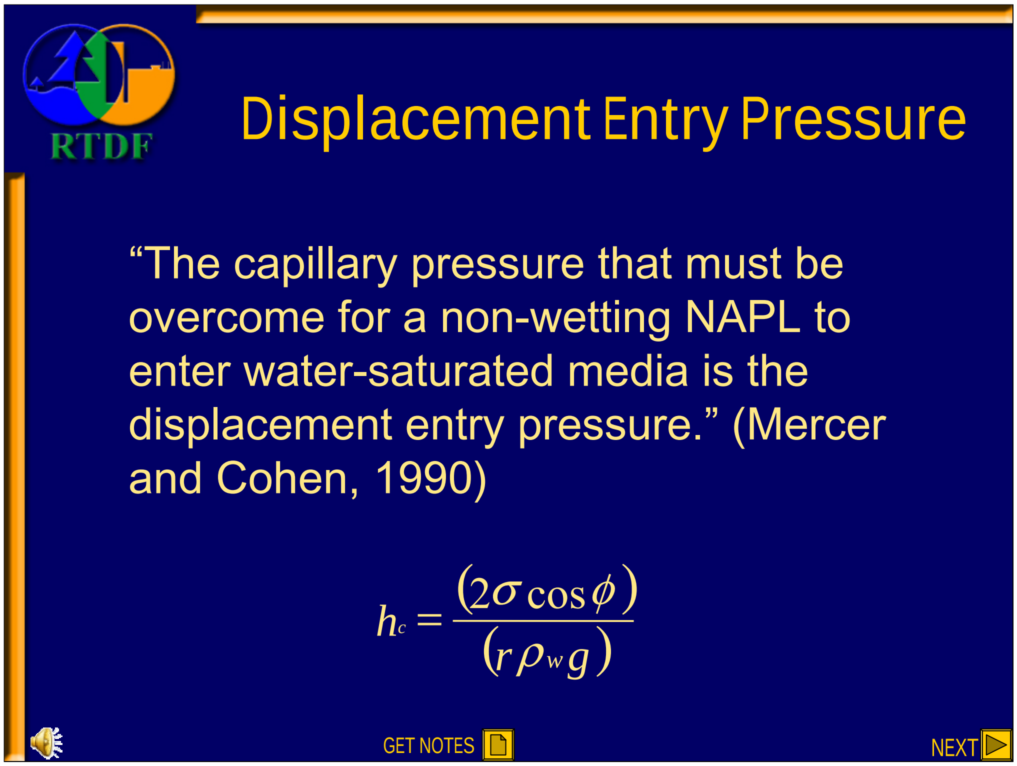

The capillary pressure that must be overcome for a non-wetting NAPL to enter water-saturated media is called the **displacement entry pressure (Mercer and Cohen, 1990)**. The pressure in the LNAPL phase is primarily related to the depth from the top of the LNAPL to water (the head) and the continuity of LNAPL above the water table. The LNAPL traveling down from a release displaces an amount of water in proportion to the height of LNAPL above.

In the equation shown,

h_c = capillary rise of the wetting fluid

r = radius of the largest pore throat

rho $(\rho)_w$ = density of water

g = gravitational constant

sigma (σ) = interfacial tension between LNAPL and the wetting fluid, and

phi (ϕ) = the contact angle measured into the water

You will recall from the generalized capillary pressure curves on slide 15 that the capillary pressure at nearly 100% water is much greater in clays and silts than in sands. This is because the pore throats in clays and silts are much smaller.

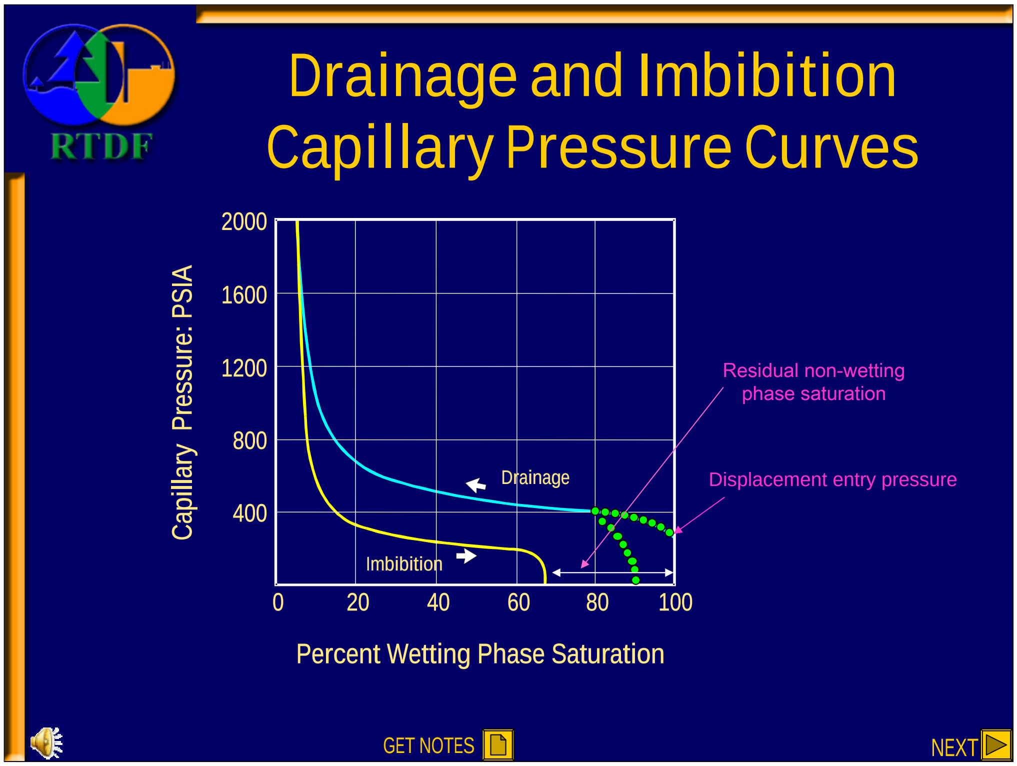

In this figure, the capillary pressure relationship for a cycle of the non-wetting phase (e.g., LNAPL) displacing the wetting phase (e.g., water) followed by the wetting phase displacing the non-wetting phase is shown. Displacement of the wetting phase from the porous media is called **drainage**. Displacement of the non-wetting phase is called **imbibition** because the wetting phase is imbibed, or pulled into, the soil.

Complete capillary pressure curves are generated in two steps: First, the non-wetting phase (the LNAPL or air) displaces the wetting phase. The initial pressure that must be exerted to drive the non-wetting phase into the soil is termed the displacement entry pressure. In a standard laboratory test, the pressure on the LNAPL, or non-wetting phase, is increased until no additional wetting phase, or water, can be displaced from the soil. This point is called the irreducible water saturation.

In the second step, the wetting phase displaces the non-wetting phase. Laboratories refer to the process of developing both drainage and imbibition curves as generating “the complete wetting history.” Note in the figure above that the imbibition curve does not follow the drainage curve. During imbibition, a portion of the non-wetting phase becomes trapped in the pores. The final non-wetting phase saturation on the imbibition curve is the “residual non-wetting phase saturation”.

It is important to understand that the value of the residual non-wetting phase saturation is strongly dependent on the volume of water displaced during the initial drainage cycle. For example, if the drainage curve displaced water to only 80% saturation, imbibition could take place and likely generate a very small “residual saturation.” In other words, the starting and ending points of the imbibition curve depend on the volume of water displaced. Also note that there is some debate about whether drainage or imbibition curves should be used to predict saturation distribution. Most of the published literature use drainage curves and incorporate a small residual by simple addition uniformly across the predicted profile. Some work has been developed that uses an imbibition curve.

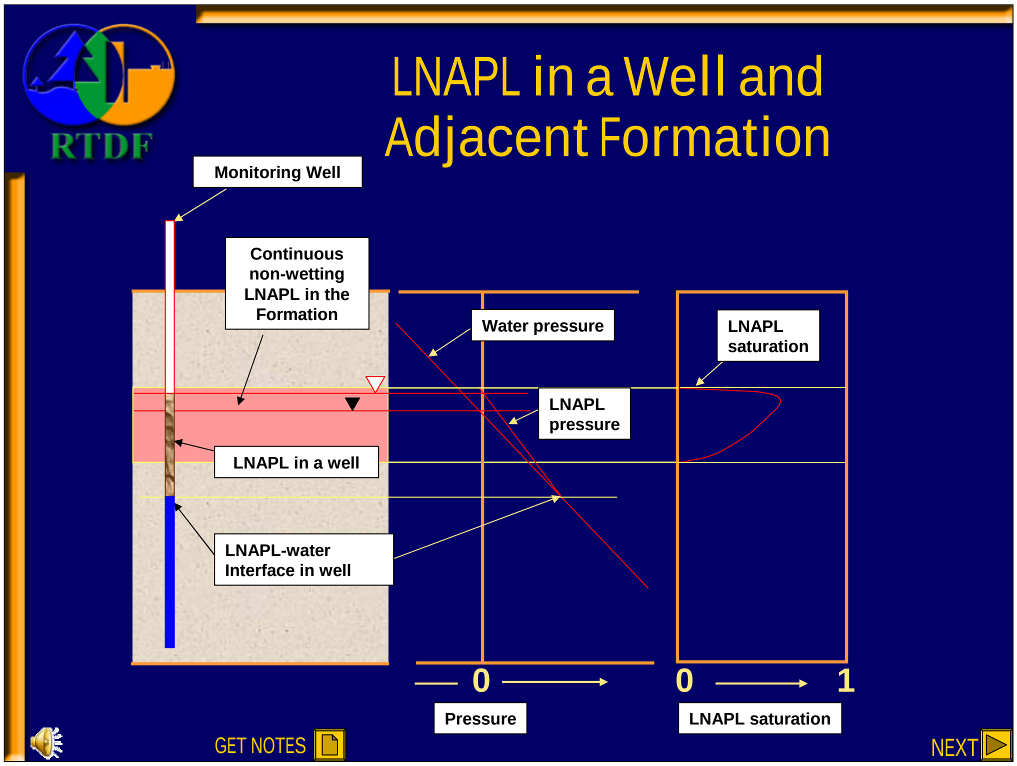

Before we discuss the calculation of LNAPL saturation distribution in the subsurface, it would be useful to examine the complex relationship between LNAPL thickness in a well and the volume of LNAPL in the formation. This figure from **API** follows Farr et al (1990). It presents a simple case in which LNAPL has migrated laterally into a uniform porous media where the water table is stable. The left-hand panel shows that LNAPL in a well extends below the LNAPL in the formation. Within this extension, the pressure difference between the LNAPL in the well and the water in the formation is not great enough to push the water out of the formation. In other words, the capillary pressure is less than the displacement pressure. The extension of LNAPL in the well below the elevation in the formation increases as the porous media become finer and as the densities of the liquids become more similar.

The center panel of this figure focuses on the pressures in the surficial aquifer in relation to the LNAPL thickness measured in the monitoring well. If LNAPL is present in the aquifer, the LNAPL surface (or LNAPL table) occurs at the air-LNAPL interface. The thickness of LNAPL in the well is the difference between the air-LNAPL interface elevation and the water-LNAPL interface elevation. LNAPL pressure starts at atmospheric pressure at the air-LNAPL interface and increases with depth. However, because the LNAPL has a different density than water, the LNAPL pressure gradient is different than the water pressure gradient. The LNAPL and water gradients intersect where the LNAPL and water pressures are equal, which establishes the water-LNAPL interface. The pressure difference between LNAPL and water at any given depth is the LNAPL-water capillary pressure.

The right-hand panel of the figure illustrates that the fraction of the pore space filled (saturated) with LNAPL changes vertically. Moving upward from the LNAPL-water interface, the pressure difference between the LNAPL and the water increases. As this occurs, the LNAPL saturation increases. When air begins to occupy pore space along with LNAPL and water, which occurs at the top of this figure, LNAPL saturation decreases.

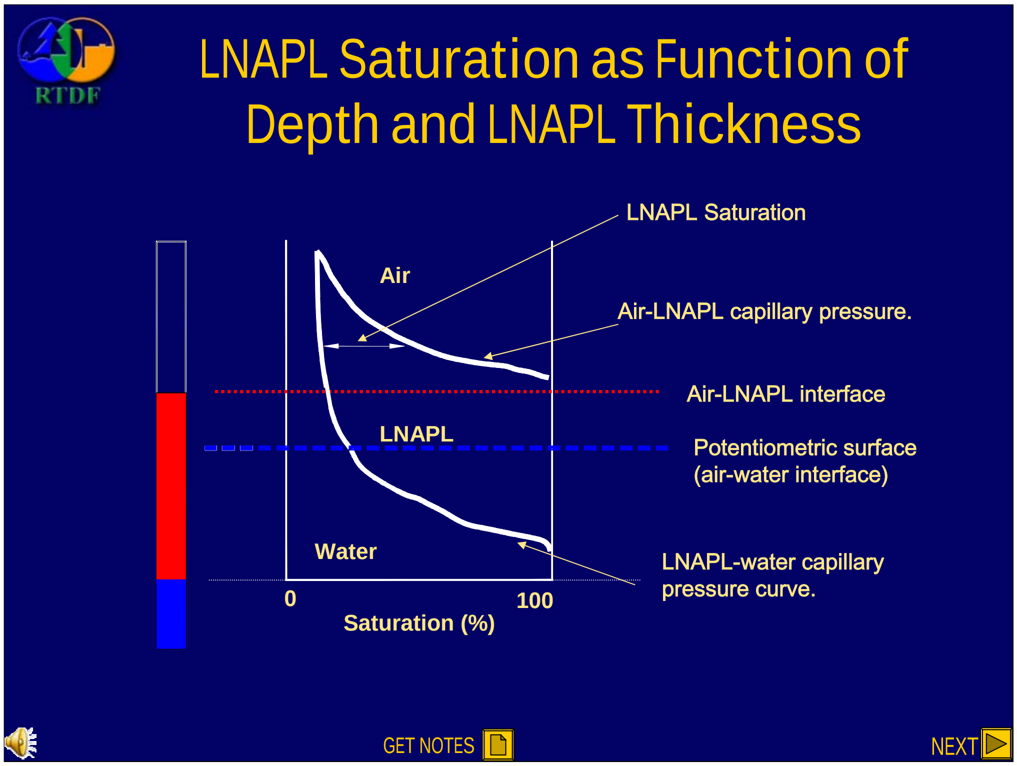

Now that we know that capillary pressure is a function of depth, we can convert this into the saturation of LNAPL as a function of depth.

The well schematic on the left shows the LNAPL thickness measured in the monitoring well. The lower curve on the graph shows the change in water saturation over the thickness of LNAPL in the well, which is actually the LNAPL-water capillary pressure curve. Since the soil is saturated below the air-LNAPL interface, the pore space that is not filled by water is filled with LNAPL. The total liquid saturation beneath the air-LNAPL interface is one.

We get the water saturation from the LNAPL-water capillary pressure curve, and we can determine the LNAPL saturation within the pore space by subtracting the water saturation from one. Above the air-LNAPL interface, the distribution of air, LNAPL, and water in the vadose zone is determined by the air-LNAPL capillary pressure curve. We should also note that the LNAPL and water above this interface are virtually immobile. API has developed spreadsheets based upon the published literature that can be used to perform these calculations. We need to be aware that these capillary pressure curves require the site-specific densities, and surface and interfacial tensions for the air-LNAPL-water combination.

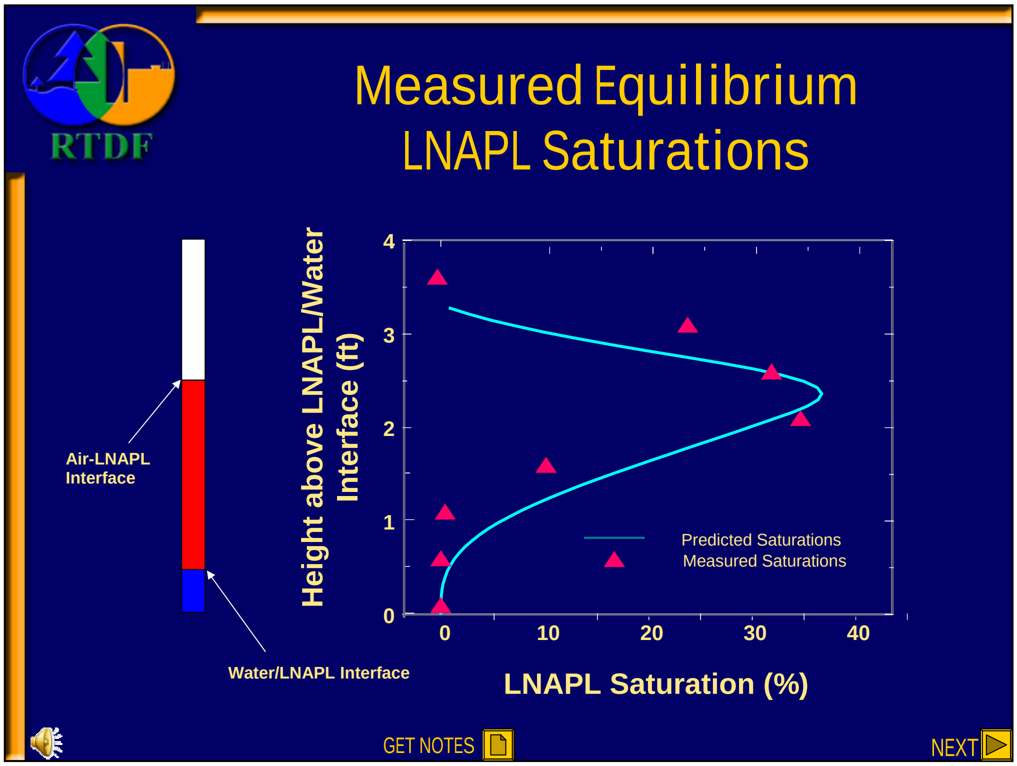

This figure shows the theoretical LNAPL saturation profile for an unconfined, steady-state aquifer and compares the calculated profile to measured LNAPL saturations at various heights above the LNAPL-water interface. The trend of decreasing LNAPL saturation with depth below the air-LNAPL interface is not unique to the amount of measured LNAPL thickness in the well (in this case, about 2.5 feet). The general characteristic shape of the LNAPL profile derives from the shape of the capillary pressure curve, as shown on Slide 22, regardless of the LNAPL thickness in the well.

Measured fluid saturations, represented here by the triangles, were obtained from core sampling in the field. We will talk more about core sampling and proper procedures for collecting, preserving, and testing cores later in the course.

In this case, core plugs were taken and analyzed for the volume of LNAPL in the pore space. Capillary pressure measurements were made from the same core. Fluid samples were obtained to determine density, interfacial tension, and surface tension values.

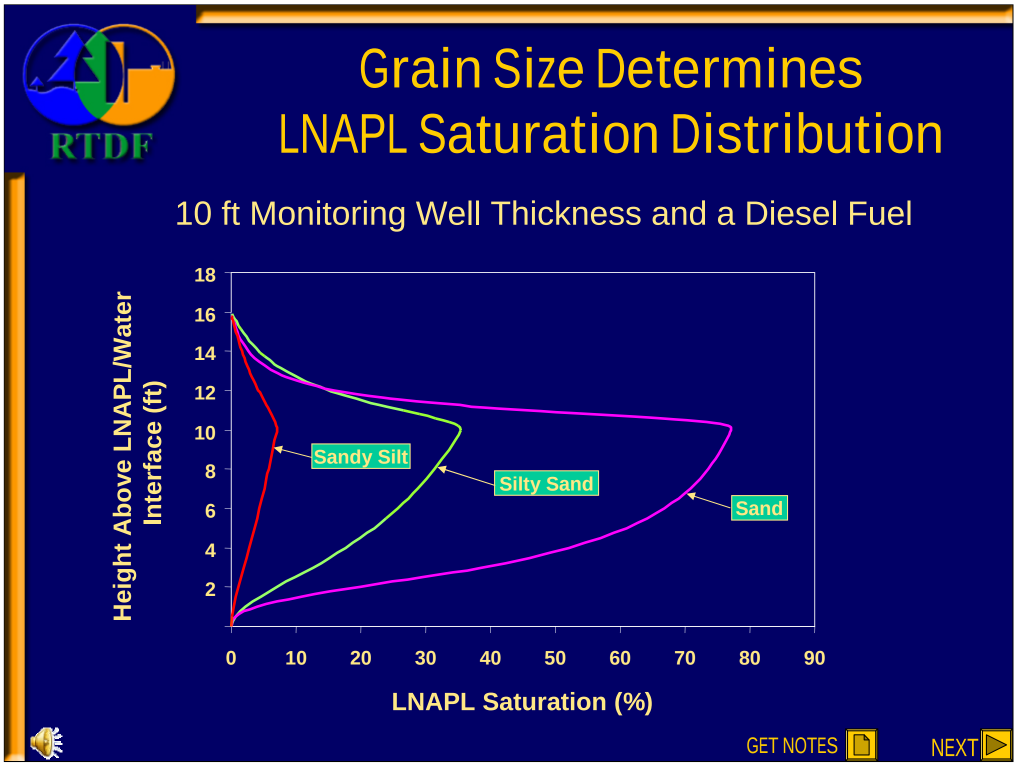

Grain size determines the LNAPL saturation distribution. For a given grain size, LNAPL thickness in a monitoring well, and LNAPL-water combination, we can calculate the LNAPL saturation for different grain sizes using the capillary pressure parameters.

This figure was generated using a LNAPL thickness of 10 feet in the monitoring well and diesel LNAPL-water combination. In the figure, we can see that, in sandy silt, the maximum LNAPL saturation with a LNAPL thickness of 10 feet is only about 7%. In a sand with the same LNAPL thickness in the monitoring well, LNAPL saturations can reach 77%. We understand from our previous discussions of capillary pressure that, in the sand, LNAPL can displace water much more easily than in the silt. Thus, higher LNAPL saturations are possible.

In practice, high LNAPL saturations are rarely measured. Of 212 analyses performed at BP refining sites, the highest saturation found was 56%. 83% of all samples had LNAPL saturations lower than 10%. In fine-grained media, maximum saturations were typically 2-5%; in coarse-grained media, maximum saturations typically were 10-56%.

API has compiled a ***Light Non-Aqueous Phase Liquid (LNAPL) Parameters Database***. In general, LNAPL capillary pressure parameters appear to be different than for agricultural soils whose capillary pressure curves are often used to calculate saturation distributions. It is speculated that the difference is caused by the compaction of porous media at LNAPL sites. This difference probably also leads to the difference between the maximum saturations calculated with default parameters.

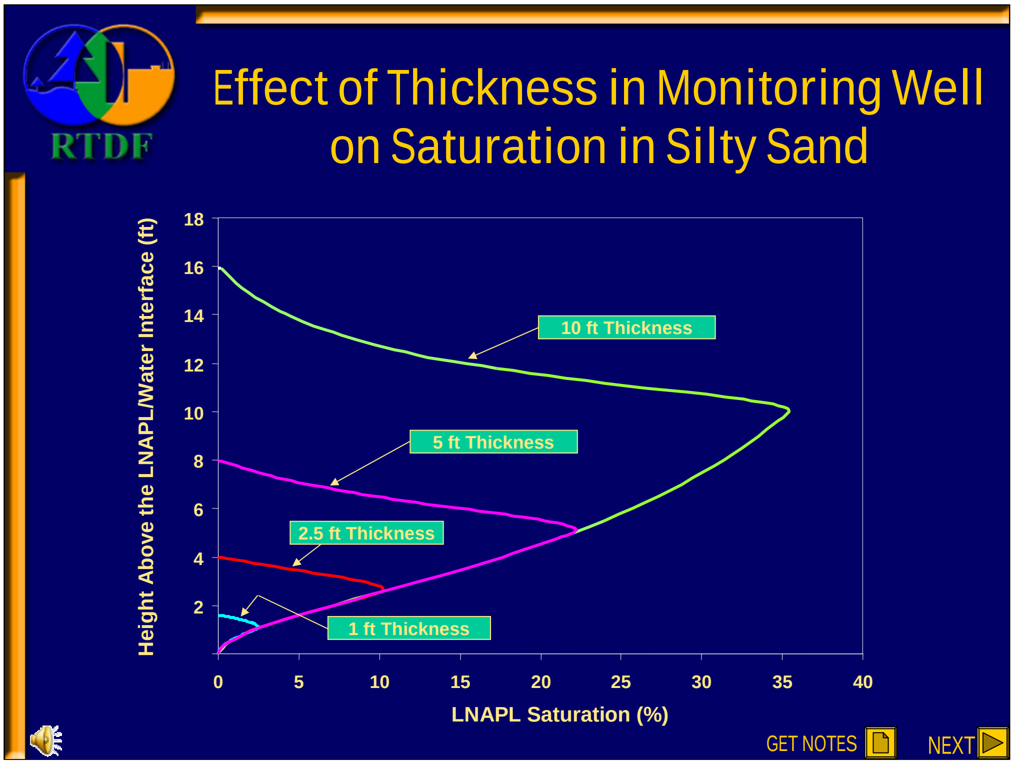

This slide illustrates that LNAPL (diesel fuel) saturation distributions vary in silty sand with differing LNAPL thicknesses measured in monitoring wells. We can see that for a 10-ft thickness of diesel fuel in a monitoring well, the maximum saturation in silty sand is predicted to be about 36%. If the diesel fuels thickness were 1 foot, the maximum saturation would be predicted to be less than 5%.

In summary, if we have capillary pressure curves and homogeneous media and know the LNAPL thicknesses measured in monitoring wells and the fluid properties, we can estimate the saturations of LNAPL in media of various grain sizes.

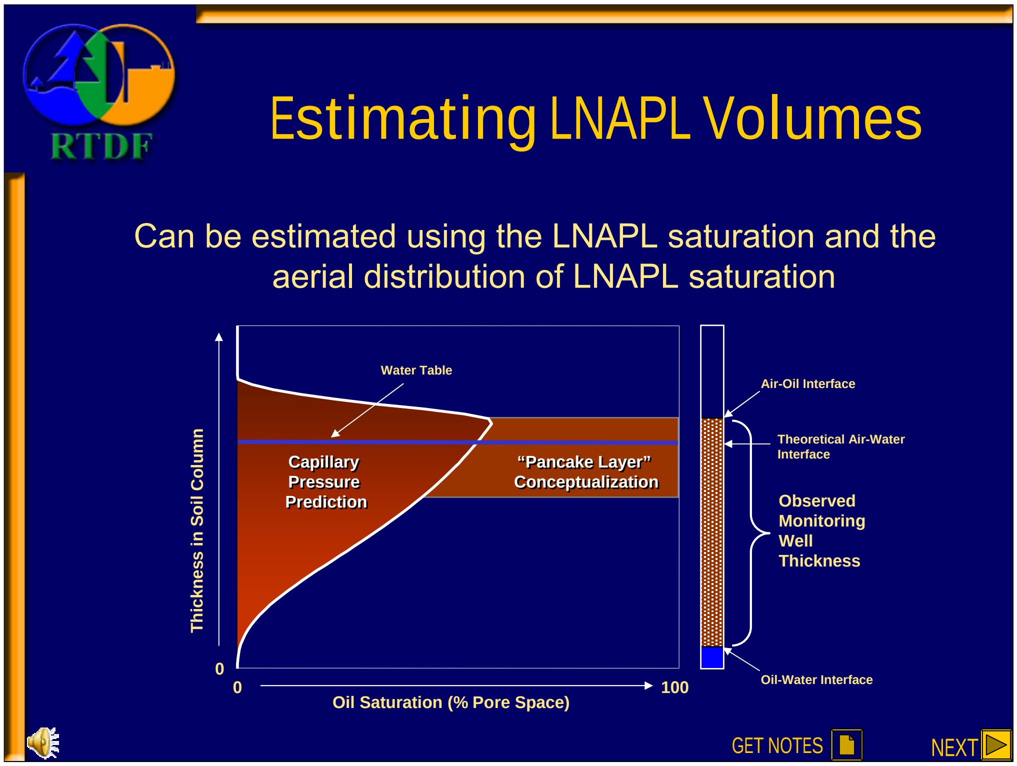

The volume of LNAPL present, given the saturation values and distribution, can be calculated in spreadsheets that use a numerical integration of the predicted saturation. The volume can be represented as follows:

Consider a 1-foot cube of soil containing the distribution depicted in the figure above. The distribution profile on the left is based on capillary pressure behavior, which shows how LNAPL saturation changes with depth. Note that the actual thickness of the LNAPL interval in the soil is roughly equal to the measured LNAPL thickness in the well.

If just the soil and water were removed from the cube, there would be a few inches of LNAPL left in the cube. This is called the "**specific volume**" of LNAPL in the soil and is expressed in $feet^3/feet^2$ (or often simplified to just feet). This specific volume of LNAPL is the same as the volume you would calculate by integrating the capillary pressure distribution curve.

This slide also depicts a typical LNAPL saturation profile generated using the old pancake model. Because the pancake model assumes 100% LNAPL saturation, the thickness is typically reduced by applying various "rule-of-thumb" correction factors to the measured well thickness. This has resulted in the misunderstood concept of "true" versus "apparent" LNAPL thickness.

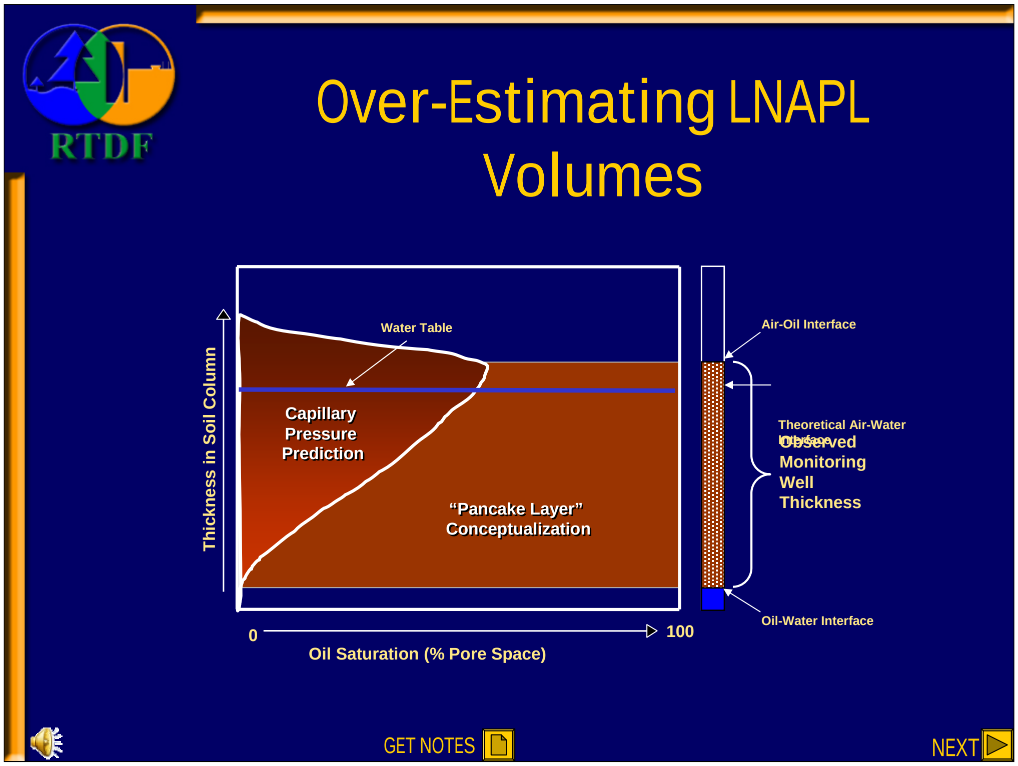

This slide illustrates how LNAPL volume can be significantly overestimated using the pancake model. It is not uncommon for analysts to assume that the pancake layer is equal in thickness to the measured LNAPL thickness in the monitoring well. By assuming a 100% LNAPL saturation, the calculated LNAPL volume would be much higher than what actually exists in the soil.

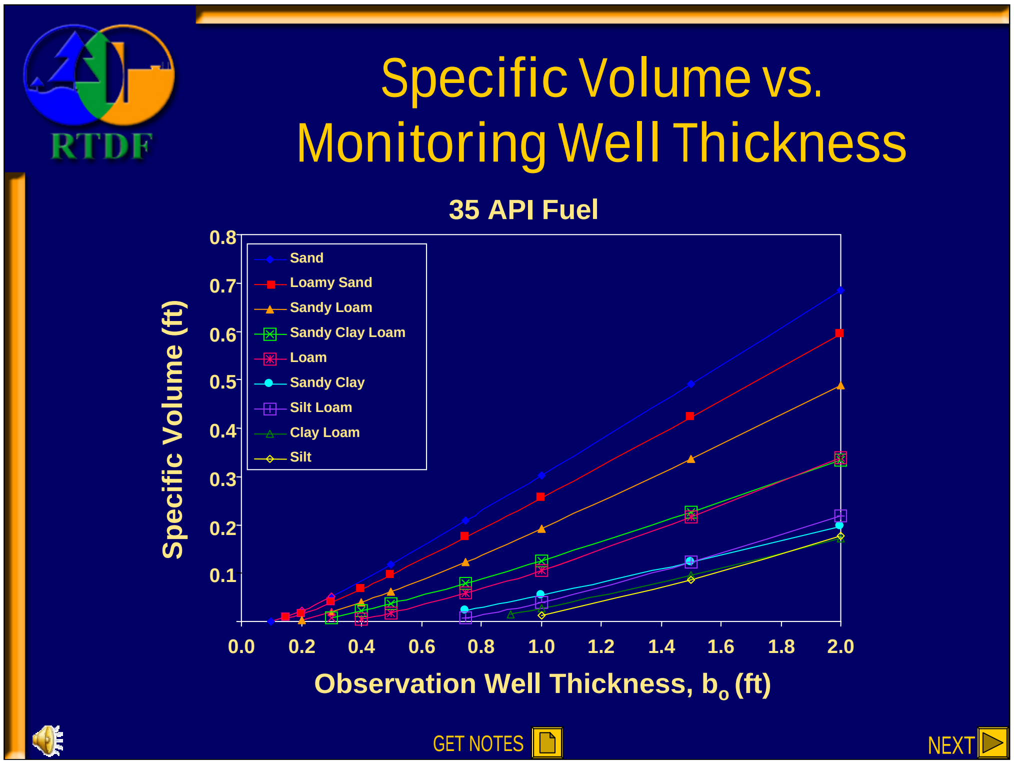

This graph illustrates how LNAPL thickness in a monitoring or observation well is related to the actual thickness of a 35 **API gravity** fuel (fresh diesel) in media of different grain sizes. The media parameters were taken from **Carsel and Parrish** for agricultural soils.

In a recent compilation of data, the capillary parameters for agricultural soils are not the same for similar soil types in surficial aquifers, probably because of different degrees of compaction.

This graph is important because it shows that the specific volume of LNAPL in the subsurface is much less than estimated using the pancake model and the LNAPL thickness in the monitoring well. This is because porous media contain a large amount of water in addition to the LNAPL.

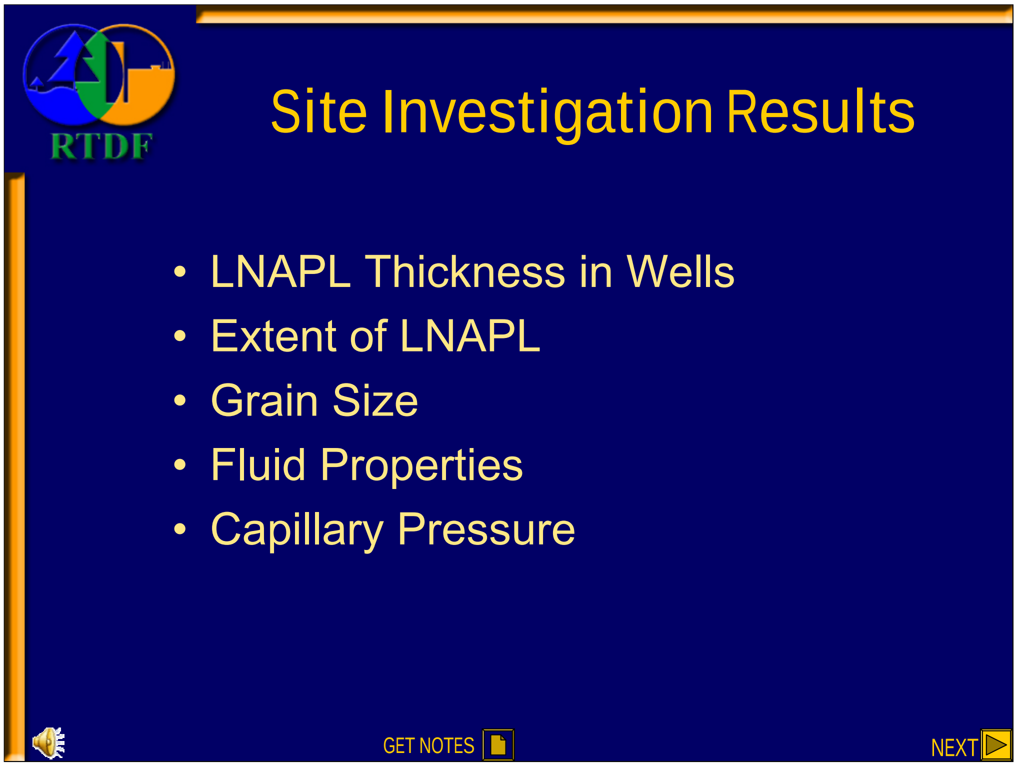

A typical site investigation determines the LNAPL thickness in the wells, the extent of LNAPL, and the grain size of the porous media. These could be sufficient to estimate the volume of LNAPL in the subsurface using default parameters from the literature (Carsell and Parrish) for fluid and capillary properties. However, recent testing of these parameters indicates that they may not be applicable to surficial aquifers due to differing degrees of compaction.

The API has developed a database that can supply the necessary default parameters dependent upon soil type and grain size. Later in the course, we will discuss how to obtain core samples and fluid property measurements.

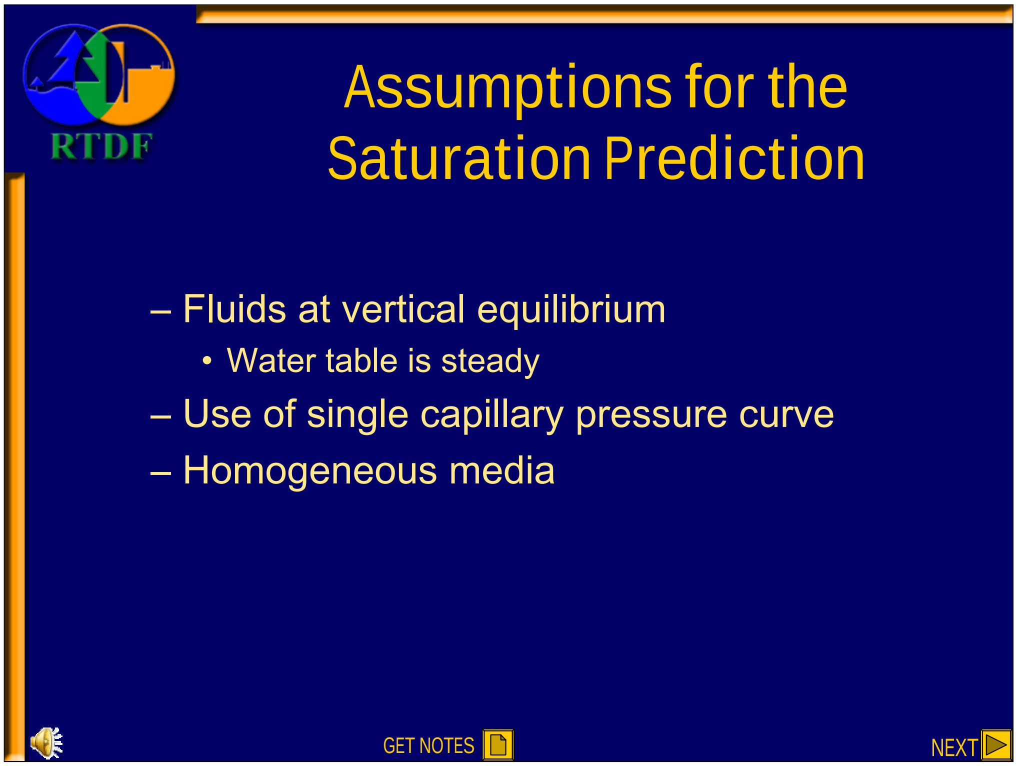

LNAPL saturation predictions typically are based on a set of assumptions. These include:

- Fluids are at **vertical equilibrium**; the water table is steady.
- A single capillary pressure curve is used.
- Media are homogeneous.

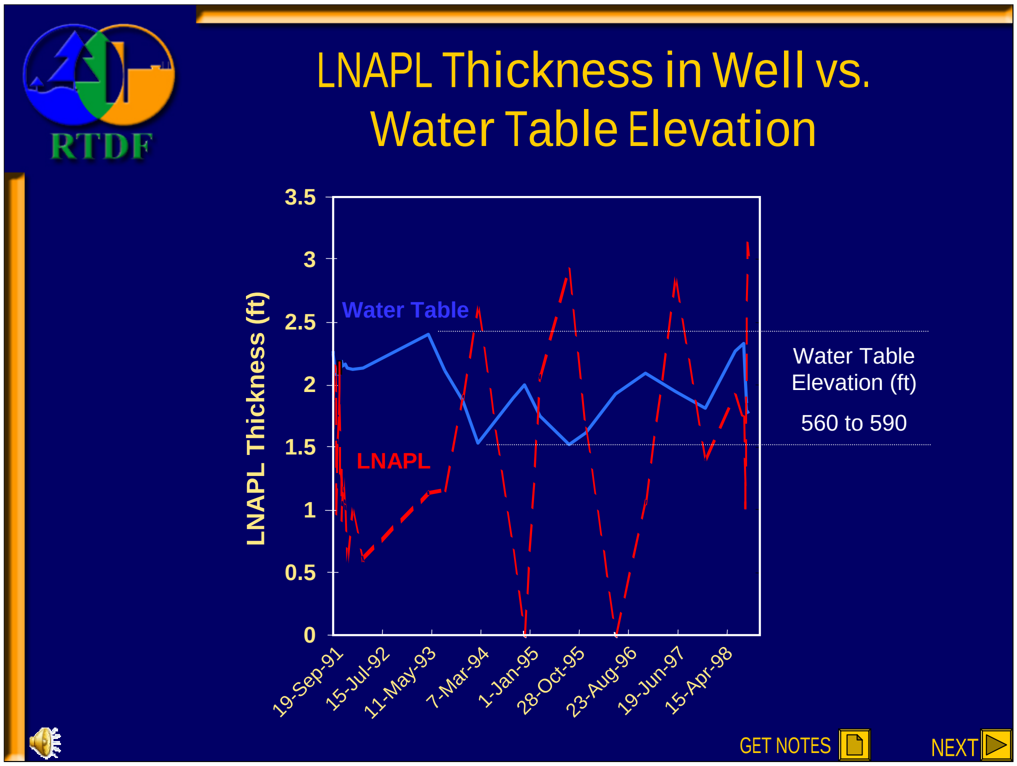

This hydrograph shows the LNAPL thickness in a well versus the water table elevation. The red line is the measured thickness of LNAPL in the monitoring well. The blue line represents the change in water table elevation. What is usually observed is that, when the water table elevation decreases, the LNAPL thickness in the monitoring well increases, and vice versa. While changes in the measured LNAPL thickness often are attributed to a redistribution of LNAPL in the aquifer as the water-table elevation changes, this is only part of the story. Two phenomena cause this: First, the redistribution of the LNAPL in the porous media, up or down with the water table, leaves slightly different volumes of residual LNAPL in the vadose or saturated zone. This causes a slight difference in the thickness observed in the monitoring well. Second, LNAPL and/or water migrates into a well from the soil as the water table drops or rises. The exact magnitude of the response is difficult to predict, because it depends upon the rates at which fluids can enter and leave a well, which, in turn, depend upon the conductivities of the water and LNAPL in the porous media. Kemblowski and Chang presented a theoretical analysis in *Groundwater* in 2000.

Following a water table rise or fall, the fluids are not in equilibrium with the soil, and some time is required to re-establish the equilibrium. Since the theory requires fluids at equilibrium with the soil, there is a question about whether we can predict saturations and volumes with monitoring well thicknesses. The case studies, discussed later, suggest that we can.

LNAPL thickness levels in monitoring wells can vary by many feet over time, because the re-equilibrium process may be slow. For low-viscosity fluids, such as gasoline, in permeable media, such as sands, the re-equilibrium process is much faster than it would be for lube oil in silt. For example, the re-equilibrium of the gasoline in sand might take 1 day, while the re-distribution of lube oil in silt could take months.

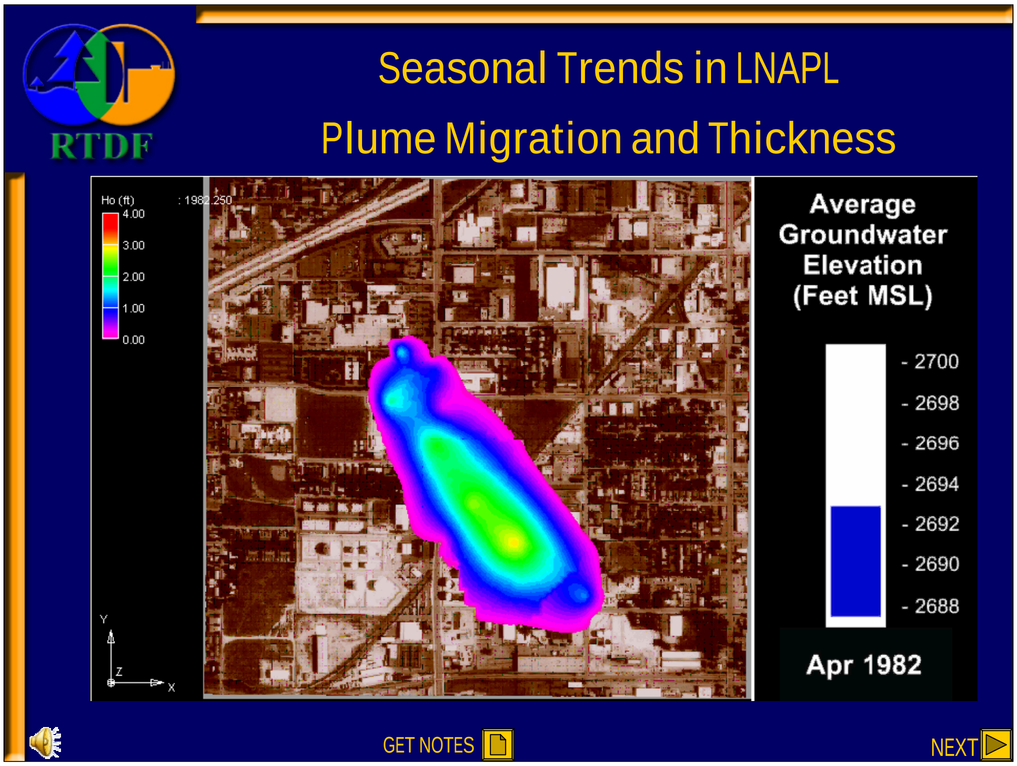

The animation in the slide illustrates a common observation at many sites that often is misinterpreted to mean that a plume is migrating or growing or that a new release has occurred.

As we saw in the last slide, seasonal fluctuations in groundwater elevation can have a pronounced effect on the measured thickness of LNAPL in a well. The animation on this slide illustrates this dramatically: it shows the changing apparent thickness and apparent size of the LNAPL plume due to fluctuations in the water table over a period of about 5 years. In this map, areas of greater measured-LNAPL thicknesses are shown in red or yellow or green. The blue and pink areas are less thick. Note the scale in the upper left corner.

The water table fluctuates over about 10 feet on a seasonal basis. The scale on the right shows the water table elevation and date.

You should note that, although measured-LNAPL thickness in monitoring wells changes quite dramatically over time, the overall position of the plume does not. Also, these short-term changes in groundwater elevation probably do not cause a significant redistribution of LNAPL in the formation – the timing for that depends upon the conductivity of LNAPL in soil; certainly a gasoline in course sand re-equilibrates in a shorter time than a lube oil in silt.

Care must be taken when applying the theories presented in this course to real-world situations that might be affected by fluctuating water tables. The real-world examples near the end of the training illustrate how this can affect results, but show that good predictions and understanding can still be obtained.

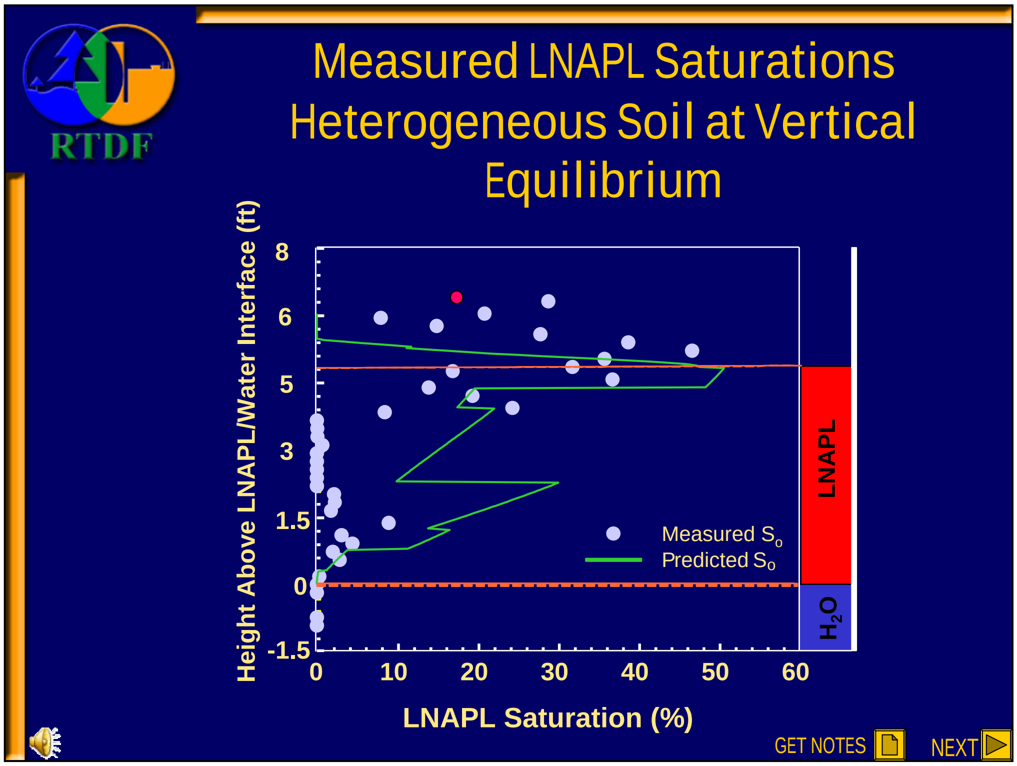

This figure illustrates the effect of a heterogeneous soil on the saturations, which can be measured. It also shows the potential agreement you can get between the theoretical and the measured values, if you have capillary pressure curves for each of the various subsurface layers. Technology and tools needed for estimating saturations and developing capillary pressure curves are currently available, and have been successfully demonstrated at many large-scale sites.

The real-world cases near the end of the training will present examples of how the theory can be applied successfully to heterogeneous geologies and fluctuating water tables. For example, Case Study #1, presented on slides 82 and 83, used the data from the figure above.

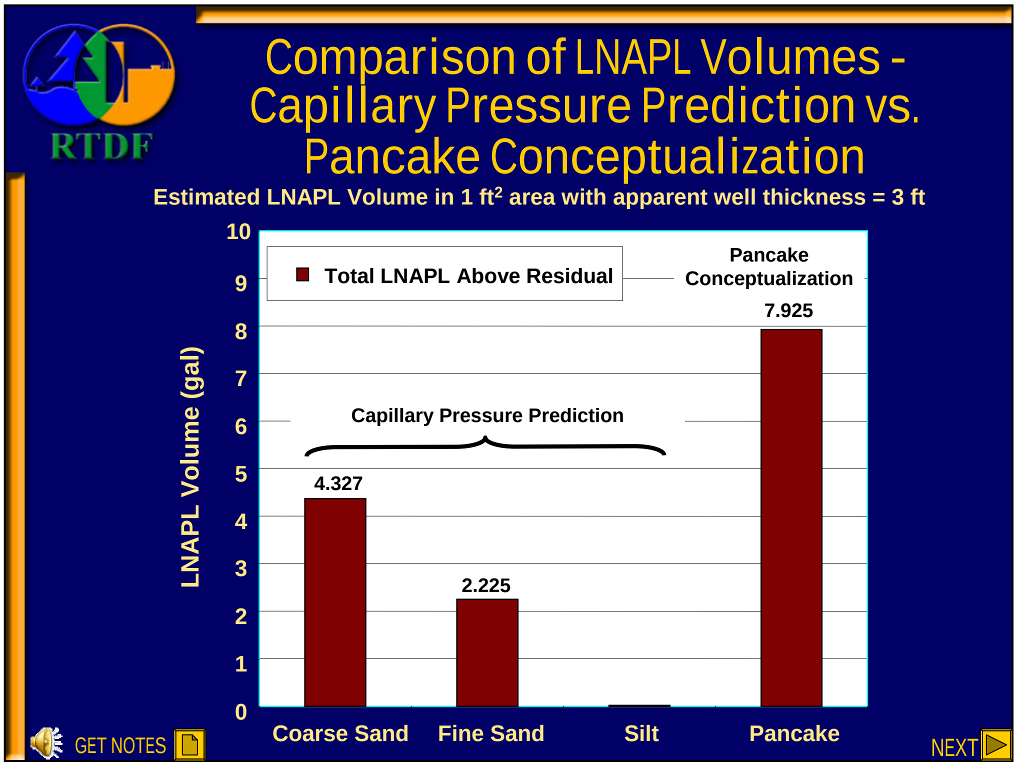

This slide compares the estimated volumes of LNAPL in different types of porous media generated from capillary pressure prediction and from "pancake model" conceptualization. "Pancake models" of the past assumed a uniform saturation independent of porous media type. The specific volume is highly dependent on the media type, as well as the LNAPL type. The volumetric data by media type can be transferred into a useful graph that shows how the specific volume in the media changes with monitoring-well thickness.

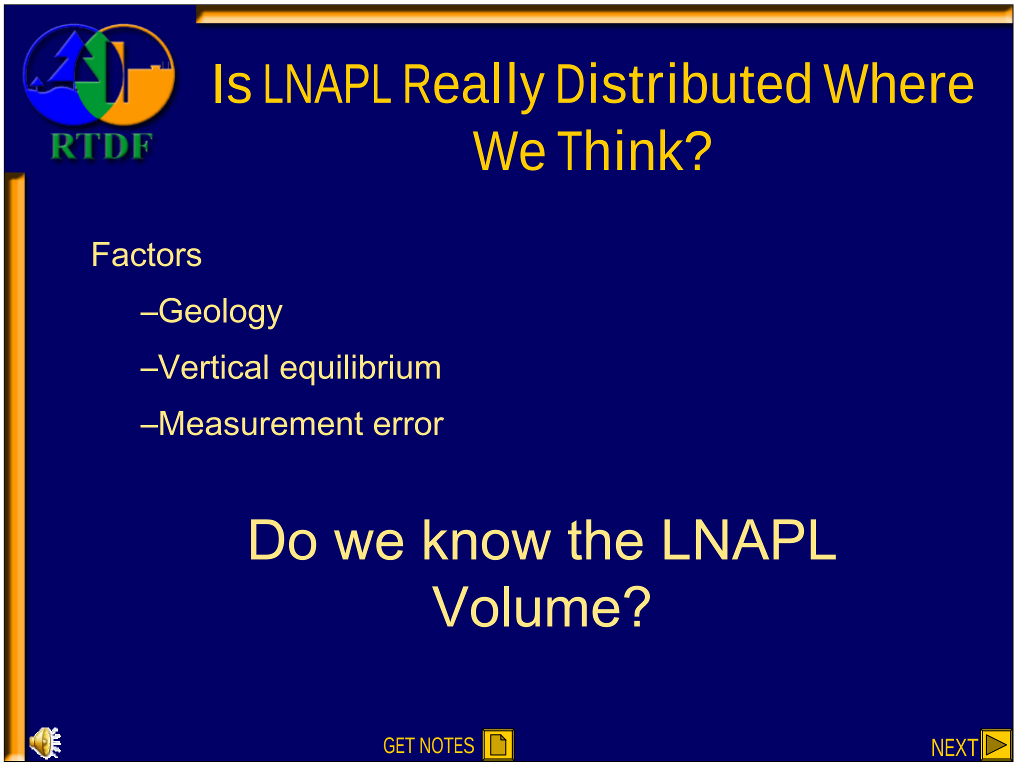

Is LNAPL really distributed where we think it is? If we know the geology, have measured the porous media and fluid data, and understand the history of the site, it is likely that we understand the distribution of LNAPL.

Do we know the LNAPL volume? Probably, but perhaps not as well as we know its distribution near a well. Geology can vary significantly over short distances, and residual LNAPL saturation is likely distributed throughout the vadose zone near the source. However, we think we can make a good estimate of the volume. Support for this will be shown in the real-world case studies.

There are a variety of factors that limit our ability to understand LNAPL distribution and to estimate its volume in the subsurface. Geology may vary, fluids may not be in vertical equilibrium, and LNAPL saturation measurements may be incorrect. As with all site assessment, additional data always will provide more detailed information that may contribute to our understanding, but collecting this data also may strain existing resources. Project teams must use their good judgment in determining the proper balance for their site.

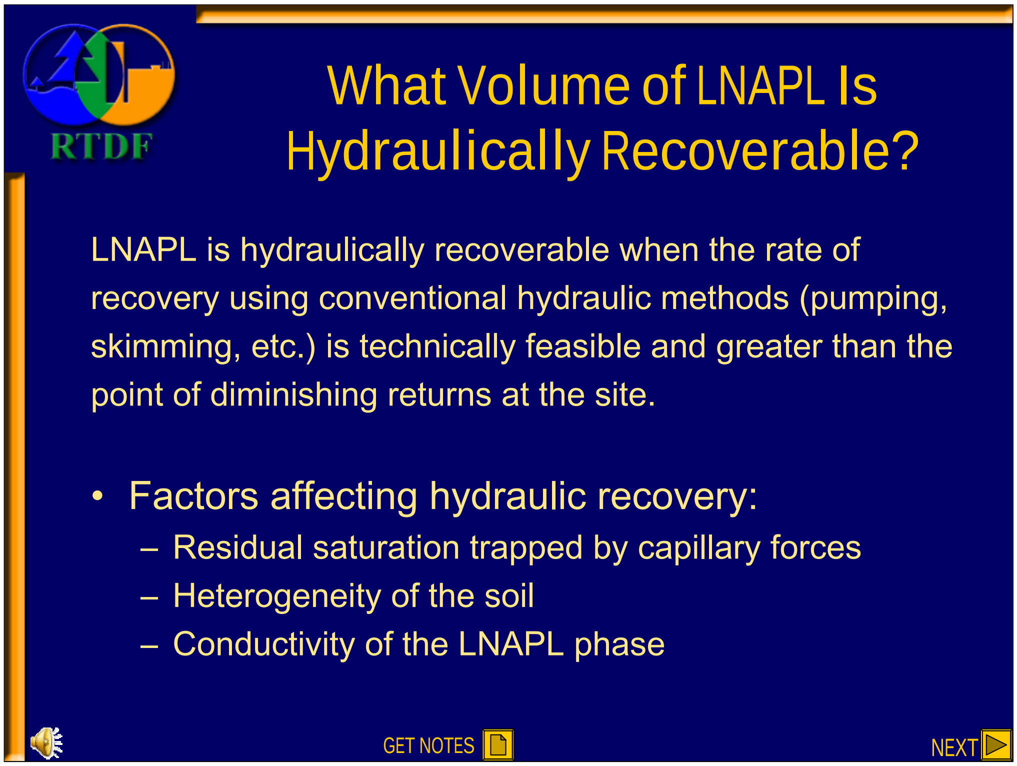

Now that we understand what parameters are needed to calculate LNAPL volume in the subsurface, how do we determine what portion of that volume is ultimately recoverable?

For purposes of this training, we define LNAPL as hydraulically recoverable when the rate of recovery using conventional hydraulic methods (pumping, skimming, etc.) is technically feasible and is greater than the point of diminishing returns — that is, when the system begins to recover decreased incremental volumes over rapidly increasing time periods. LNAPL recovery by volatilization or enhanced methods such as steam is beyond the scope of this training.

The factors that affect recoverability (the volume that can be recovered) are residual saturation trapped by capillary forces, heterogeneity of the media, and conductivity of the LNAPL phase.

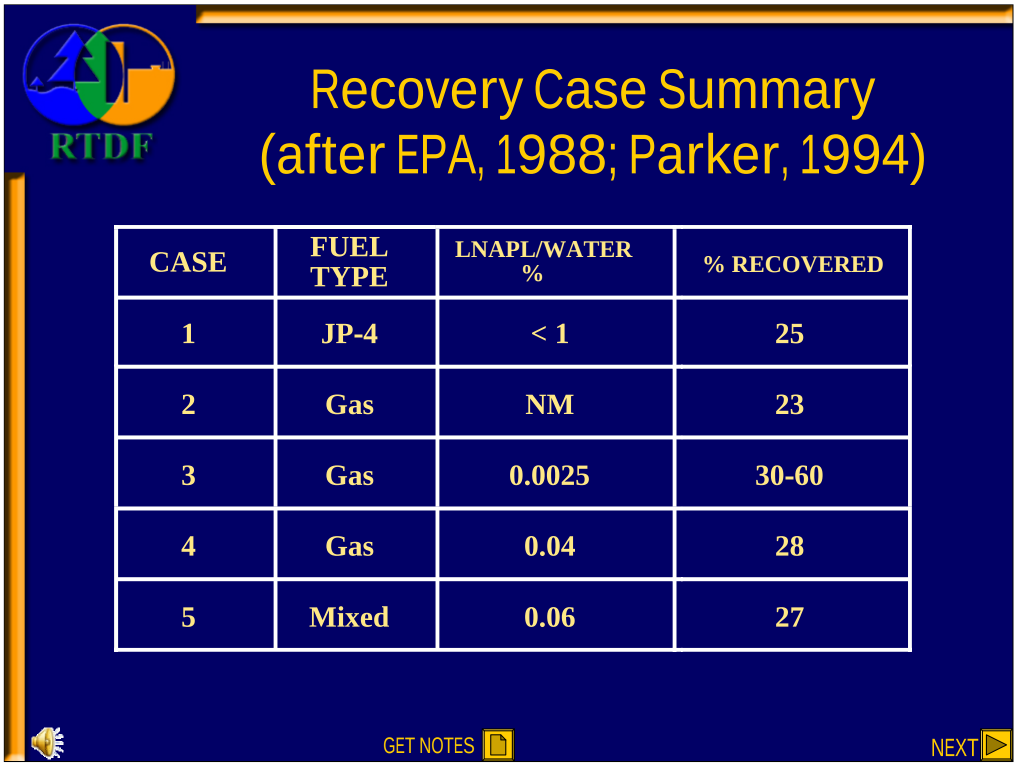

CASE	FUEL TYPE	LNAPL/WATER %	% RECOVERED
1	JP-4	< 1	25
2	Gas	NM	23
3	Gas	0.0025	30-60
4	Gas	0.04	28
5	Mixed	0.06	27

This table, developed by **Beckett and Lundegard**, documents the ultimate measured recoveries obtained at 5 different sites for different fuel types. The low recoveries are due to capillary forces, geology, and conductivity of the LNAPLs.

The third column indicates that the recovery was stopped when the percentage of produced LNAPL to water was relatively low.

We have previously discussed residual saturations and the effect of heterogeneity. Now let's discuss LNAPL **relative permeability**.

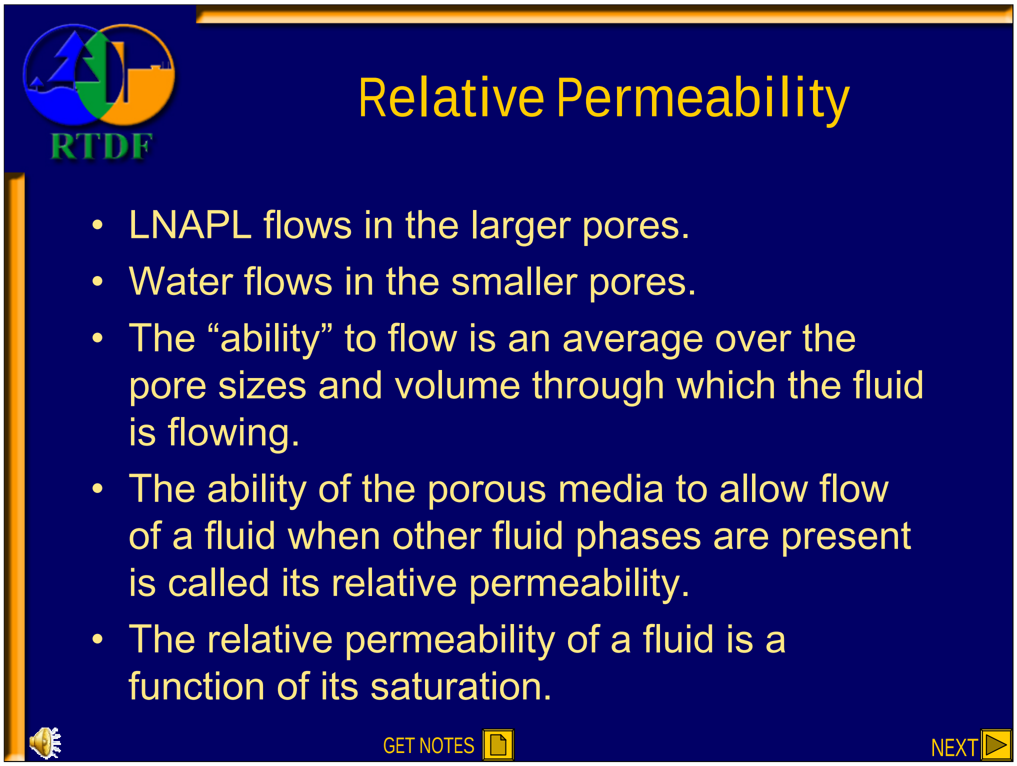

Relative permeability is one of the most important parameters affecting the flow of LNAPL in porous media.

LNAPL flows in the larger pores. Water flows in the smaller pores. The ability to flow is an average over the pore sizes and volume through which the fluid is flowing.

The ability of the porous media to allow flow of a fluid when other fluid phases are present, relative to its ability to allow flow of that fluid when no other fluid phases are present, is called its relative permeability.

The relative permeability of a fluid depends on its saturation and the saturation of other fluids present. Relative permeability is fluid-specific and ranges from 0 to 1.

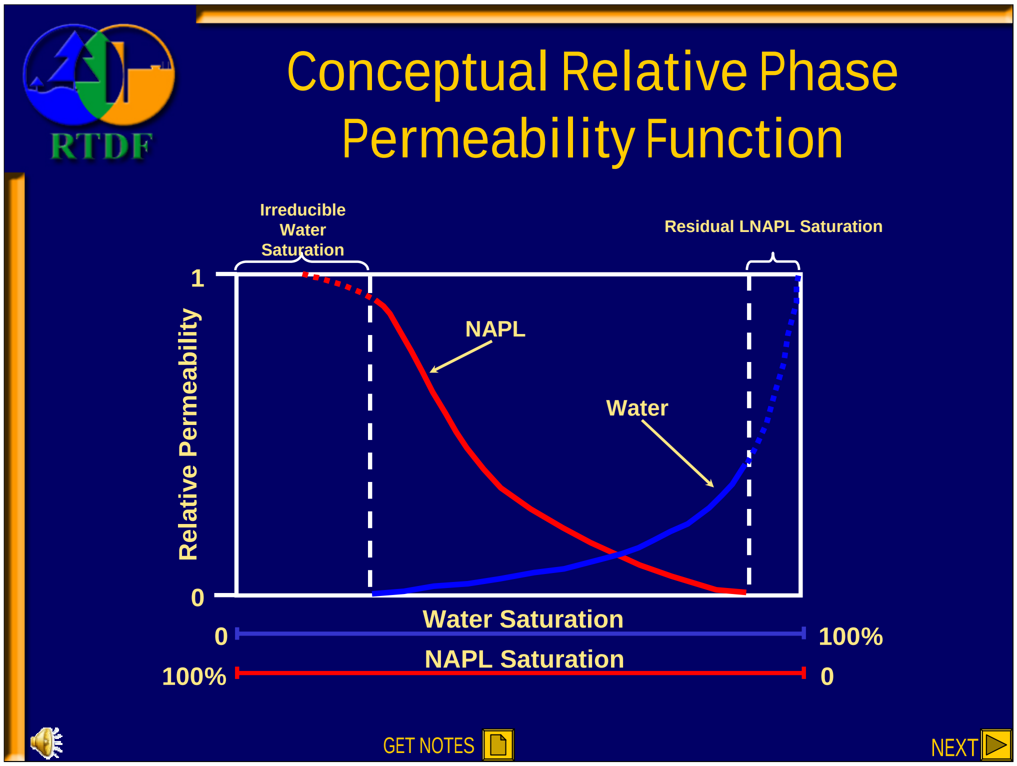

This figure shows conceptual relative permeability curves of the water (wetting) and the LNAPL (non-wetting) phases in a porous media as a function of their saturation. Perhaps it is easiest to understand these curves from the basis of the experiment that is run in order to measure the relative permeability. Remember: Relative permeability is a function of the saturation of the phase in the porous media.

In our experiment, a sample of soil is placed in a core holder and secured. Then, it is filled with water. At one end of the soil core, a constant ratio of LNAPL and water is injected. The pressure gradient across the core is measured, and the fluids leaving the soil core are collected. When the gradient across the core is steady, or constant, and the ratio of fluids leaving the core is constant, the flow is considered to be at steady state.

Several methods can be used to measure saturation. One might measure the collected volumes and use the total porosity to determine the saturation. Often x-rays are used in the oil production business.

In practice, an unsteady-state test is run with mathematical methods to analyze the changing gradients across the core and the changing LNAPL-to-water ratios produced to arrive at the relative permeability curves.

As depicted, these relative permeability curves are “drainage” curves in keeping with the drainage capillary pressure curves. Some hydrologists and engineers prefer to use the imbibition curves since they are thought to better reflect the displacement of LNAPL by water during the hydraulic recovery process.

As an alternative to laboratory tests, models based upon the capillary pressure curves can be used to estimate relative permeability.

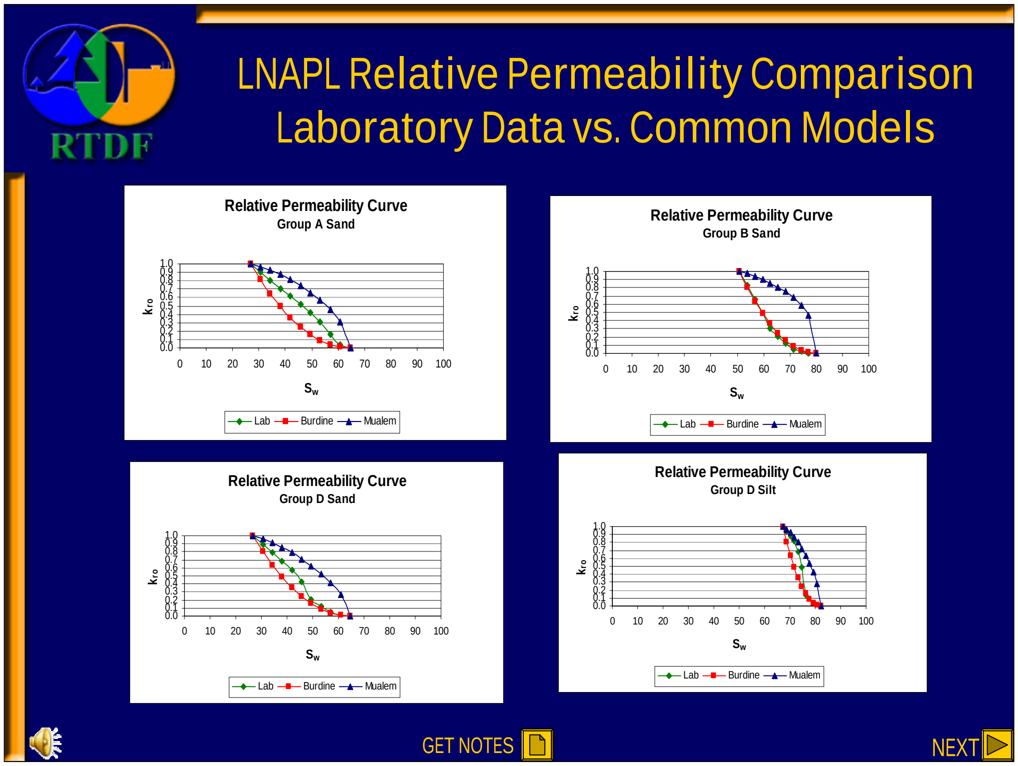

Two models -- the **Burdine** and the **Mualem** models – are used to estimate relative permeability. They are based on models of pore size distribution and the association of permeability to the pore sizes. Generally, the Mualem model estimates a slightly greater relative permeability than Burdine. This is likely due to the way permeability is associated with pore size distribution.

The curves shown here compare Burdine and Mualem estimates to laboratory-measured water-LNAPL relative permeability. The Burdine model provides a better fit to the laboratory data, except in the Group A Sand case (where it would under-predict recovery rate). In the other three examples, Burdine provides an acceptable match over the lower range of LNAPL saturation. LNAPL accumulations in aquifers typically would be at the lower range of LNAPL saturation. In all these cases, the Mualem model over-predicts the LNAPL recovery rate. Generally, Mualem is believed to provide better predictions in clays; Burdine in sands.

In the field, capillary pressure and relative permeability can vary significantly over a few inches, and assumptions for the recovery models (to be discussed later) can be easily violated. Thus, hydrogeologists and engineers need to use good professional judgment when deciding whether models or laboratory measurements will provide the best overall estimates of field performance at their sites.

Now let's discuss the conductivity of LNAPL.

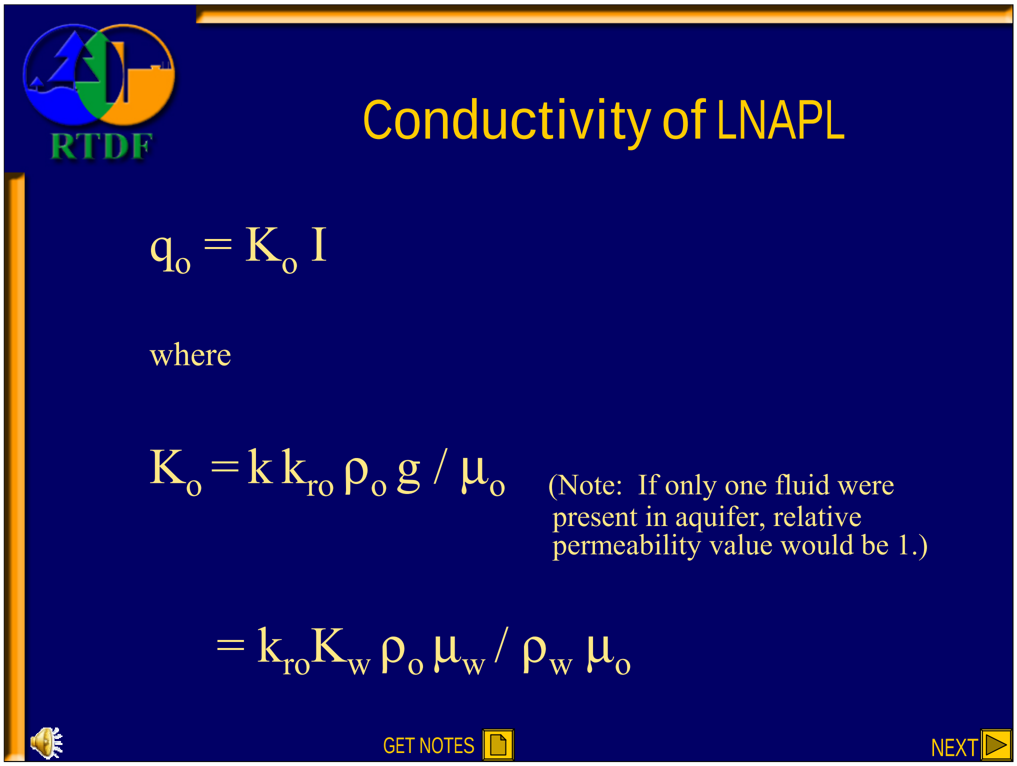

You can calculate the flow rate of LNAPL in the same way you would calculate the flow rate of water. The Darcy velocity of LNAPL (subscript "o" denotes LNAPL), q_o, is equal to the conductivity of LNAPL, K_o, multiplied by the gradient, I (the slope of the LNAPL-air interface).

The conductivity of LNAPL (K_o) is expressed similarly to that of water. It is a function of:

k, the permeability of the porous media, multiplied by the

rho $(\rho)_o$, the LNAPL density, multiplied by

g, the gravitational constant, and then divided by

mu $(\mu)_o$, the LNAPL viscosity.

Note that if only a single fluid were present in an aquifer, the relative permeability would have a value of 1.

For multi-phase flow, when water and LNAPL are present in the subsurface, the relative permeability, k_{ro}, is also included in the conductivity equation.

LNAPL conductivity also can be calculated from the conductivity of groundwater, since the viscosity and density of water both have a value of about 1. Multiply the conductivity of groundwater (subscript "w" denotes groundwater) by the density of the LNAPL at field temperature, and then, divide by the viscosity of the LNAPL.

Note that LNAPL conductivity is inversely proportional to its viscosity. So, the conductivity of a fuel oil with a viscosity about 6 times that of water would be 6 times less than the conductivity of gasoline, which has a viscosity slightly less than water. This will be graphically illustrated later.

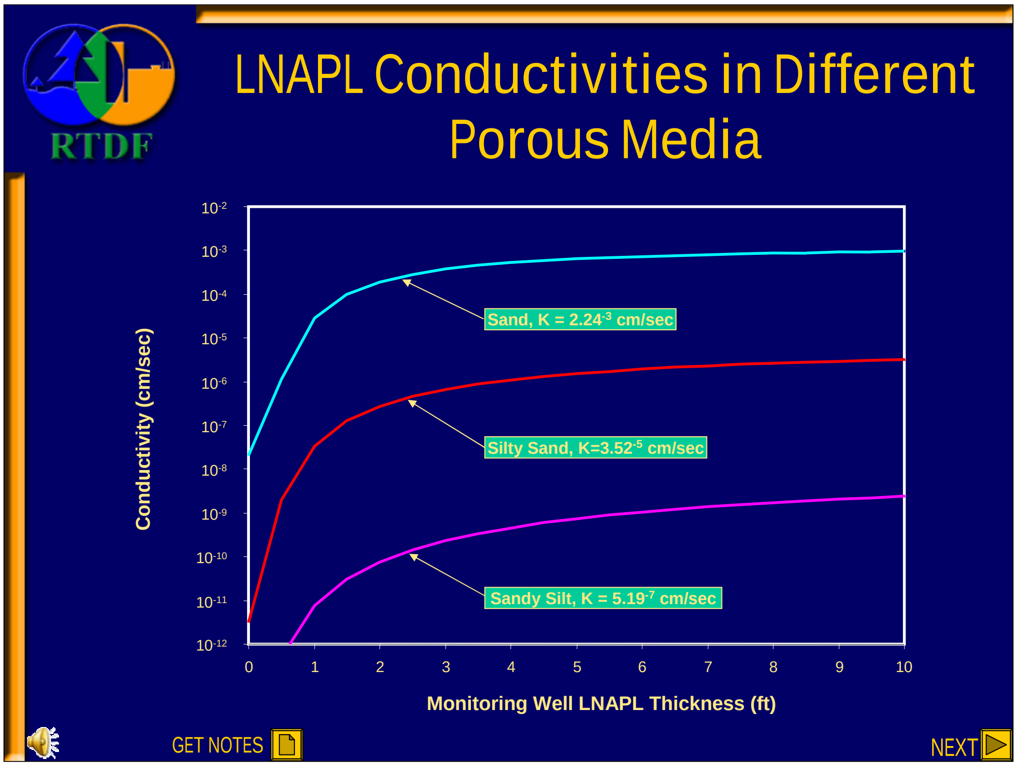

This slide shows the vertically averaged value of LNAPL conductivity, which varies along the LNAPL saturation curve, at different monitoring well thicknesses in three porous media. The Burdine model and gasoline fluid properties were used in these calculations.

LNAPL conductivity is largely a function of the permeability of the porous media. It is clear, however, that the conductivity of LNAPL decreases by orders of magnitude as the thickness of LNAPL in a monitoring well and its volume in the subsurface decrease. This is why recovery of LNAPL is so difficult when well thickness is small.

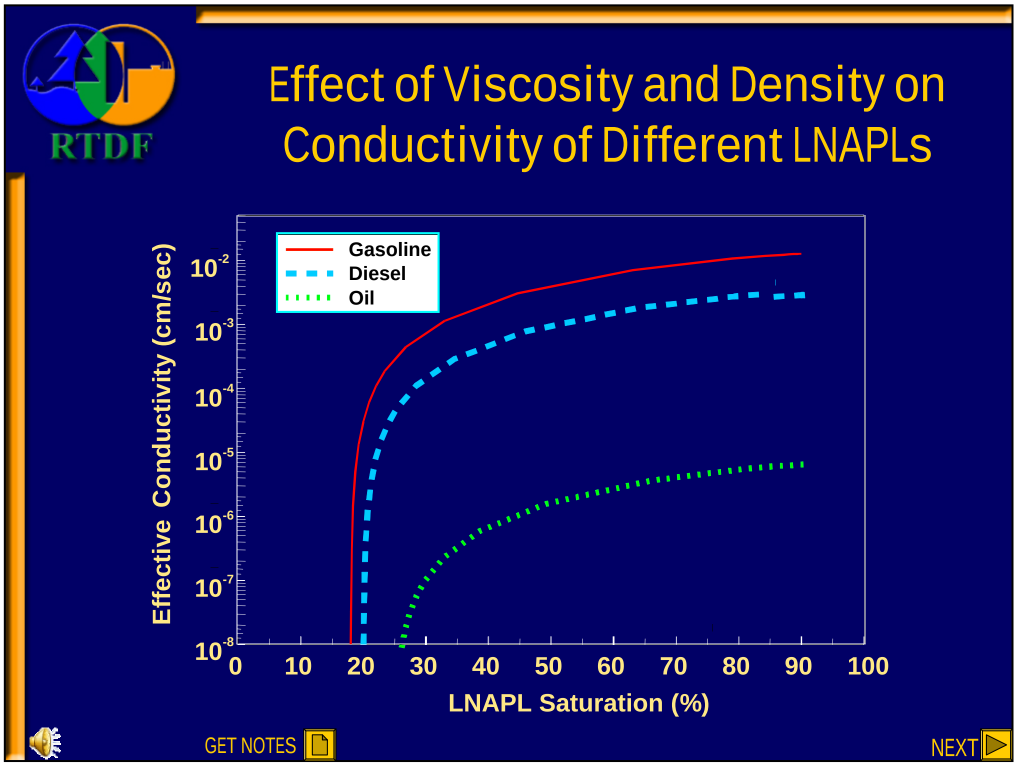

This figure illustrates how the density and viscosity of different LNAPLs affect their conductivity. Note that there are order-of-magnitude changes in conductivity as LNAPL saturation decreases.

You will recall from the equation for conductivity, that LNAPL conductivity is inversely proportional to its viscosity. Gasoline has a viscosity of about 0.7 **centipoise**. Crude oil has a viscosity on the order of 50-100 centipoise. Notice that the effective conductivity of crude oil in comparison to gasoline is considerably reduced, primarily due to viscosity. Oil will have a density somewhat greater than gasoline. This increases conductivity slightly, but not to the degree that the viscosity is decreasing it.

Conductivity is sensitive to relative permeability. A decrease in effective LNAPL conductivity as LNAPL saturation decreases is the result of relative permeability reductions and the decreases in LNAPL saturation, which will be discussed on the next slides.

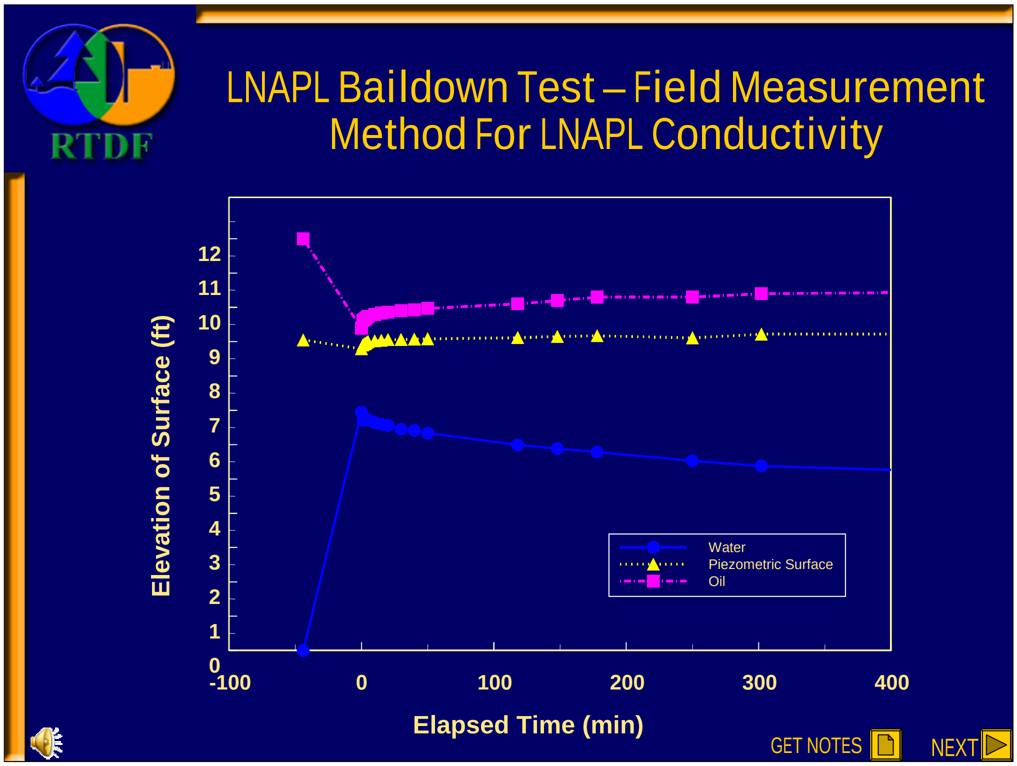

One way to check a LNAPL relative permeability estimate is with a **baildown test**. An LNAPL baildown test is performed and analyzed in much the same way as a water baildown test, but there are some important differences. First, instead of the water being evacuated from the well, only the LNAPL is removed. In practice, this is hard to do. We often try to do it with a vacuum truck rather than a bailer.

Instead of monitoring only the water-air interface, both the water-LNAPL and LNAPL-air interfaces need to be monitored versus time. The figure shows a plot of such data.

There are two methods for analyzing the data. One was developed by **Lundy and Zimmerman et al**; another was developed by **Huntley**. Typically, we use both and compare them to theory.

There are practical limitations to the baildown test. First, there must be enough LNAPL in the well to measure it and determine changes in thickness of LNAPL flow into the well. Second, the conductivity of the LNAPL must be high enough that the LNAPL flows back into the well. The test may not be practical for high viscosity liquids (about 10 centipoise or higher) or low permeability media. Several days may be required for the LNAPL to flow into the well, which can be a problem if the potentiometric surface also changes.

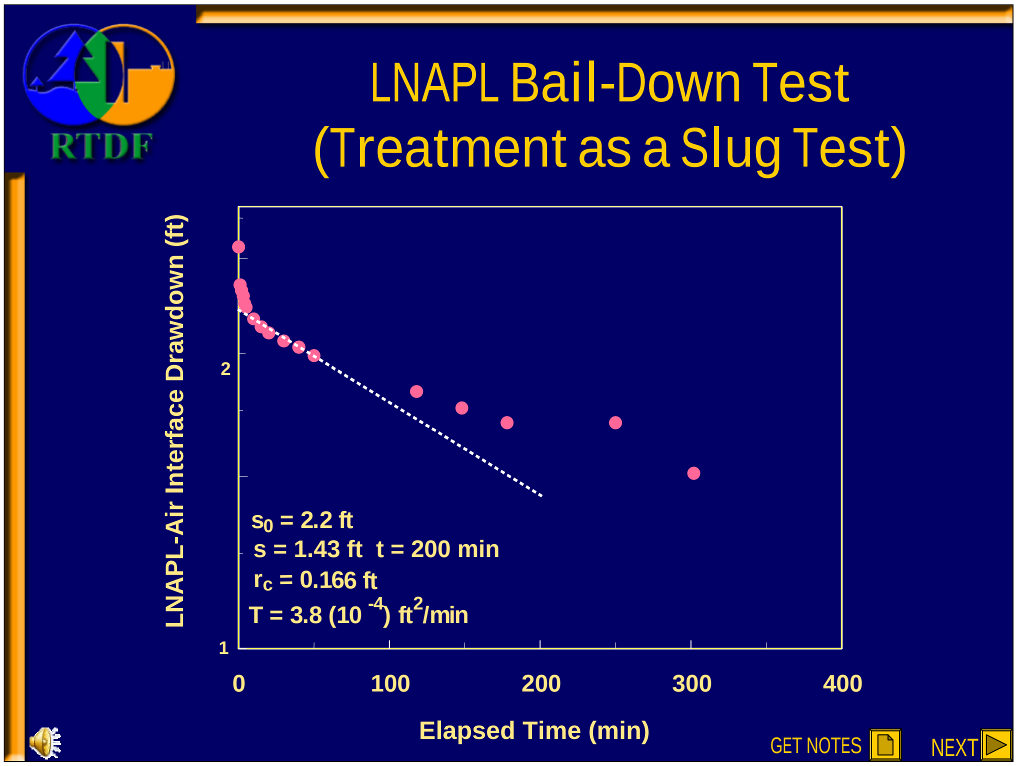

This analysis uses the Huntley method of plotting the LNAPL drawdown — that is, the original LNAPL elevation minus the subsequent elevation versus time.

With the **Bouwer and Rice** type of analysis of baildown or slug test data, the LNAPL transmissivity can be calculated.

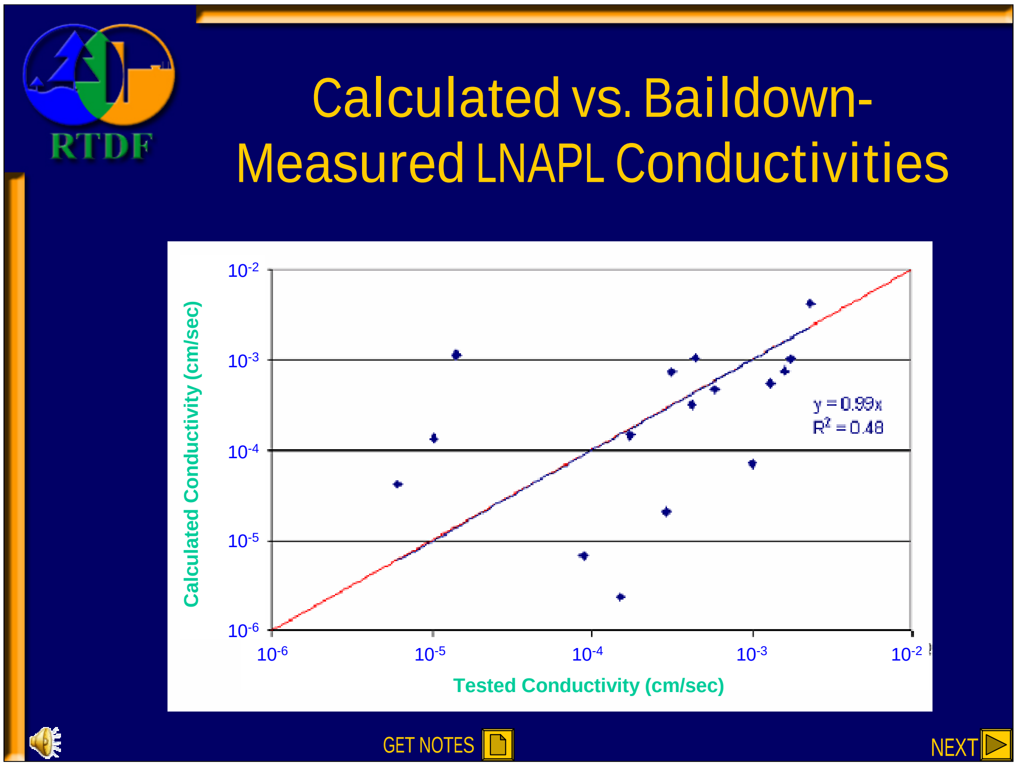

This graph illustrates the agreement we can expect between calculated and baildown-measured LNAPL conductivities. The calculated conductivities were obtained using site-specific capillary pressure and relative permeability data and the interpretation methods presented in this training. The scatter in data points is due largely to the varying distance between tested wells and the corresponding borings used for the calculated conductivities. Normal sampling, testing, and data evaluation factors also contribute to the scatter. Professional judgment needs to be used when interpreting these data.

It is also important to recognize that this methodology provides an estimate of LNAPL conductivity where none was available previously. The agreement shows that we can expect a reasonable <u>initial</u> conductivity prediction.

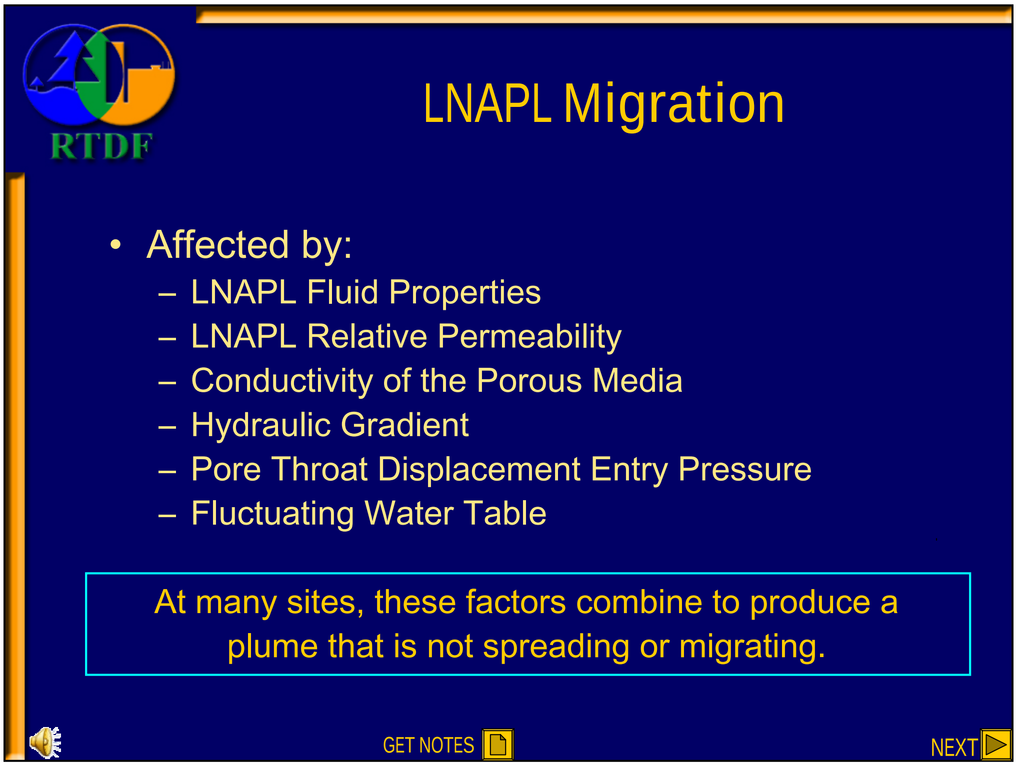

Now that we have discussed LNAPL conductivity, we can begin to look at the migration of the LNAPL phase.

LNAPL migration is affected by several factors, including its conductivity, the groundwater hydraulic gradient through **Darcy's Law**, the pore throat displacement entry pressure, and a fluctuating water table.

As we have just seen, LNAPL conductivity depends on its fluid properties, its relative permeability, and the conductivity of the porous media.

How pore throat displacement entry pressure and a fluctuating water table affect LNAPL migration may be less well understood. Recall from the capillary pressure curves that a certain pressure needs to be applied to the LNAPL for it to move through a pore throat. This is called the displacement entry pressure. If the upgradient pressure is not sufficient at the leading edge of a plume to force LNAPL through the pore throats in the media, the LNAPL cannot migrate.

In a clean coarse sand, the displacement entry pressure is lower, and the plume can spread more easily. In a very fine grained media, the displacement entry pressure can be quite high and effectively prevents the LNAPL from migrating.

A fluctuating water table can prevent the LNAPL from migrating because, as the water table rises, the LNAPL can become trapped as residual. This effect will be illustrated shortly.

At many sites where releases have been stopped, these factors combine to produce a plume that is not spreading or migrating. This has been illustrated in previous slides. In addition, case study #5 (slides 100-106) demonstrates that LNAPL plumes do not continue to migrate after some initial period.

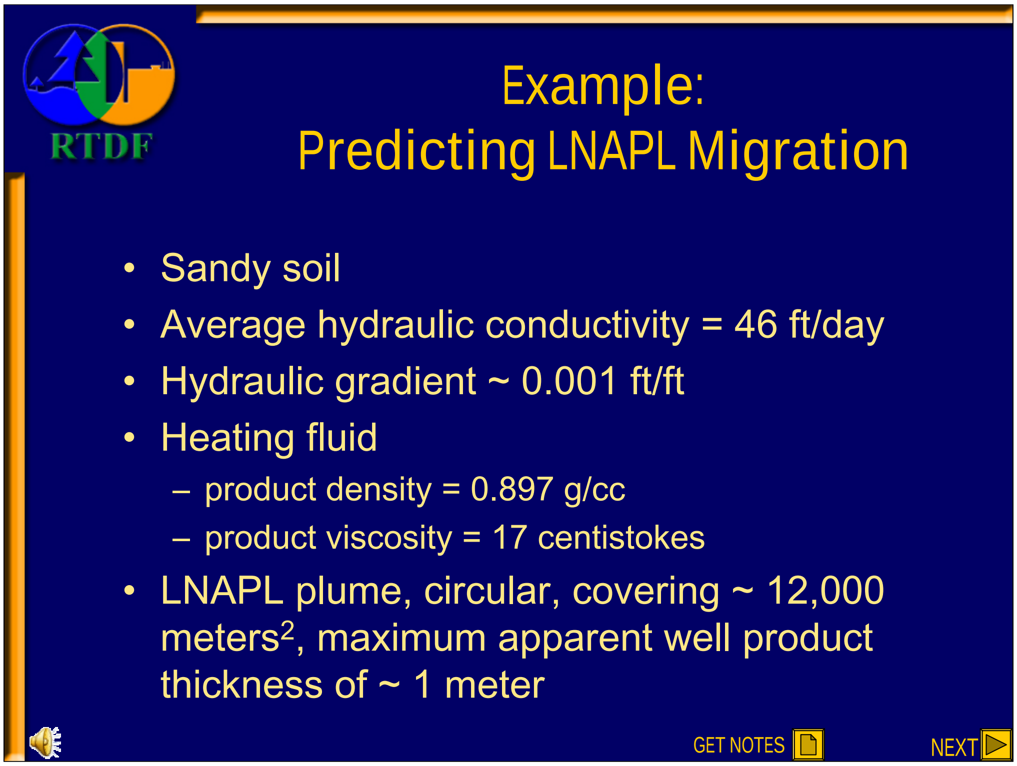

In this example, a numerical model is used to predict the potential migration of an LNAPL plume.

The soil is a sand with a high conductivity of 46 ft/day. The hydraulic gradient is about 0.001 ft/ft, so we would expect that groundwater would move about 35 ft/yr, assuming a porosity of about 0.5. Not a high velocity.

The LNAPL is a heating oil with a density of 0.897 and a viscosity of about 20 times that of water. You can see the plume size on the next slide.

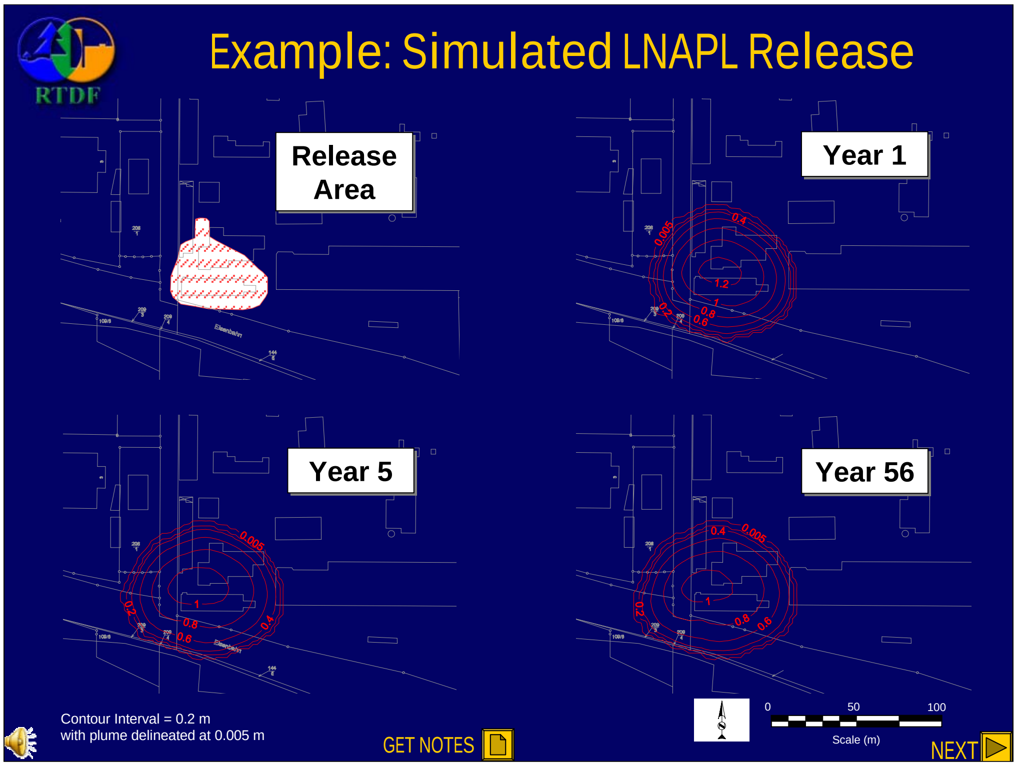

This figure shows the simulated migration of a plume of about 1,500 m^3 of LNAPL over 56 years. The images represent predicted well-product thickness measurements. While growth in the plume from release to Year 1 is clear, the plume appears to grow only slightly over the next 56 years.

Certainly, the small gradient, which produces a low groundwater flow rate, has had an effect, but groundwater has moved about 600 meters over the 56 years. The LNAPL plume, however, has not.

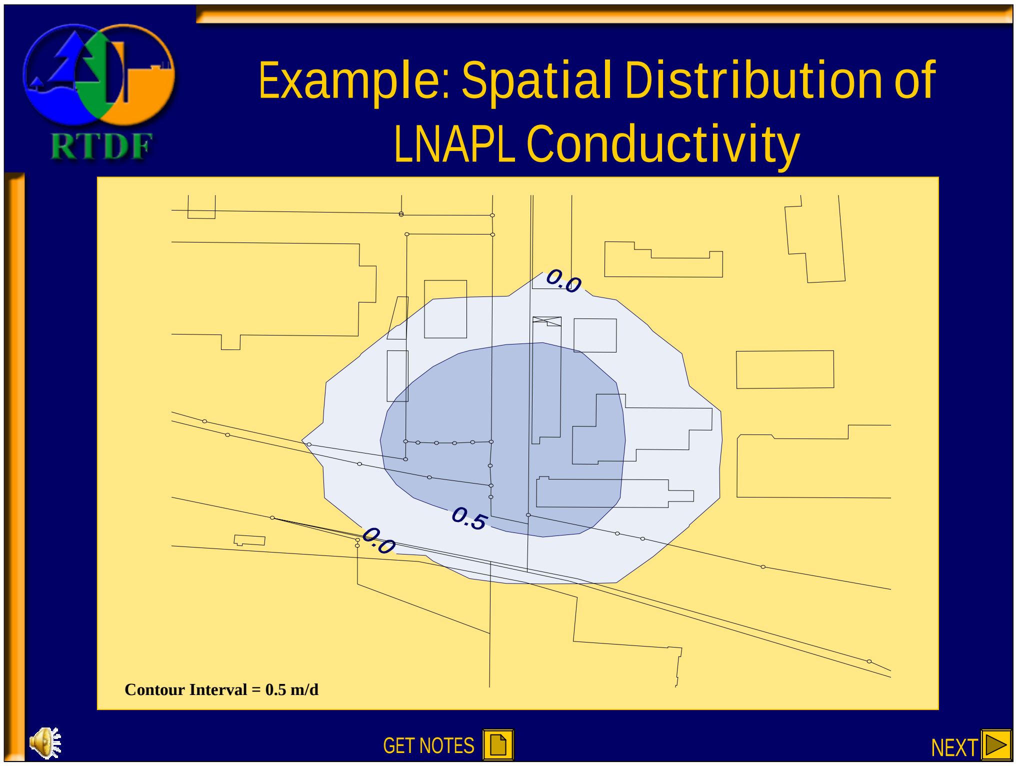

This slide shows the conductivity of the LNAPL. Note that there is LNAPL conductivity in the center, where LNAPL saturation is greater than residual saturation (and thus relative permeability is greater than zero). However, no conductivity is apparent at the edge where LNAPL saturation is less than or equal to residual saturation. Thus, a well at the center of the plume would be more likely to contain LNAPL that is recoverable than a well near the edge of the plume.

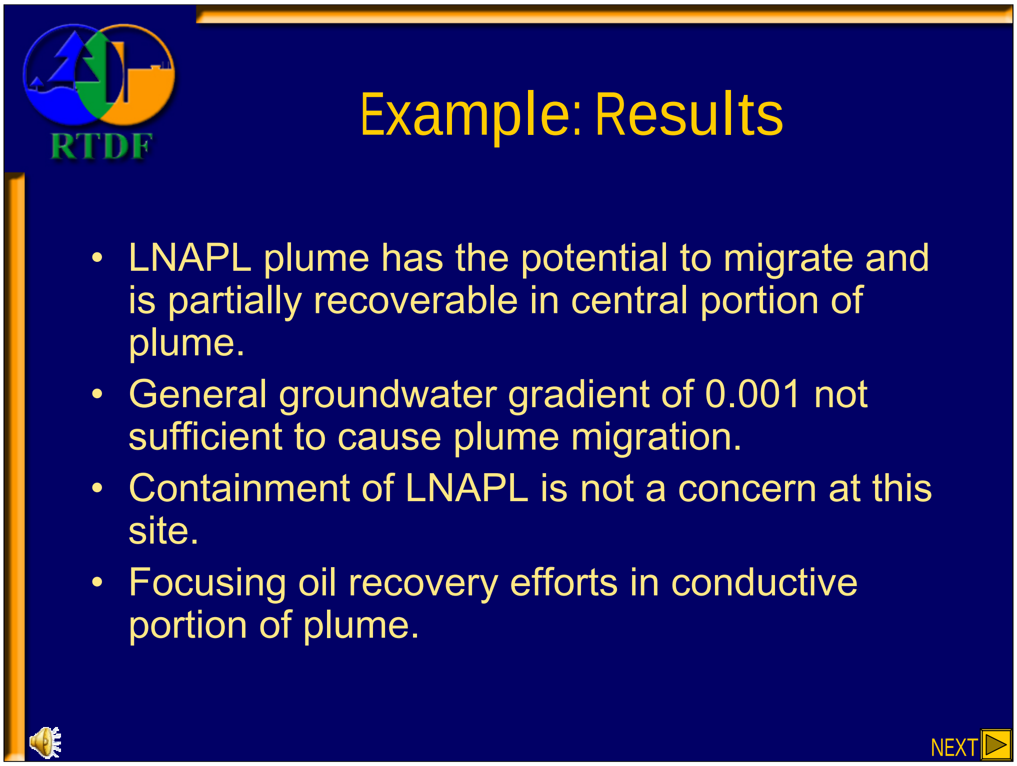
RTDF
Example: Results
• LNAPL plume has the potential to migrate and is partially recoverable in central portion of plume.
• General groundwater gradient of 0.001 not sufficient to cause plume migration.
• Containment of LNAPL is not a concern at this site.
• Focusing oil recovery efforts in conductive portion of plume.
NEXT

Read slide.

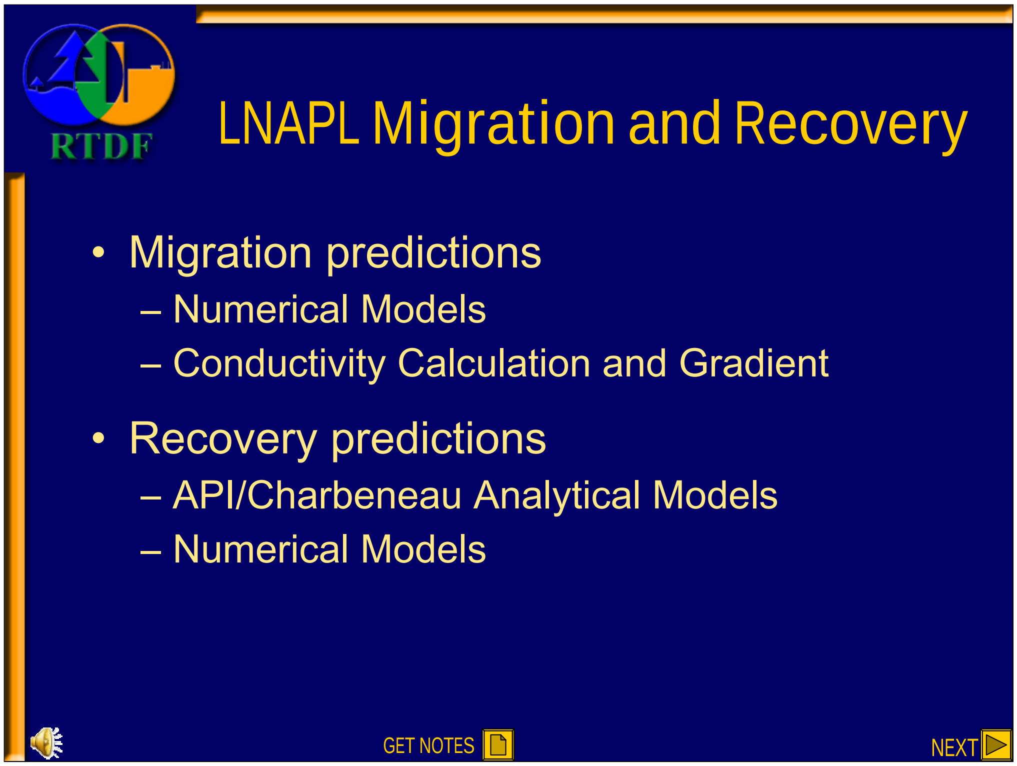

The spreading of LNAPL plumes can be predicted using numerical models, such as the **Areal Multiphase Organic Simulator (ARMOS)** or the **Multiphase Areal Remediation Simulator (MARS)**. These can be obtained from vendors.

The **Hydrocarbon Spill Screening Model (HSSM)** also can be used. HSSM depends upon the head pressure in the LNAPL (due to the connectivity of the LNAPL in the vadose zone), the thickness at the water table, and the conductivity of the LNAPL. At the edges of the spreading LNAPL, it also depends upon the displacement head pressure, which affects the LNAPL's ability to enter a pore.

As with many numerical models, HSSM is difficult to run. Using a simplified calculation method is an alternative. This would involve using capillary pressure and relative permeability data combined with fluid-level gauging measurements from wells within the LNAPL plume. In theory, as LNAPL thickness decreases toward the edge of the plume, the calculated LNAPL seepage velocity would approach zero. This is conservative, since it does not account for the need to overcome the displacement head pressure. To account for displacement entry pressure, fluid-level data can be used to estimate whether the plume is stable or potentially migrating (i.e., whether sufficient driving force, or "head," exists within the plume to overcome displacement pressure head at the edge of the plume).

We also can use simple analytical models or more complicated numerical ones to make recovery predictions, which we will discuss next. The analytical models are based on the same assumptions and concepts as HSSM, but incorporate them into spreadsheets for ease of use. Several numerical models are available, but they are difficult to run. Generally, they are used by experts dealing with complex situations. All of these models deal with liquid flow. Only a few include vapor or air flow, and they have some limitations and instabilities when the simultaneous movement of air, LNAPL, and water is simulated.

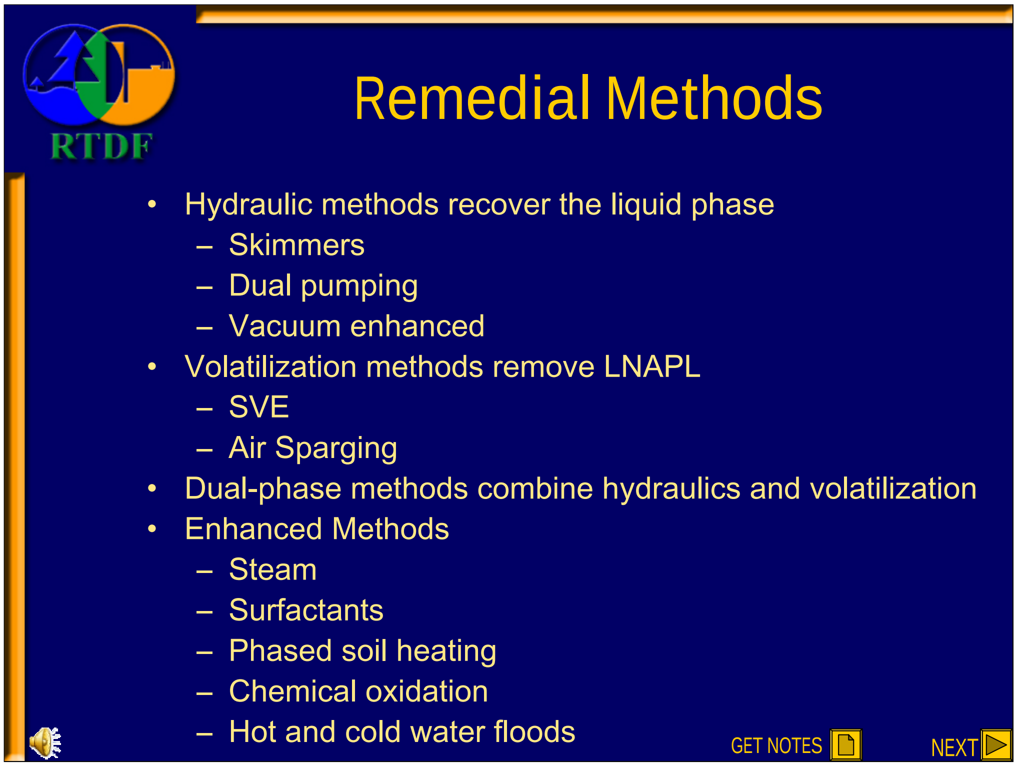

There are many remedial methods for removing LNAPL, and they can be grouped as shown.

Hydraulic methods, such as skimmers, dual pumping, and vacuum enhanced, recover only the liquid-phase LNAPL present in the well by mechanical removal. Volatilization methods, such as soil vapor extraction (SVE) and air sparging, remove the LNAPL by volatilizing the liquid phase and capturing it as a vapor. Dual-phase methods, such as vacuum trucks, combine hydraulic methods for liquid-phase removal with volatilization methods for vapor removal.

These technologies can be enhanced to allow for removal of greater amounts of LNAPL. For example, steam reduces LNAPL viscosity and increases its volatilization. Surfactants reduce interfacial tension and allow residual LNAPL to escape from the small pores and flow to a capture zone. In addition to reducing interfacial tension, surfactants (and cosolvents) increase solubility and enhance LNAPL removal via dissolution.

For most enhanced remedial methods, the prediction of recovery is not currently possible; however, predictions can be made for hydraulic methods.

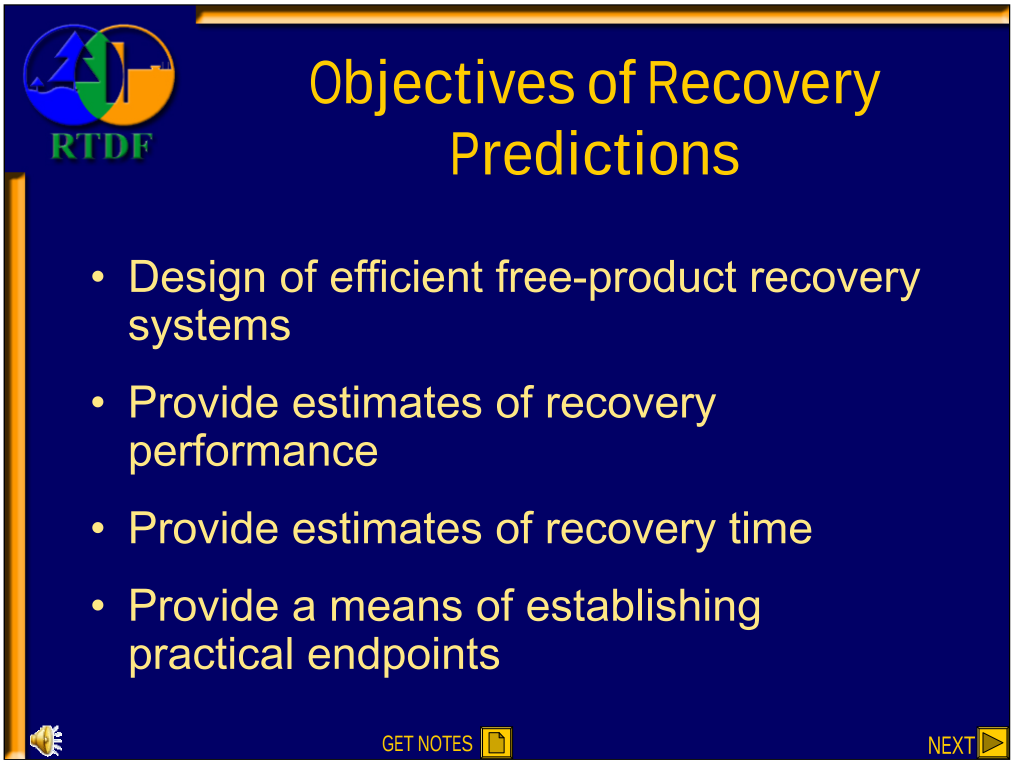

The objectives of recovery predictions are to:

• Design efficient free-product recovery systems using trenches, skimmer wells, and single- and dual-pump wells;

• Provide estimates of recovery performance;

• Provide estimates of recovery time; and

• Provide a means of establishing practical endpoints.

In the next few slides, we will describe recovery predictions using analytical models. This discussion will help clarify the relationship between the porous media and fluid properties and the understanding developed earlier.

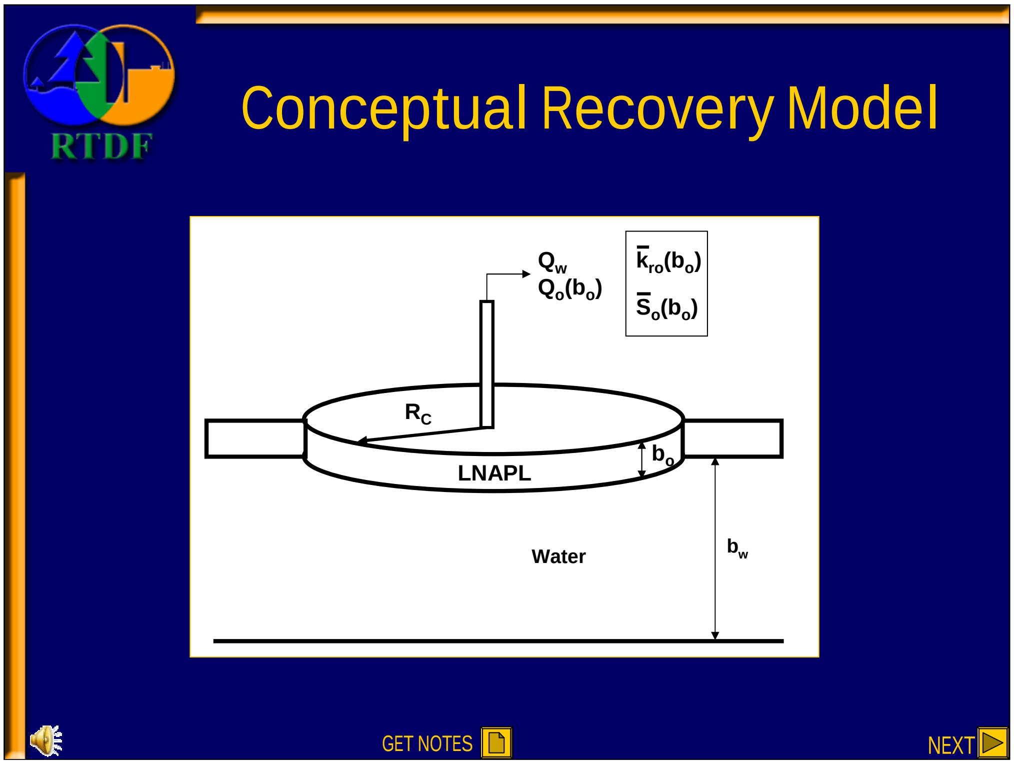

This simple picture is used to show the important parameters that affect recovery. While the analytical models seem to revert to a "pancake model" type at first glance, this is just for illustrative purposes.

These parameters include: The radius of capture (R_c), or the radius of LNAPL that can flow into the well, and the extraction rates for water (Q_w) and air (Q_o) from the well. Note that, for skimmers with no vacuum enhancement, the air and water extraction rates are zero.

As we know from the previous discussion of conductivity, the relative permeability (k_{ro}) and saturation (S_o) are important. Finally, the monitoring well thickness (b_o) and the thickness of the saturated zone (b_w) also are needed.

What is not explicitly shown on the figure is the residual saturation in the vadose and saturated zones.

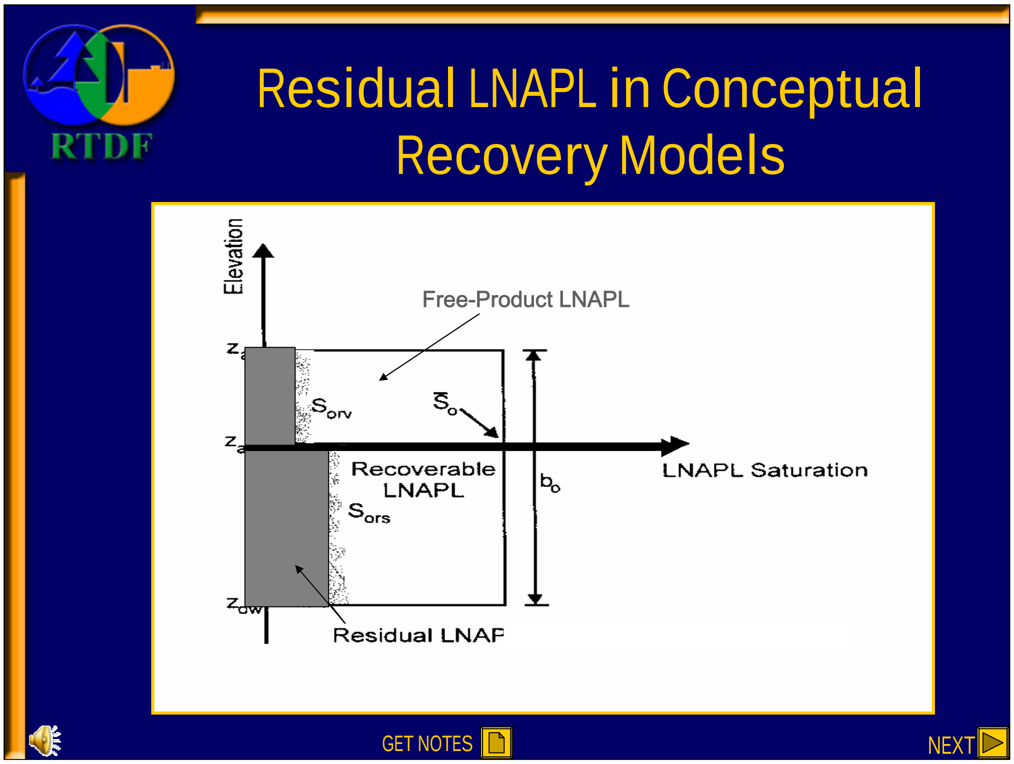

In recovery models, the residual saturations in the vadose and saturated zones are added to the distribution calculated using the capillary pressure curves, the fluid properties, and the monitoring well thickness. In essence, the calculated LNAPL distribution in the subsurface is shifted to a higher saturation equivalent – the S_{ors} in the saturated zone, or the S_{orv} in the vadose zone.

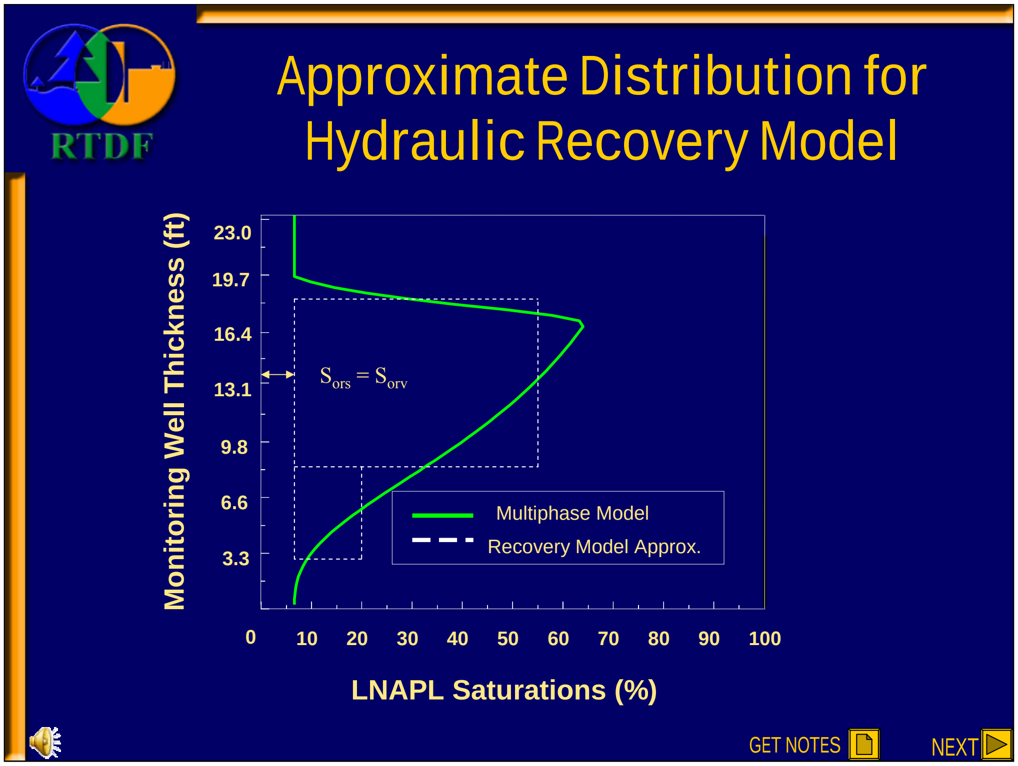

On a previous slide, we used a “pancake” figure for illustrative purposes. For actual recovery predictions, the distribution of LNAPL is approximated by a series of pancakes.

Shortly, we will see how this is related to the capillary pressure and the LNAPL distribution. In this figure, it is assumed that the residual saturation in the saturated and vadose zones is the same; however, this is not generally the case.

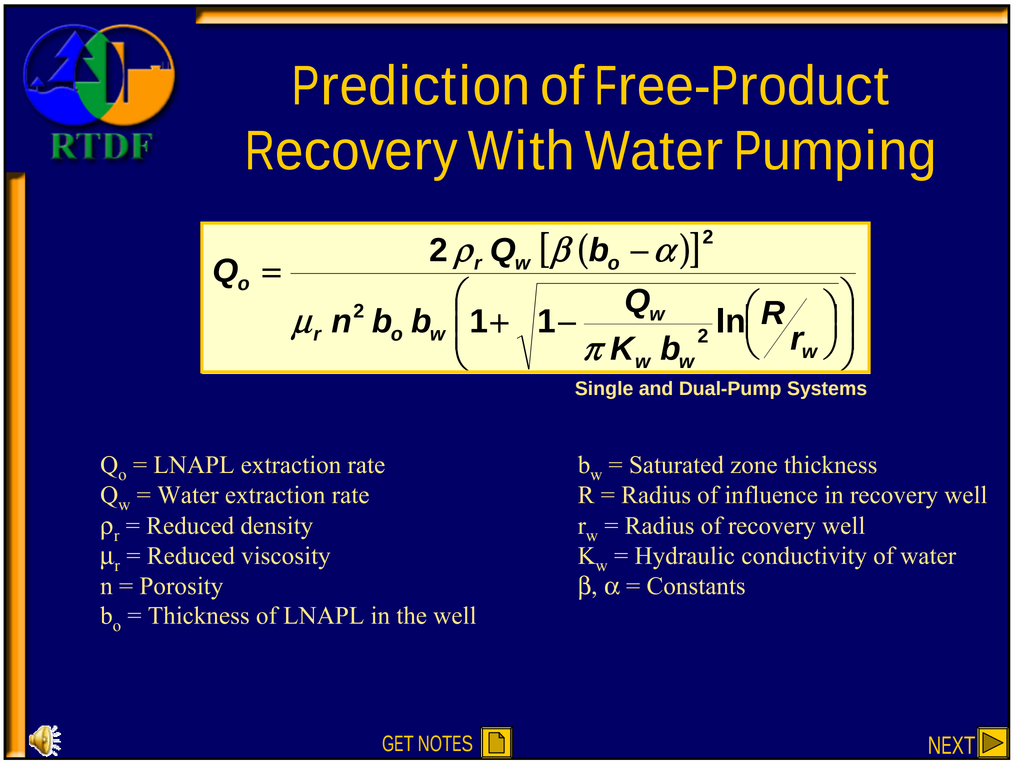

This slide presents the analytical expression for hydraulic LNAPL recovery by a dual-phase LNAPL/water pumping system. It can be easily incorporated into a spreadsheet.

Q_o = the LNAPL extraction rate;

Q_w = the water extraction rate;

rho $(\rho)_r$ = the reduced density (defined by the density of LNAPL divided by the density of water);

mu $(\mu)_r$ = the reduced viscosity;

n = the porosity;

b_o = the thickness of LNAPL in the monitoring well;

b_w = the saturated zone thickness;

R = the radius of influence of the recovery well;

r_w = the radius of the recovery well;

K_w = the hydraulic conductivity of water.

Beta (β) and alpha (α) are constants (related to the size of the series of pancake slices on a previous slide). In this equation, LNAPL recovery is determined by water drawdown. Water drawdown is determined by water production, and there is a weak dependence on aquifer hydraulic conductivity.

From this relatively simple equation, it is easy to see the expected effects of various parameters on the LNAPL recovery. For example, the viscosity of the LNAPL occurs in the denominator and is inversely proportional to the LNAPL recovery rate. In other words, if LNAPL viscosity increased by a factor of three, we could expect the LNAPL recovery rate to be reduced by a factor of three, and the time required to recover an equivalent amount would be increased by a factor of three.

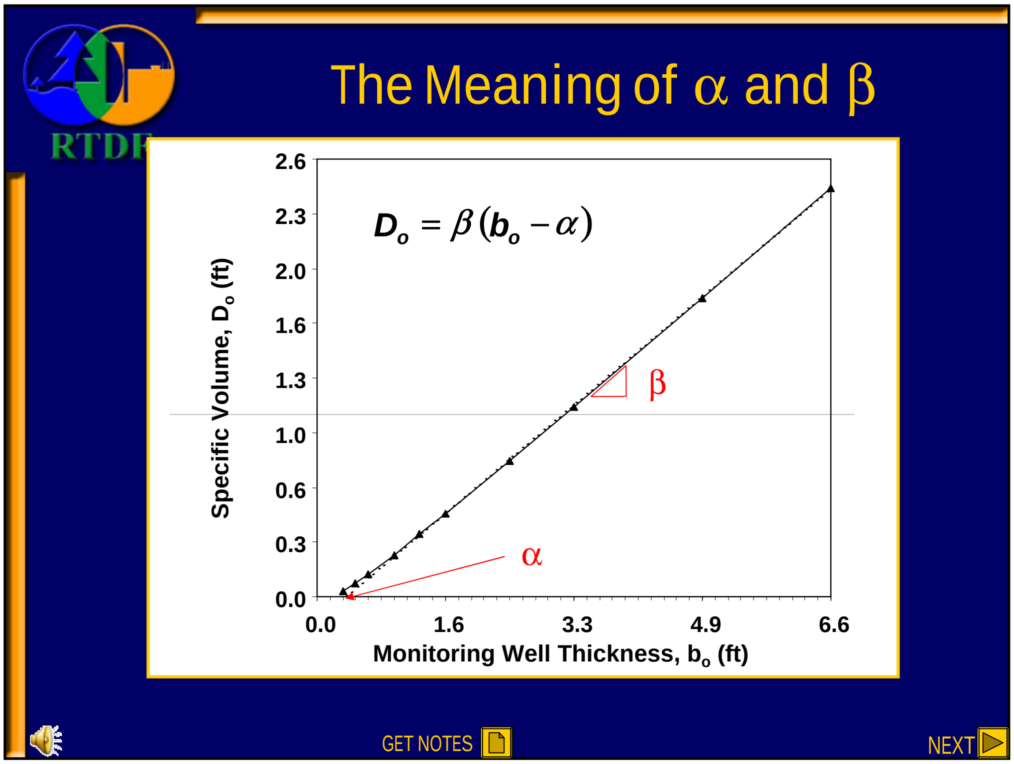

The solid curve in this figure relates LNAPL thickness in the monitoring well to the specific volume, or formation free-product volume.

Recall that this is calculated by integration under the LNAPL distribution curve calculated from the capillary pressure curve for specific fluid pairs.

The curve can be approximated by a series of straight lines. Each of the straight lines defines the thickness of a pancake slice. This is the source of the α and β values discussed on a previous slide, and one can now see how the recovery is related to the distribution of the LNAPL in the subsurface.

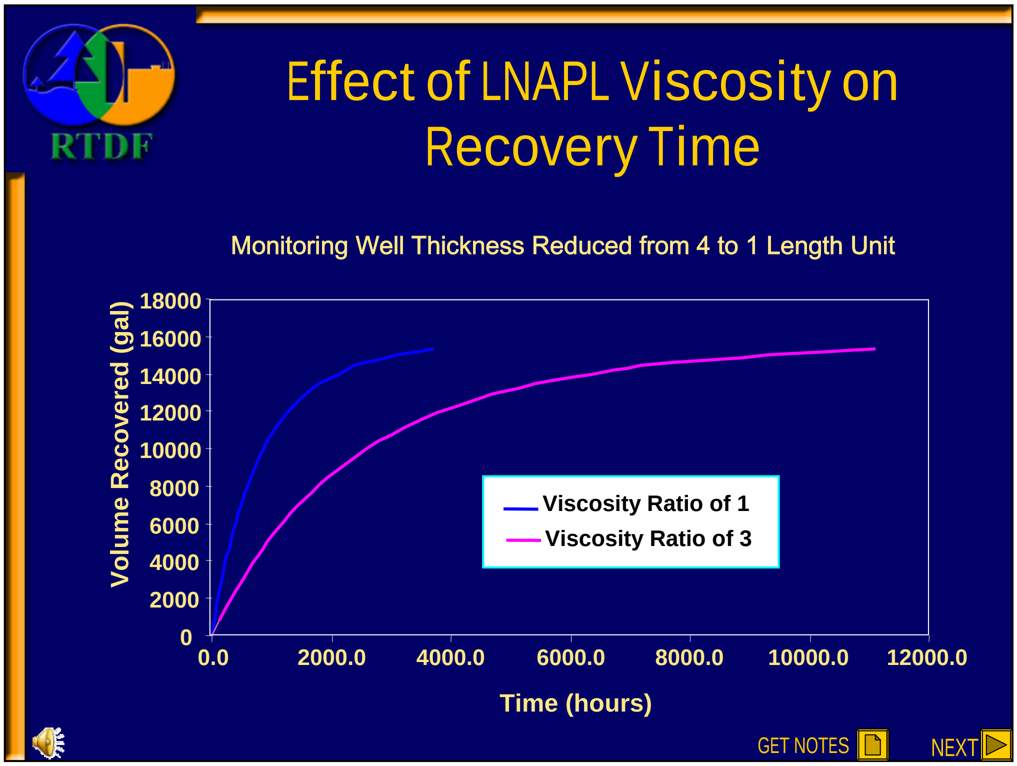

In the expression for LNAPL recovery, the rate of recovery was inversely proportional to the viscosity of the LNAPL.

This graph shows volume recovered versus time for two LNAPL products with different viscosities. The lower curve is for a product with a viscosity 3 times that of the one represented by the upper curve.

To recover 14,000 gallons of low-viscosity product, it takes 2,000 hours. To achieve the same recovery for the product with a viscosity 3 times higher, it would take about 6,000 hours, a threefold difference.

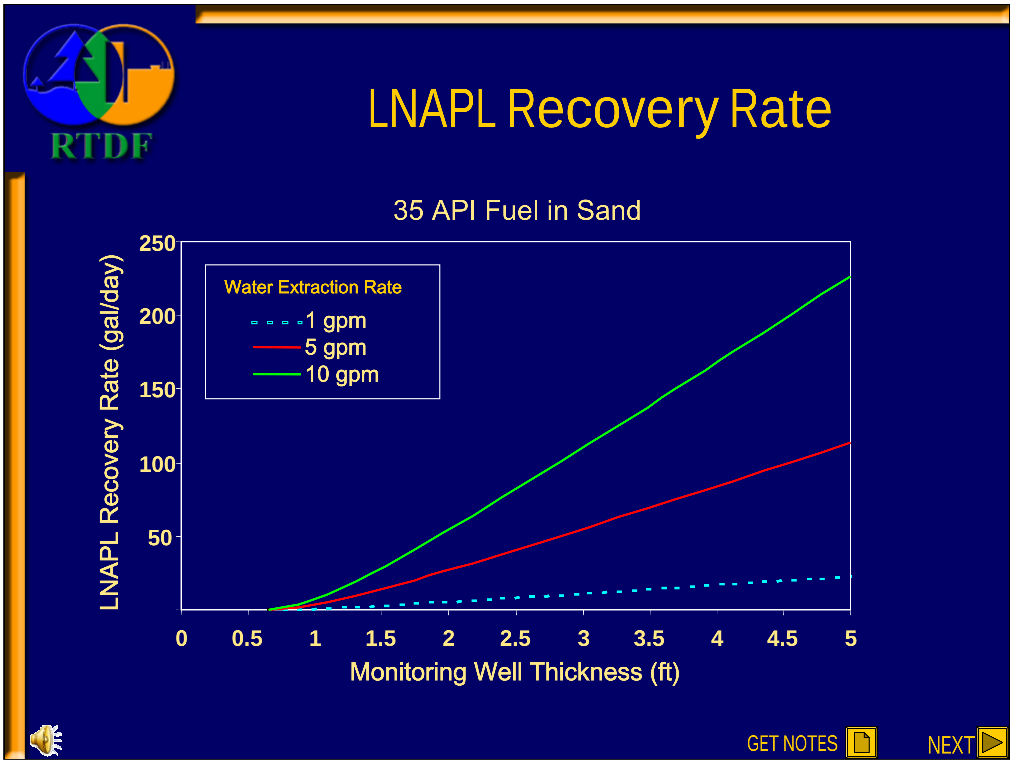

This slide plots the LNAPL recovery rate for a 35 API fuel (fresh diesel) in sandy soil versus time at various water-extraction rates. As the water extraction rate increases, the LNAPL recovery rate also increases.

Again, this follows from the expression for LNAPL recovery given earlier.

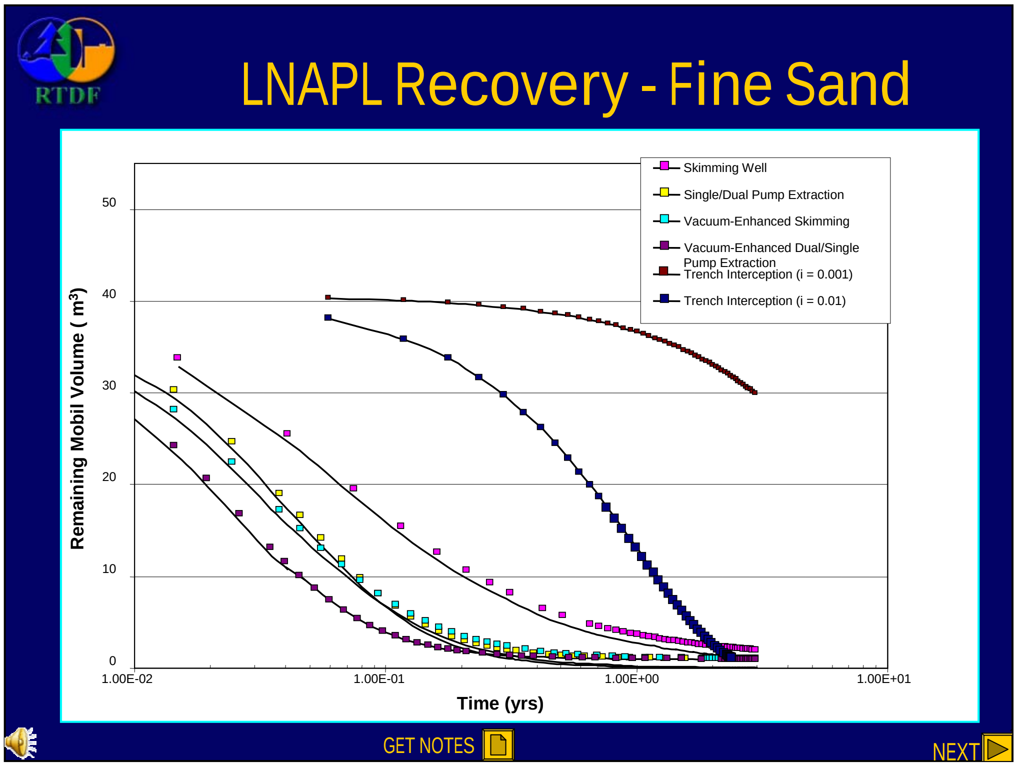

This figure illustrates the comparison of recovery predictions that can be made using the API spreadsheets.

This figure shows the remaining volume of mobile or recoverable LNAPL as a function of time for various hydraulic recovery techniques. Note that the application of vacuum is generally beneficial, because it increases the gradient toward the recovery well. The slowest is an interceptor trench that recovers LNAPL that has migrated to the trench due to only the natural gradient of the air-LNAPL interface.

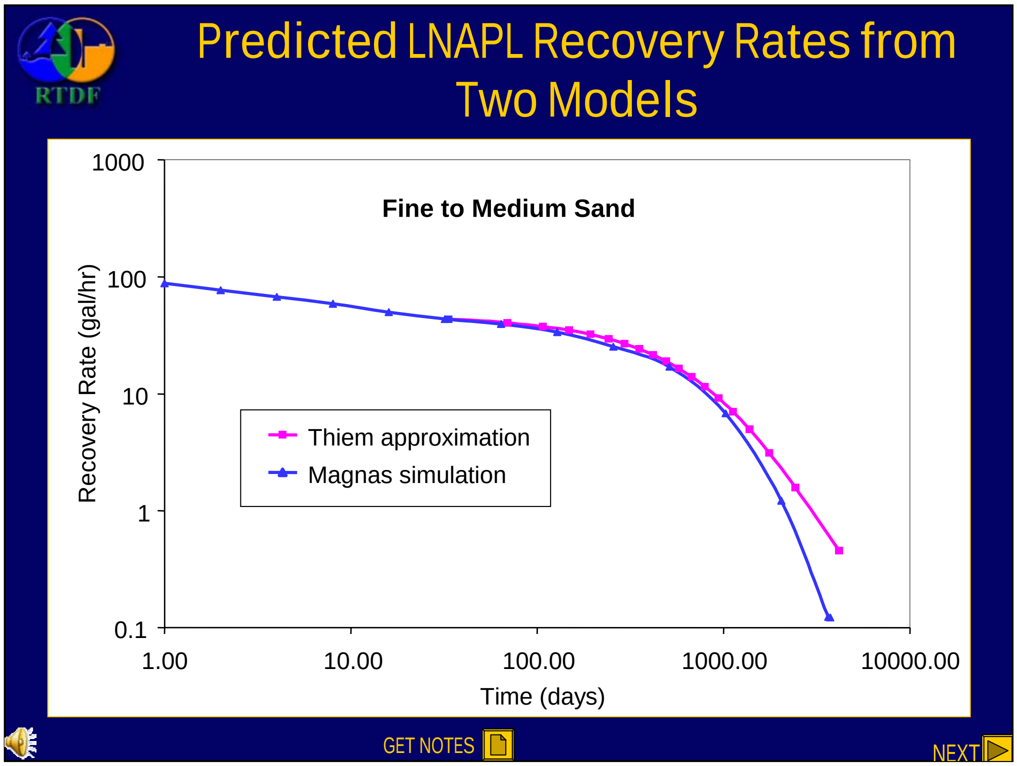

This figure shows a comparison of predicted recovery rate versus time from an analytical model (the **Thiem Approximation**) and a complex numerical model (the **Magnas Simulation**). In this fine sand, the comparison is quite good; in finer grained material, the comparison is not so good.

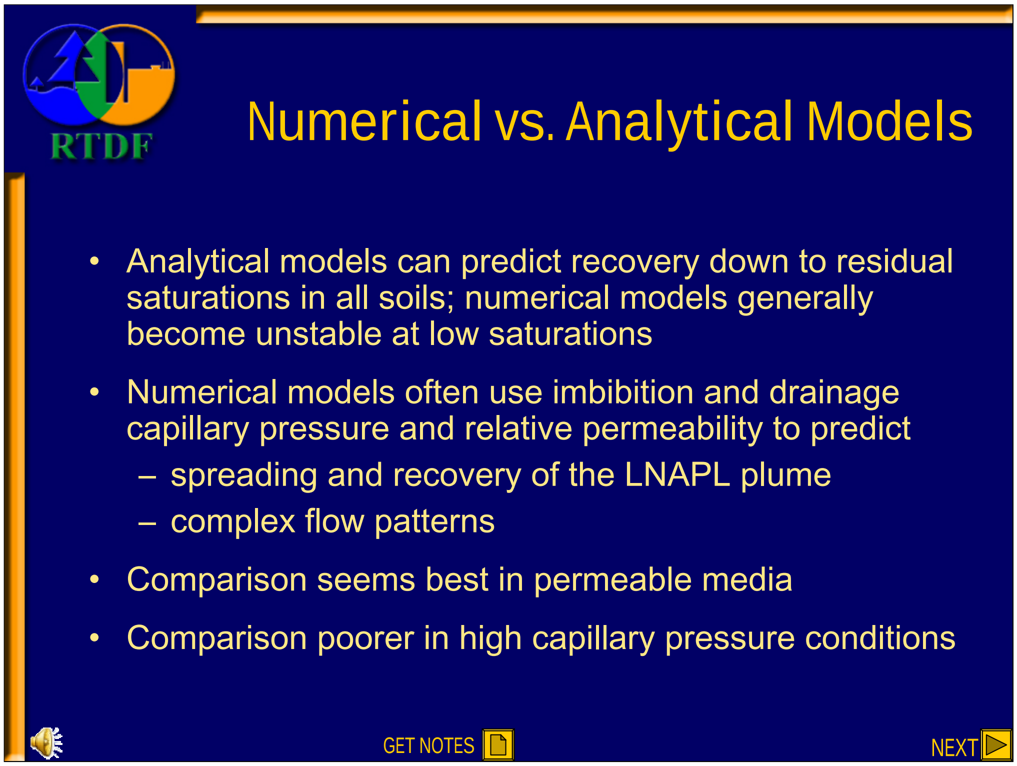

There has been limited comparison between the analytical models derived by **Charbeneau** and the various numerical models put forth. To date, none of the comparison studies have been published. The following statements are made, based on experience, but they are not likely to hold with all models in all media.

- Analytical models can predict recovery down to residual saturations in all media.
- Numerical models generally become unstable at low saturations. Numerical models often use imbibition and drainage capillary pressure and relative permeability to predict spreading and recovery of the LNAPL plume and complex flow patterns.
- The comparison of analytical and numerical models seems best in permeable media. The comparison is poorer in high capillary pressure conditions.
- We do not know whether analytical or numerical models will provide the more accurate predictions without calibration; it probably depends on the conditions.

It is likely that both analytical and numerical models can make good predictions, provided that field conditions do not violate the assumptions of the models and that proper calibration is made.

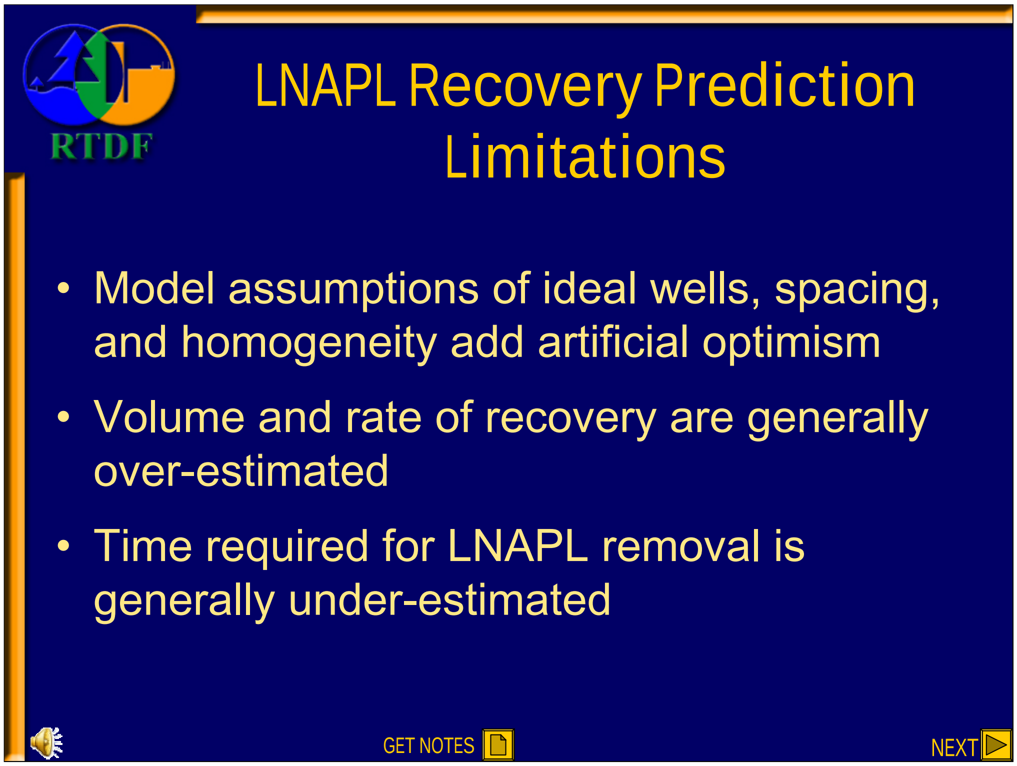

Predicting LNAPL recovery has several limitations.

The models assume ideal wells, spacing, and homogeneity, all of which add artificial optimism.

Generally, we would expect predictions to over-estimate the volume and rate of recovery. On the other hand, they generally under-estimate the time required to remove the LNAPL.

Predicted LNAPL saturations, conductivities, and recoverability should be compared to field measurements whenever practical. This will provide confidence in the predictions.

Some of this will be illustrated in the real-world case studies that we will discuss at the end of the course.

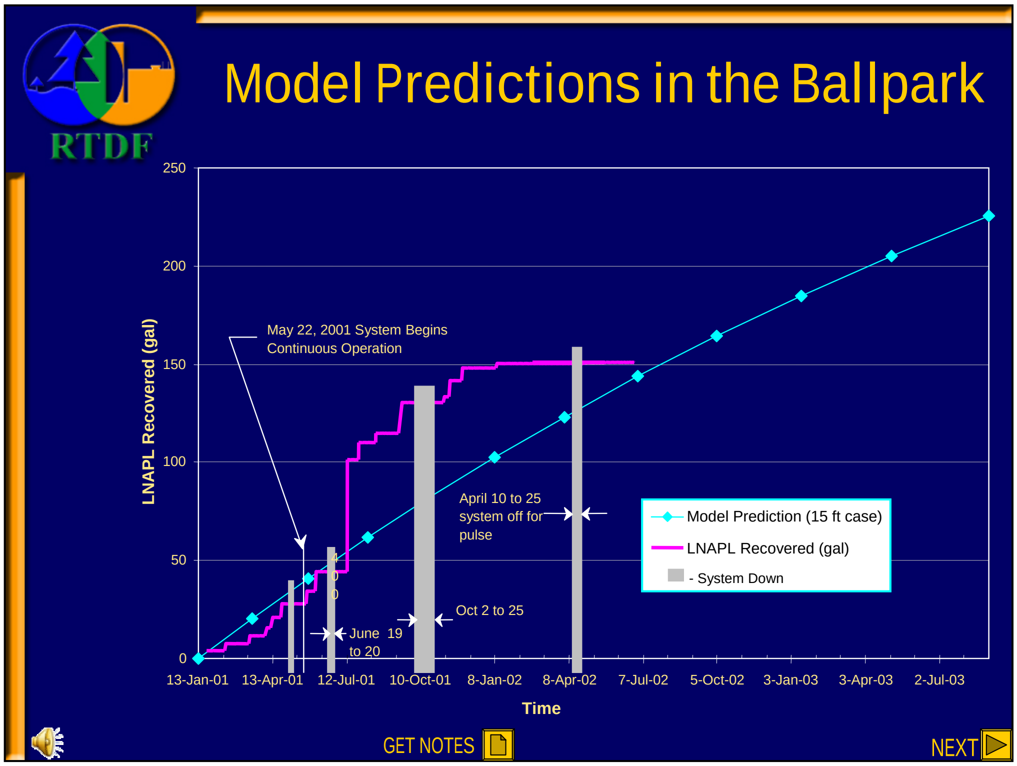

Even though there are limitations, model predictions are generally "in the ballpark."

This is a plot showing the LNAPL recovered from a very tight soil over a period of time. It compares the recovery predicted with a model (the smooth blue curve) with the actual measured recovery (the dark pink curve). This example involves a vacuum-assisted skimming system, which can be modeled using the API equations.

The LNAPL in this example is a degraded diesel with few light ends, so there is only liquid recovery and no vapor recovery. Despite the fact that the recovery is not smooth, there is very good agreement between the predicted and actual recoveries.

It is worth noting that this recovery prediction was made with no calibration of the model. This comparison gives us confidence that our new understanding and quantitative calculations are providing a sound basis for understanding the distribution and movement of LNAPL and its potential for recovery.

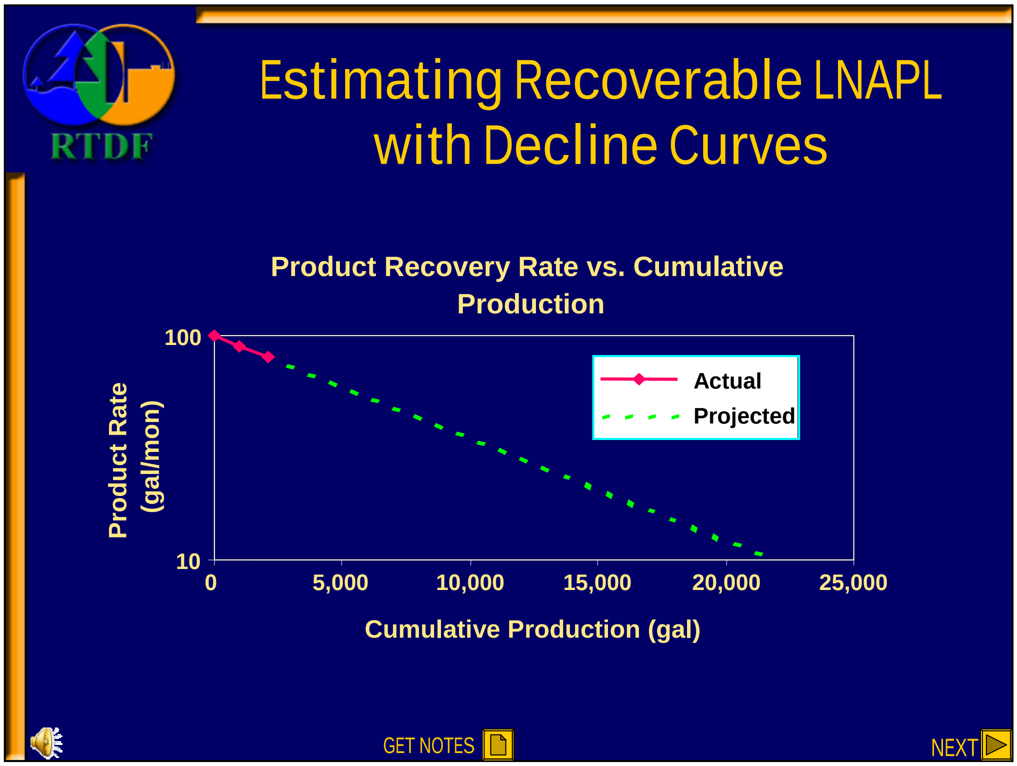

Obtaining the parameters for running the API spreadsheets can be quite costly and will require specialized training and good judgment. In the absence of running models, the petroleum industry has developed graphical techniques for evaluating recovery well performance.

Decline curve analysis is a standard method in petroleum engineering for estimating total recoverable LNAPL and evaluating well performance. It involves plotting LNAPL recovery rate versus cumulative recovery, as shown in this slide. We offer it as a tool that experienced professionals find useful. The details of the technique can be found in the *Petroleum Engineering Handbook*.

In a mature LNAPL recovery system (a system that has been fully developed and operates efficiently), there is a linear relationship between LNAPL recovery rate and cumulative recovery on a semi-log plot of LNAPL recovery rate versus the cumulative recovery.

Deflections from an established straight-line decline curve indicate changes to the recovery system. Theoretically, a recovery-rate trend that falls below the established decline would suggest a decrease in efficiency or problems with the system (e.g., fouling of recovery wells, pump problems, or wells being taken off line). A trend that rises above the established decline generally indicates an increase in recovery capacity (e.g., adding new wells, larger pumps, or well-stimulation treatments). It is important to recognize that, although these changes affect the rate of recovery, they do not change the volume of recoverable LNAPL. For example, if an older recovery well is rehabilitated, the rate of recovery will increase. Once a new straight-line trend is established for the well, the decline rate will be steeper and will project out to the same ultimate recoverable volume. Well stimulation will only shorten the recovery time.

The value for ultimate recoverable LNAPL is obtained by extrapolating the straight-line function to some practical endpoint value of LNAPL recovery rate.

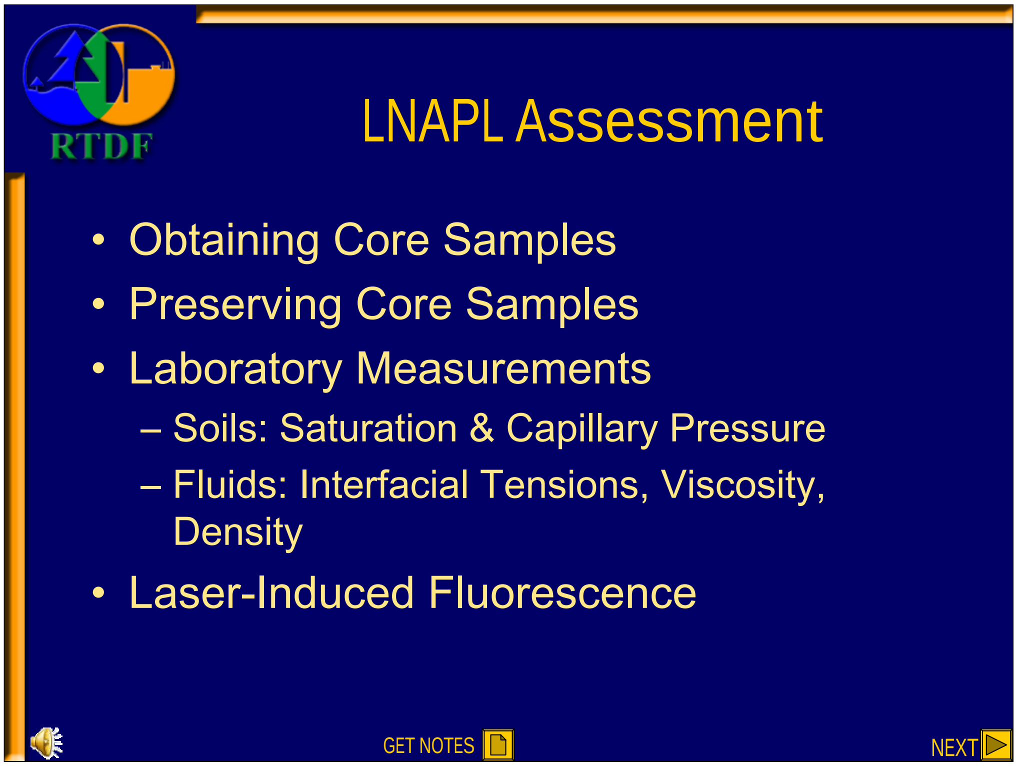

Now that you have a basic understanding of LNAPL behavior in the subsurface, let's move on to discuss some of the methods and techniques available to help in assessing a LNAPL site. These include methods for obtaining and preserving core samples, laboratory methods for soils and fluids, and a technique known as **laser-induced fluorescence (LIF).**

LIF can provide a semi-quantitative vertical distribution of LNAPL occurrence. LIF response is a function of media and LNAPL properties, and some experts have correlated LIF response and LNAPL saturation.

Solid media and fluid property measurements from **ASTM International**, API, and other organizations can provide additional information and are available on the API web site at www.api.org/lnapl.

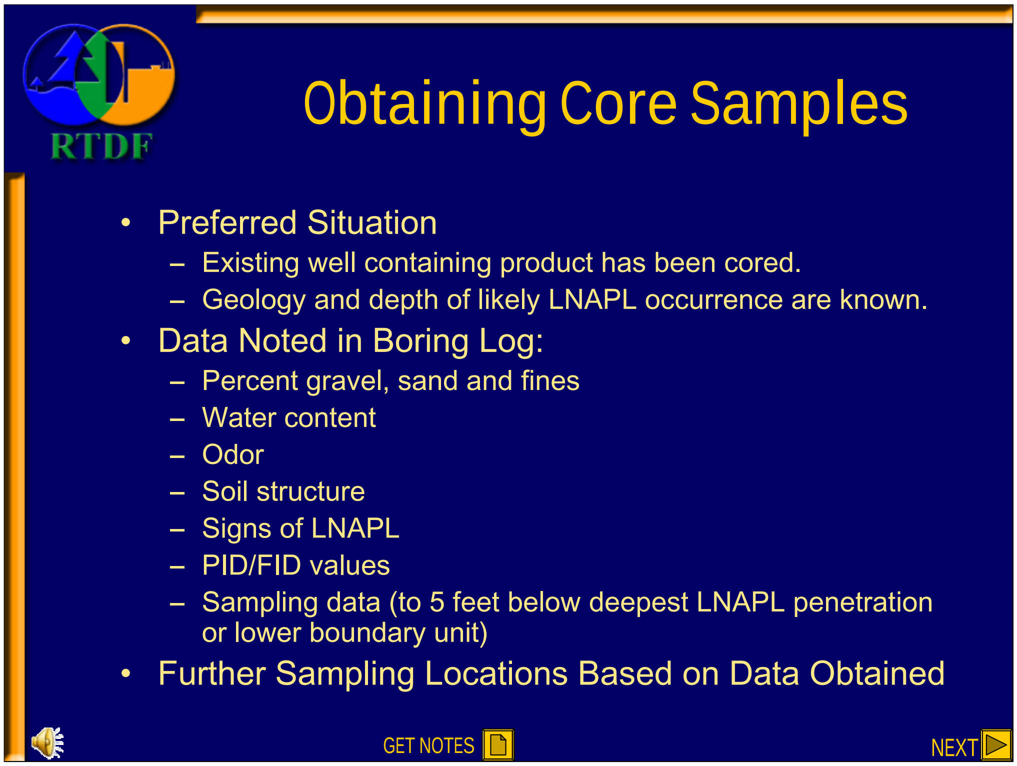

Core samples should be obtained for measuring LNAPL saturation, capillary pressure, and, in some cases, relative permeability. Cores can be photographed to study the heterogeneities and location of LNAPL. (LIF and **cone penetrometer technology**, or CPT, data also can be used to locate LNAPL and study media heterogeneity.)

The procedure outlined in the next three slides is for an **ideal** situation, one in which there are no cost restrictions. Using this procedure, the cost for a couple of borings with the associated core and fluid property tests is likely to be at least $5,000.

Bringing undisturbed cores to the surface, especially in coarser-grained materials, can be very difficult. Taking extra care to recover good cores can help you manage cost. Although large diameter cores (about 3-inch) are preferred, ¾-inch acetate sleeves with direct push techniques or using more sophisticated core retrieval devices, such as a piston, Denison, or Pitcher sampler, may provide the best means of good core recovery at such sites. Site-specific experience is invaluable in determining the best method. Fluid loss may be an issue and also should be considered both prior to core sampling and in subsequent analysis. In general, however, predicted LNAPL saturations have been in good agreement with measured LNAPL saturations, so loss of LNAPL does not appear to be a significant problem. There is some speculation that the low conductivity of LNAPL in many situations minimizes its loss during core-obtaining activities.

The preferred situation, as shown above, is one in which an existing well containing product has been cored, and the geology and depth of likely LNAPL occurrence are known. You might obtain information on LNAPL depth of occurrence from a high **photoionization detector (PID)**/**flame ionization detector (FID)** reading.

If this is not the case, a very careful boring log should be produced noting the percent gravel, sand, and fines; the water content; the odor; the soil structure; and signs of LNAPL. PID/FID values also should be noted. (The frequency of PID/FID data collection is up to the site geologist, who responds to field conditions.) Core samples should be taken to at least 5 feet below depth of LNAPL penetration or until a very competent lower boundary unit is encountered. (Sometimes, LIF is used instead of boring.)

Use the information gathered to decide the location for additional boring or use of another "undisturbed" sampling method (e.g., Shelby Tube samples) across the area of LNAPL impact. For shallow investigations (<50 feet), dual-tube direct push rigs also may be an efficient way to collect continuous cores.

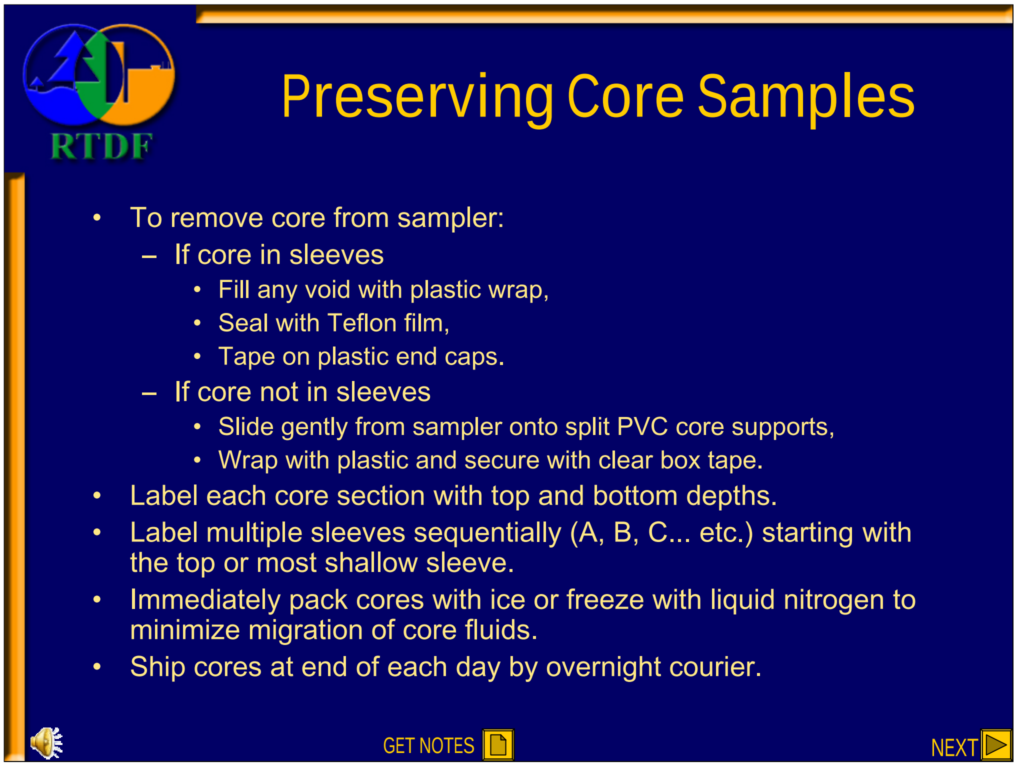

Typically, cores are preserved following the procedure outlined here; however, the procedure may vary, depending on the individuals and the laboratories involved.

To start, remove the core from the sampler as soon as possible. If the core is in sleeves, fill any void space with plastic wrap to minimize core movement. Seal the core with Teflon film and tape on plastic end caps. If the core is not in sleeves, gently slide it from the sampler onto split PVC core supports. Wrap the core with plastic wrap and secure it with clear box tape.

Each core section should be labeled with top and bottom depths. Fractions of a foot should be recorded in tenths. Multiple sleeves should be labeled sequentially (A, B, C, etc.), starting with the top or most shallow sleeve.

Place the cores in a cooler containing dry ice immediately to minimize the movement of core fluids. As alternatives, you can put the core into a cooler with frozen "Blue Ice" packs and foam packing material, or you can freeze it with liquid nitrogen.

Ship the cores at the end of each day by overnight courier.

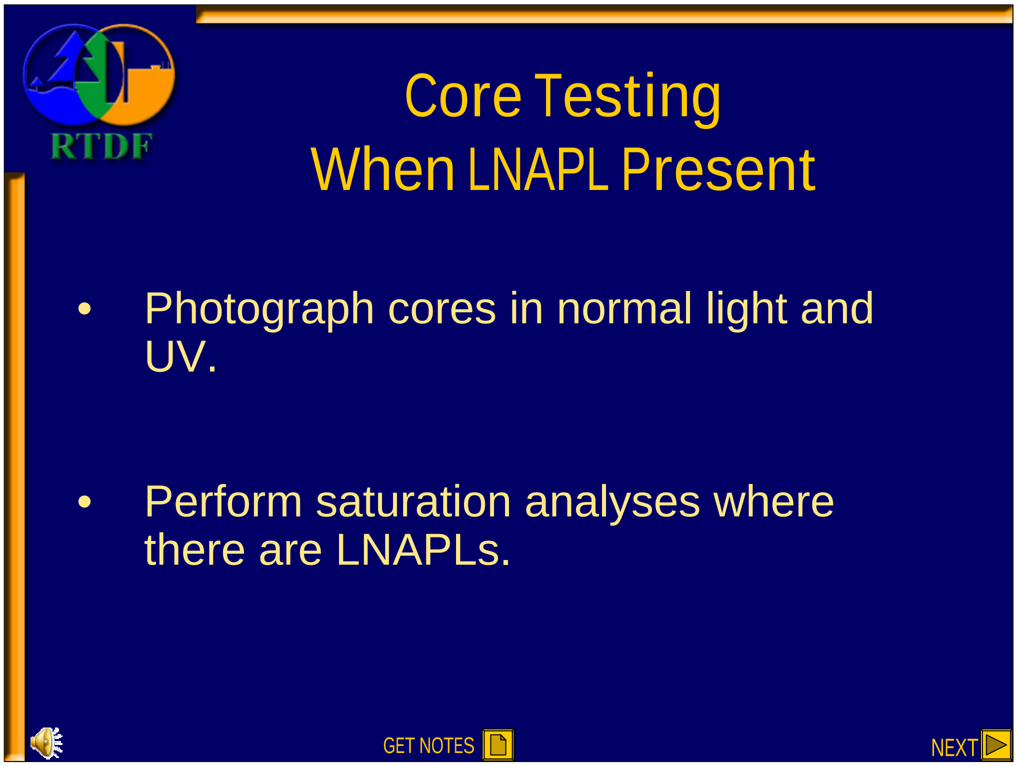

In earlier discussions, we defined what LNAPL saturation is and described the processes that influence it. This slide begins our discussion of how LNAPL saturation is measured.

The objective of core testing is to determine the solid media-fluid interaction properties that will enable us to predict LNAPL saturation and conductivity in the subsurface. If good saturation measurements are obtained, we can compare theory with experiment and improve our confidence in the predictions.

Remember, each site is different, and the project team will have to decide how many samples are needed for analysis at your site. Soil samples for laboratory testing are selected based on soil classification and LNAPL type. Soil-fluid interaction properties such as capillary pressure and relative permeability are affected by the soil structure (e.g., porosity and pore size distribution) and the physical properties of the fluids (e.g., density, viscosity, interfacial tension and surface tension). Thus, it is important to identify the various combinations of soil and fluid types present within the study area (e.g., gasoline in a sand, diesel in a silty sand). A representative number of soil samples should then be obtained for each soil-fluid combination.

The following step-by-step approach can help you obtain the basic data set for analysis. It is offered as general guidance. Project teams should modify this, as necessary, based on specific site needs.

1. Photograph cores in both natural and ultraviolet (UV) light. This helps to identify heterogeneities. It also is useful with grain size analysis to identify the lithology. UV photos identify the location of LNAPL in the cores, so direct lithology and LNAPL occurrence can be compared.

2. Perform saturation analyses (**Dean-Stark** or TPH analysis). The number of samples depends on the length of the impacted zone and may be chosen based on the UV photos. ***Methods for Determining Inputs to Environmental Petroleum Hydrocarbon Mobility and Recovery Models*** (API Publication 4711), lists the methods used to determine soil and fluid properties. Most of these are ASTM methods.

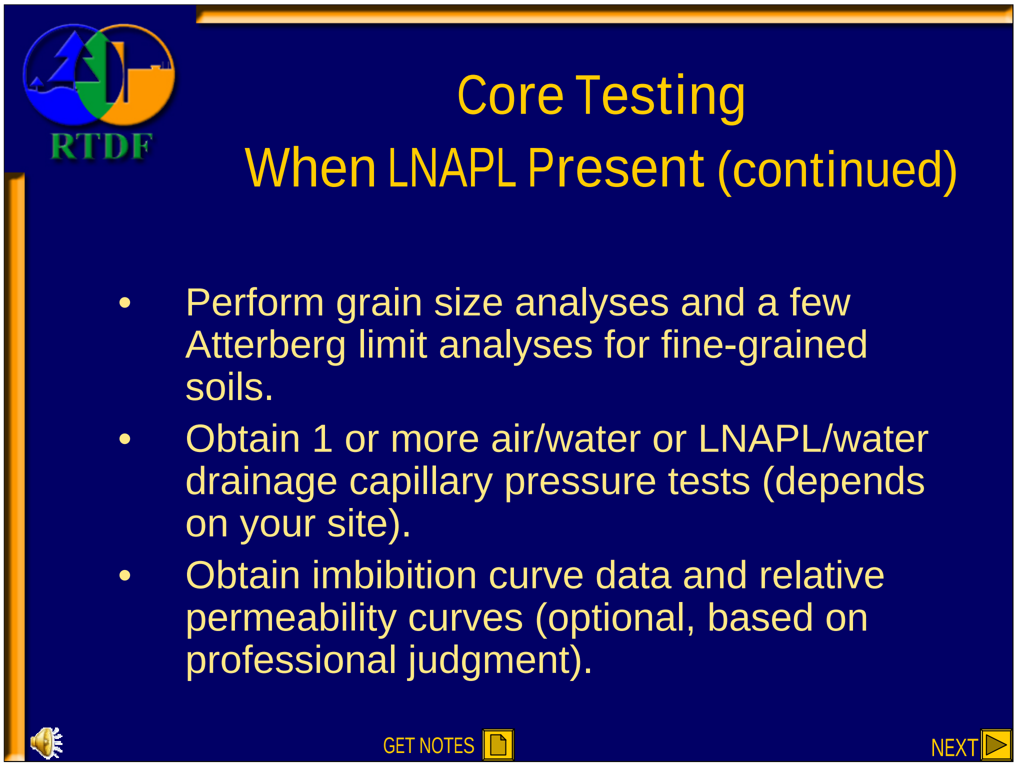

3. Perform two to five grain size analyses, depending on the heterogeneity in the core. The grain size analysis determines soil type. Also perform a few **Atterberg Limits** analyses. These are used to determine if the finer fraction of the soil (passing 200 sieve performed on particles passing a #40 sieve) is classified as clay or silt and whether it has low or high plasticity. This information allows you to use API's ***Light Non-Aqueous Phase Liquid (LNAPL) Parameters Database***, which provides capillary pressure parameters for typical soil types.
4. Obtain one or more air-water or LNAPL-water drainage capillary pressure tests. One should suffice if the subsurface is homogeneous; more would be warranted if the subsurface is heterogeneous. Locations for these tests should be chosen based on LNAPL saturation occurrence and the lithology.

A final optional task is to obtain imbibition curve data and relative permeability curves. Because of the significant costs involved, the choice to perform this task should be based on the project team's professional judgment about whether this is necessary and useful at their site.

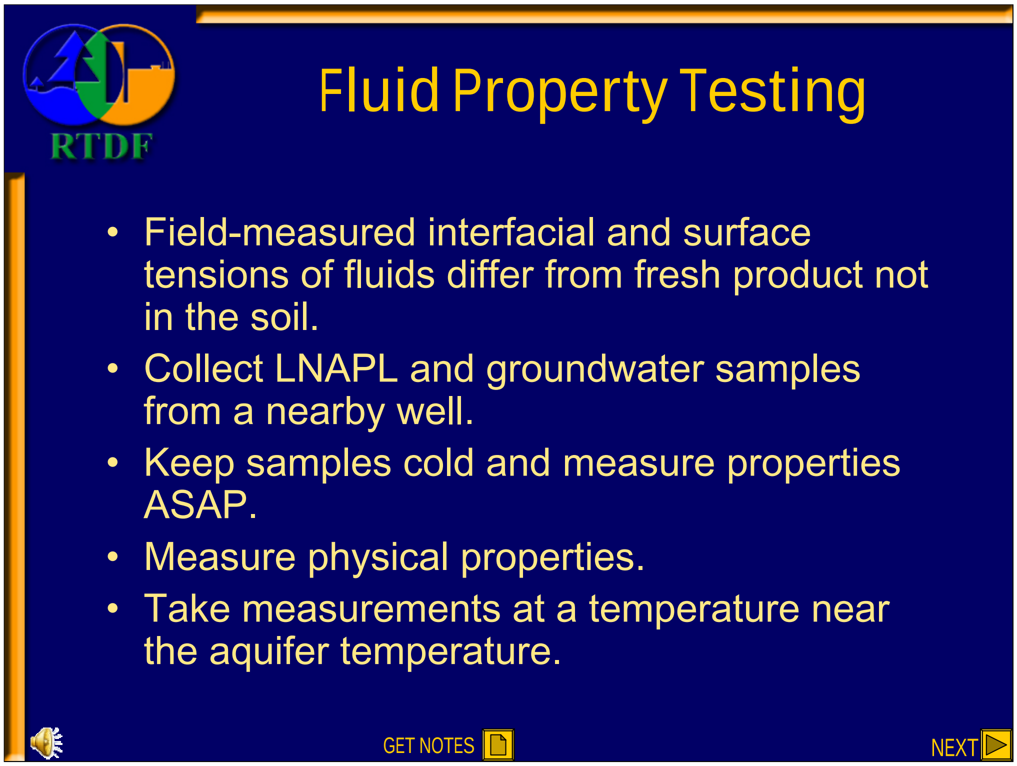

In fluid property testing, experience has shown that measured interfacial and surface tensions of fluids taken from the field are very different than those of fresh product that has not been in the soil.

LNAPL and groundwater samples should be collected from a nearby well. They should be kept cold, and the properties should be measured as soon as possible. The physical properties to be measured are: density, viscosity, surface tension, and LNAPL-water interfacial tension.

These measurements should be obtained at a temperature near the aquifer temperature; however, standard methods can be used to correct these values down to aquifer temperatures.

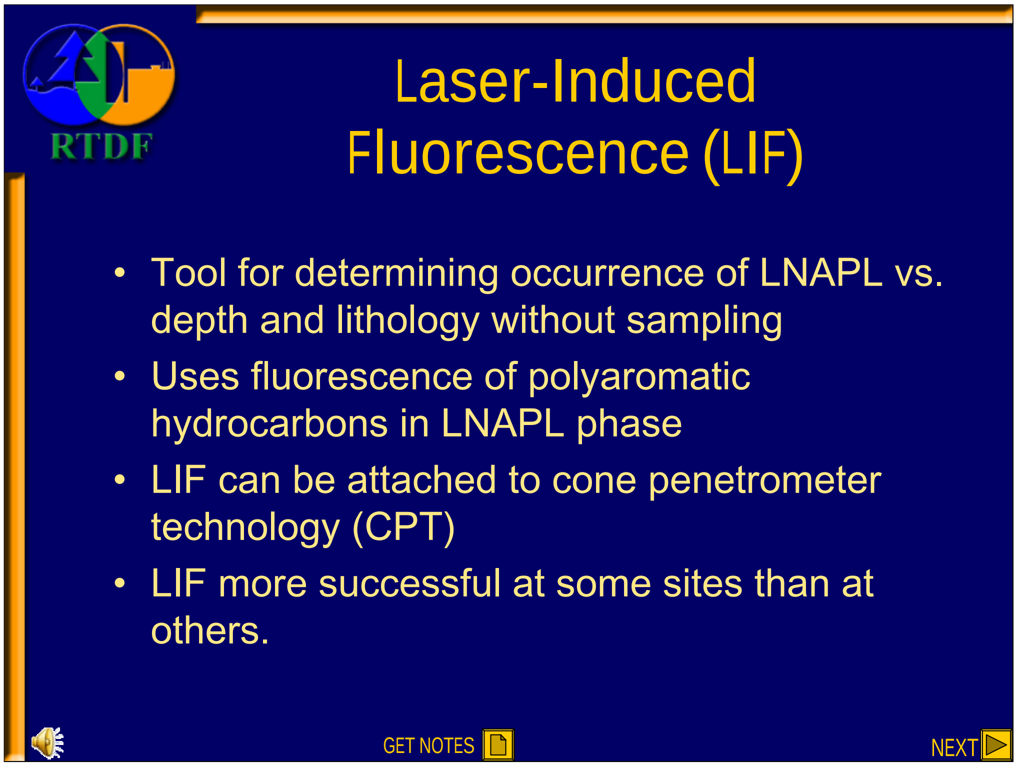

Various federal agencies contributed to the development of LIF. This tool is used to determine the occurrence of LNAPL versus depth and lithology without taking samples. LIF takes advantage of the fact that polyaromatic hydrocarbons in the LNAPL phase fluoresce when exposed to certain wavelengths of light. (Depending on the wavelength frequency used, LIF also can be used to detect other aromatics, such as benzene.)

LIF can be attached to a CPT that is pushed into the subsurface. Since only polyaromatic molecules in the LNAPL phase will fluoresce, each LNAPL product fluoresces differently. As a result, correlating the intensity of fluorescence produced with LIF and the LNAPL saturation in the subsurface is more successful at some sites than at others. An RTDF/LNAPL Cleanup Alliance Project Team has successfully used LIF at a former refinery site in Casper, WY, for example. Decisions about the use of LIF should be made by individual project teams based on the specific characteristics of their sites.

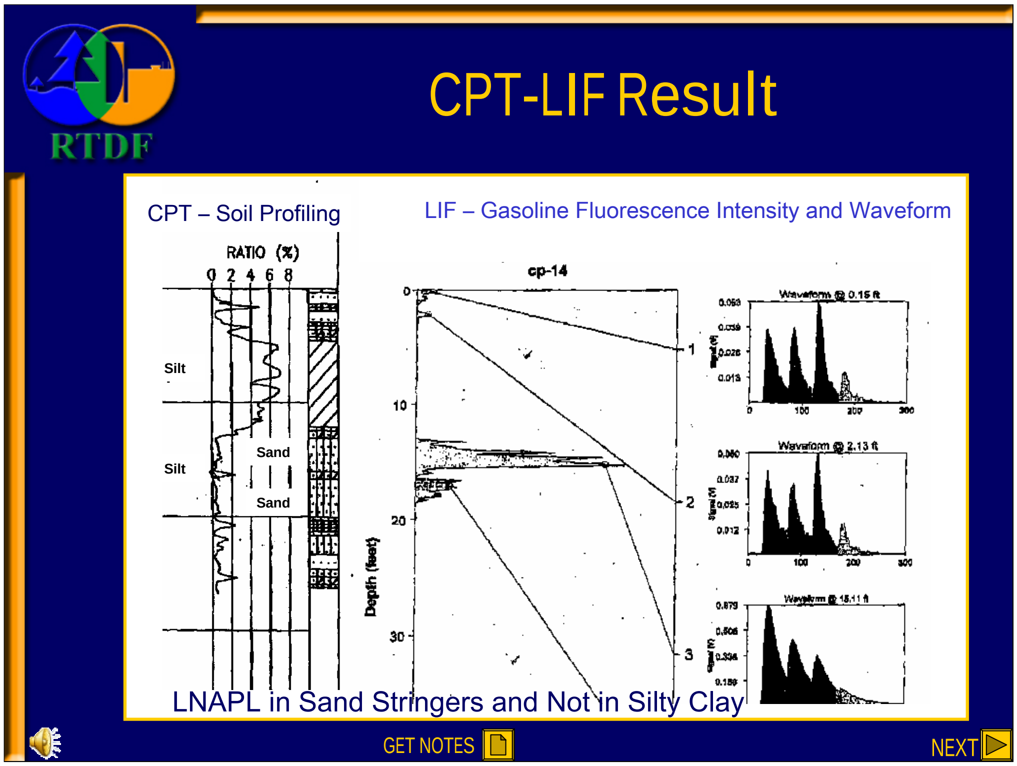

This slide shows the information that can be obtained from a CPT/LIF boring. On the left is the lithologic profile that was obtained from the cone penetrometer. We see a series of layers of silt and sand, with some of the sand containing a high degree of silt.

In the center is the intensity of fluorescence, as a function of depth, obtained with the LIF. Notice that the highest fluorescence is in the sand layer; there is virtually no fluorescence in the silt. As you recall, silt or clay-rich media with very fine pores hold water so tightly that LNAPL has difficulty entering the fine pores. This is a good illustration.

On the right is a waveform that is like a signature for gasoline with the type of LIF used at this site. LIF equipment can use single or multiple wavelengths. As a result, LIF also can sometimes provide information on LNAPL product type and other factors.

Next, we'll look at photos of cores from some real LNAPL sites and examine where LNAPL resides.

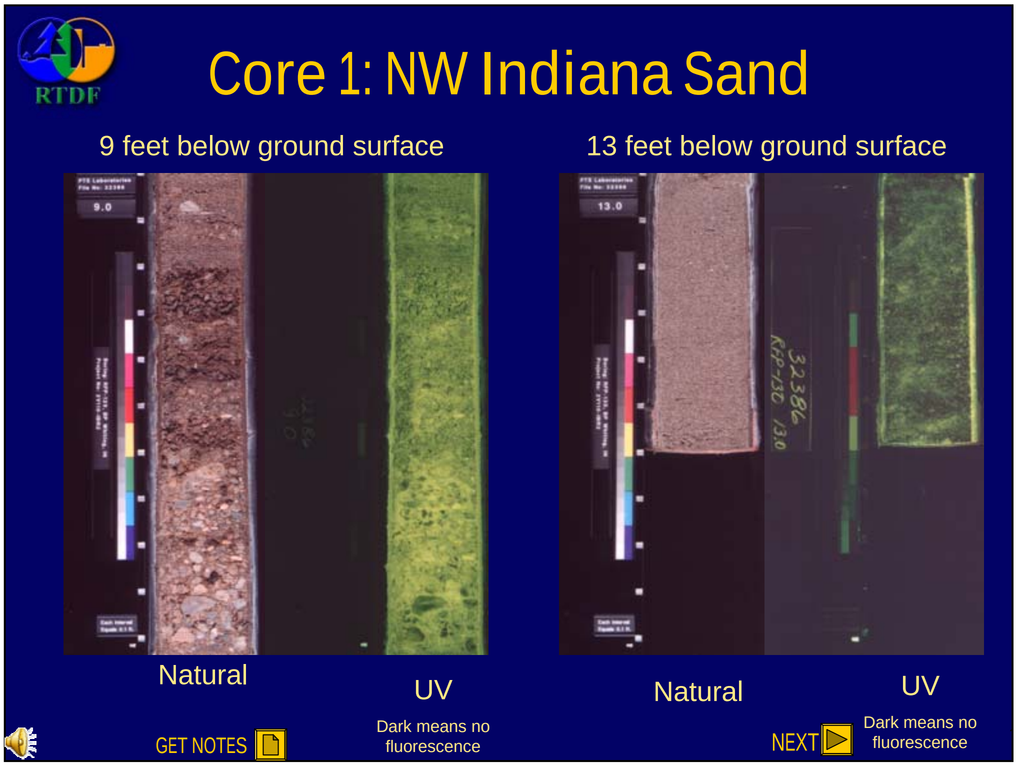

At this site, typical boring logs indicate a medium sand to about 17 feet below ground surface. The natural light photo on the left, at 9 feet below ground surface, shows that there is considerable gravel at that depth. However, over a substantial portion of the 17 feet, the core appears to be rather homogeneous like the natural light photo on the right, at 13 feet below ground surface.

The corresponding UV fluorescence photos indicate that there is LNAPL occurring over much of the interval with possibly less at depth. Remember, however, that UV photos are not calibrated in any manner, and all LNAPL does not fluoresce to the same degree. Thus, saturation measurements are needed to determine if, indeed, there is less LNAPL saturation at depth.

This is a picture of a slabbed core of Beaumont clay containing LNAPL from a site in Texas. Around the larger “macropores,” identified by the yellow circles, there is LNAPL staining. No LNAPL is observed on the majority of the core.

As you recall, the capillary pressure curves for clay-rich media indicated that water is held very tightly in the smallest pores, and LNAPL could enter only the largest pores under typical field conditions.

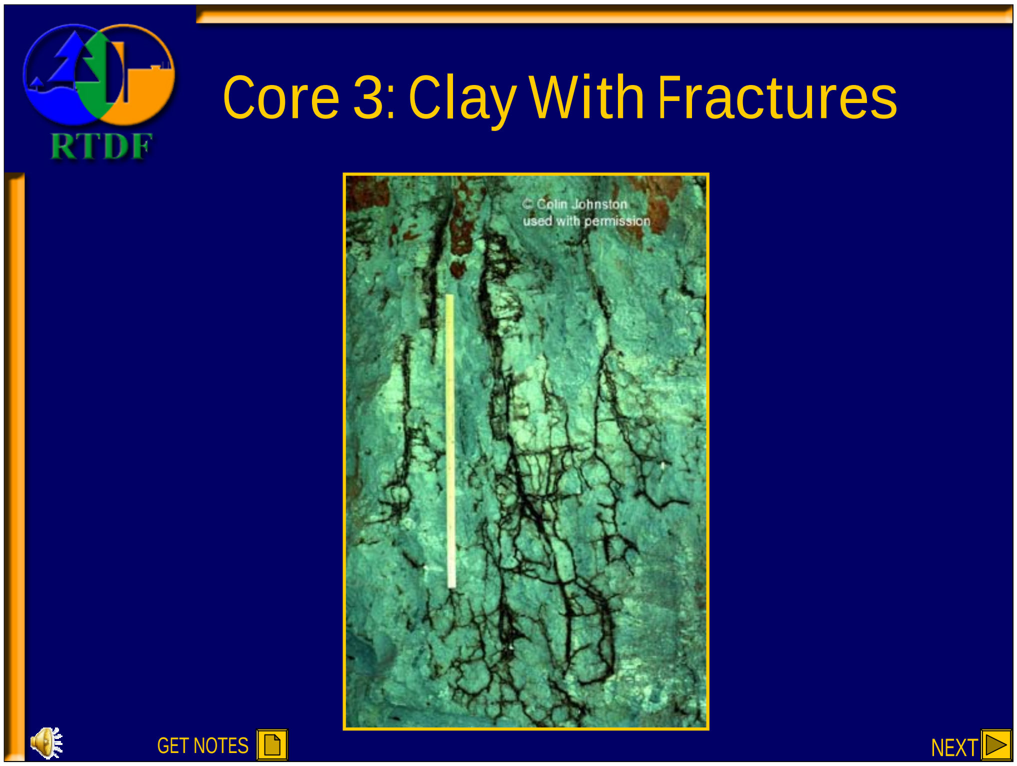

This is a picture of a clay with fractures. On the previous slide, that core was slabbed so the macropores were perpendicular to the face; in this photo, the slab is parallel to the macropores, so we can see their connectivity and detail.

We would expect the LNAPL to move within the black macropores and not enter the matrix.

This photo shows a heterogeneous sand in Texas. The natural light photo shows significant heterogeneity, and the percent of fines has been indicated on the photo. In the right UV photo, the LNAPL, indicated by the light color, is present on the coarser grained materials.

Measured saturations are provided in the photo. Note that the highest saturations occur in the sand with the lowest amount of fines. This is probably due to media with a higher content of fines having higher capillary pressures.

One might think that these photos from real cores somewhat negate the use of capillary pressures and saturation measurements to calculate the volume present and predict its recovery. On the contrary, all such information must be combined with good judgment.

Now we can appreciate better why it has been so difficult to remove LNAPL, and why recovery performance has rarely met expectations. In most cases, the volume of LNAPL that the old pancake model predicted was too conservative (i.e., over-estimated the volume), and the nature of porous media and the lower LNAPL conductivities reduce our ability to recover it.

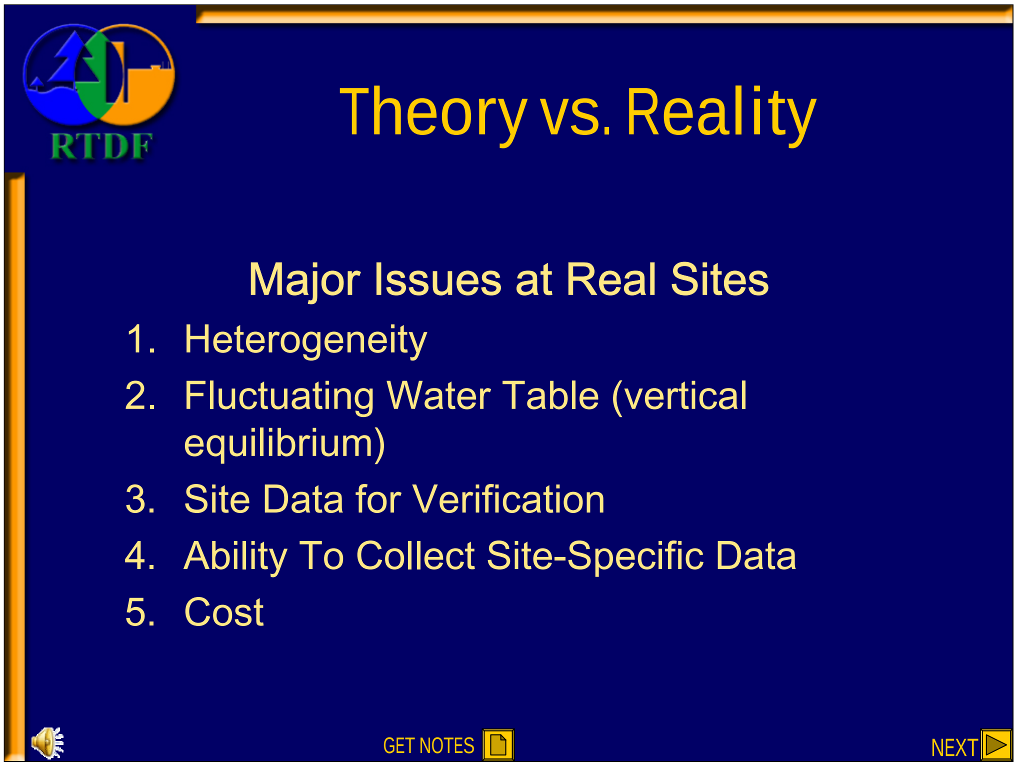

Thus far in this course, you have learned how to make good predictions and better decisions about LNAPL problems using somewhat ideal and academic concepts. We also have discussed that ideal situations are rarely encountered at real sites.

For example, we now know that the basic assumptions for the theory of homogeneous soils and vertical equilibrium are likely to be violated at most sites, since nearly all porous media are heterogeneous and water tables fluctuate. While we would like site-specific data with which to compare our predictions, these data often are not available and must be collected. Moreover, often we cannot collect all the data we need because of difficult drilling, site operations, or cost.

Project teams need to consider all these issues in planning their investigations.

Next, we will look at five site-specific examples.

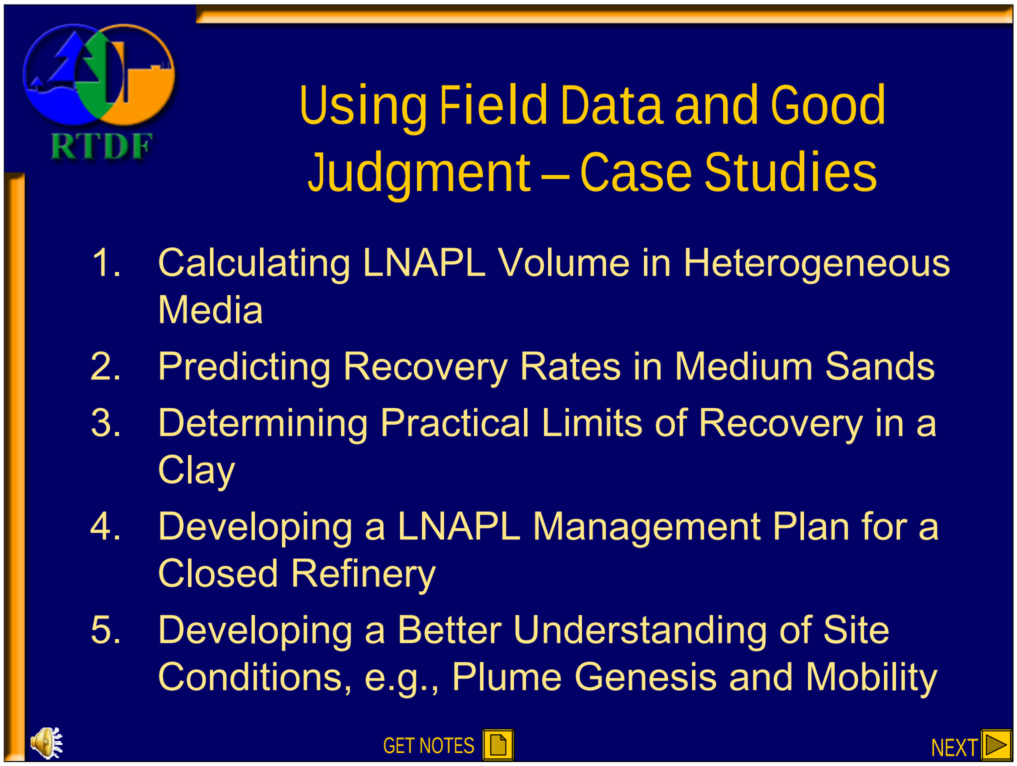

We will use five case studies to illustrate the concepts and methods discussed in this training.

Case #1 examines different methods to calculate the volume of LNAPL in heterogeneous media. This case was reported by **Huntley et al**.

Case #2 looks at predicting recovery rates in medium sands.

Case #3 focuses on determining practical limits of recovery in a clay.

Case #4 examines development of a LNAPL management plan for a closed refinery. This case was reported by **Brubaker et al**.

Case #5 describes how comprehensive investigations using borehole geophysics followed by continuous coring and petrophysical work produced a more refined understanding of site conditions, particularly plume genesis and mobility.

At all of these sites, there are geologic heterogeneity and fluctuating water tables. The sites range from clays to conductive sands. The predictions are compared with actual field results.

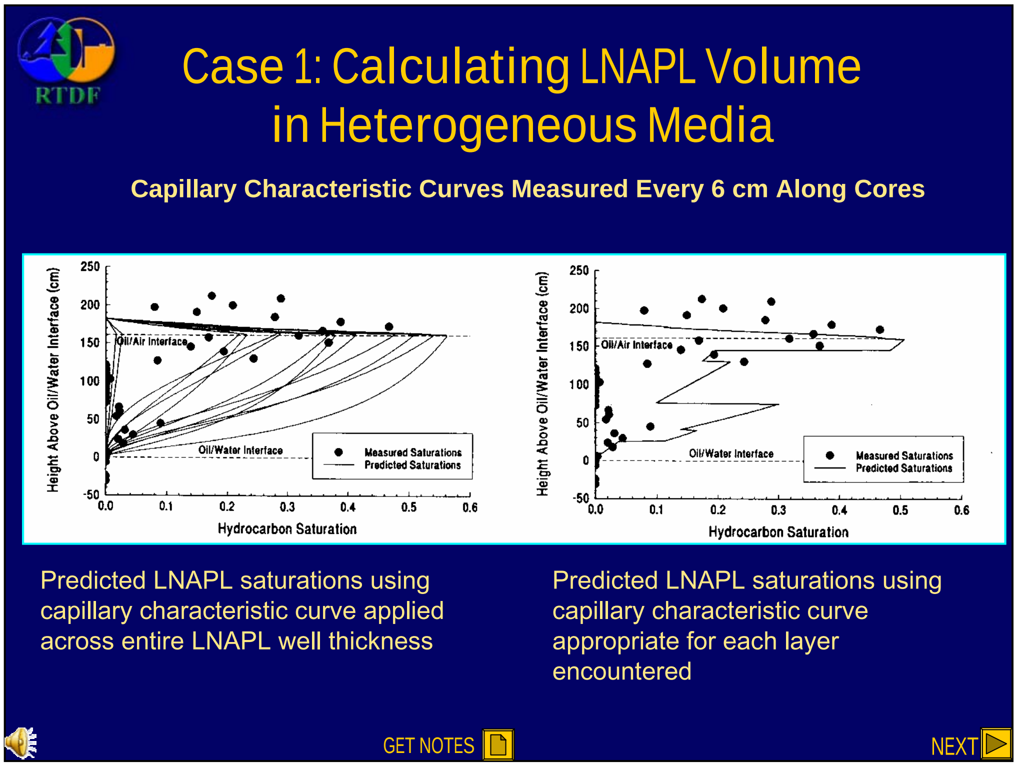

In this case, the team cored several monitoring wells measuring capillary pressure and LNAPL saturations about every 6 cm.

In the figures, the solid dots are the measured LNAPL saturations. Note that the highest saturations occur slightly above the LNAPL-air interface. The authors ascribe this to non-equilibrium drainage of a low-conductivity LNAPL. Note also that the hydrocarbon saturations are quite low and variable below the LNAPL-air interface due to the hydrostatic and capillary pressure relation and the significant variation in grain size in the media layers at the site. Sands, silty sands, clayey sands, and sandy clays were encountered.

In the figure on the left, the measured saturations are compared to calculated capillary pressure curves using the parameters measured from the cores taken along the depth. Notice the significant variation in predicted saturation profiles. We would expect this variation because of the wide range of grain sizes in this boring.

In the figure on the right, the predicted saturation distribution as a function of depth was calculated by applying the measured capillary pressure curve for each layer in the boring. This would appear to be a much better prediction, although it apparently over-predicts the saturations.

For both figures, the agreement between measured and predicted saturations is much better than you would calculate using a pancake model and the simplified models associated with it.

Case 1: Measured and Estimated Specific Volumes

		Measured (cm^3/cm^2)		Estimated From Characteristic Curves (cm^3/cm^2)		
Borehole	LNAPL Thickness in MW (cm)	Total	Below air/oil interface	Range From All Samples	Average	Calculated From Layered Profile
9	0	1.75	NA	0	0	0
10	97	6.4	2.2	1.2 to 10	5.5	4.7
11	116	6	1.2	2 to 6	4	3.5
12	161	9.7	5.2	5.8 to 25	14	13.7

Average and Calculated from layers in good agreement

Comparison to measured not quite as good, but conservative, *"in the ballpark"* and probably much better than what typically would have been estimated in past

GET NOTES NEXT

This table compares the measured and calculated LNAPL specific volumes from the monitoring wells and soil measurements by Huntley et al. There are four boreholes. The LNAPL thickness measured in the installed monitoring wells is given in the second column. The third and fourth columns give the LNAPL specific volumes for the saturation measurements for the total length and below the LNAPL-air interface. The difference is likely due to non-equilibrium drainage.

The fifth column is the range of estimated specific volumes calculated from the capillary pressure curves measured along the depth. These would come from the numerical integration of the curves in the left figure on the previous slide. The average value (sixth column) is the average of those curves.

The final column on the right shows the estimated specific volumes calculated from predicted layer profiles, which were derived using the appropriate capillary pressure curve for each layer encountered. These correspond to the figure on the right in the previous slide.

There is good agreement between the estimated specific volume averages of all curves and the estimates calculated from specific layers. This is not to say that one method is better than another, however, or that they are equivalent. Working at real sites, the project team must decide how to deal with heterogeneity, and no one rule applies. We will see two different methods in subsequent examples.

The comparison between the measured and calculated specific volumes is not quite as good, but the calculated estimates are "in the ballpark" and probably much better than similar estimates developed in the past.

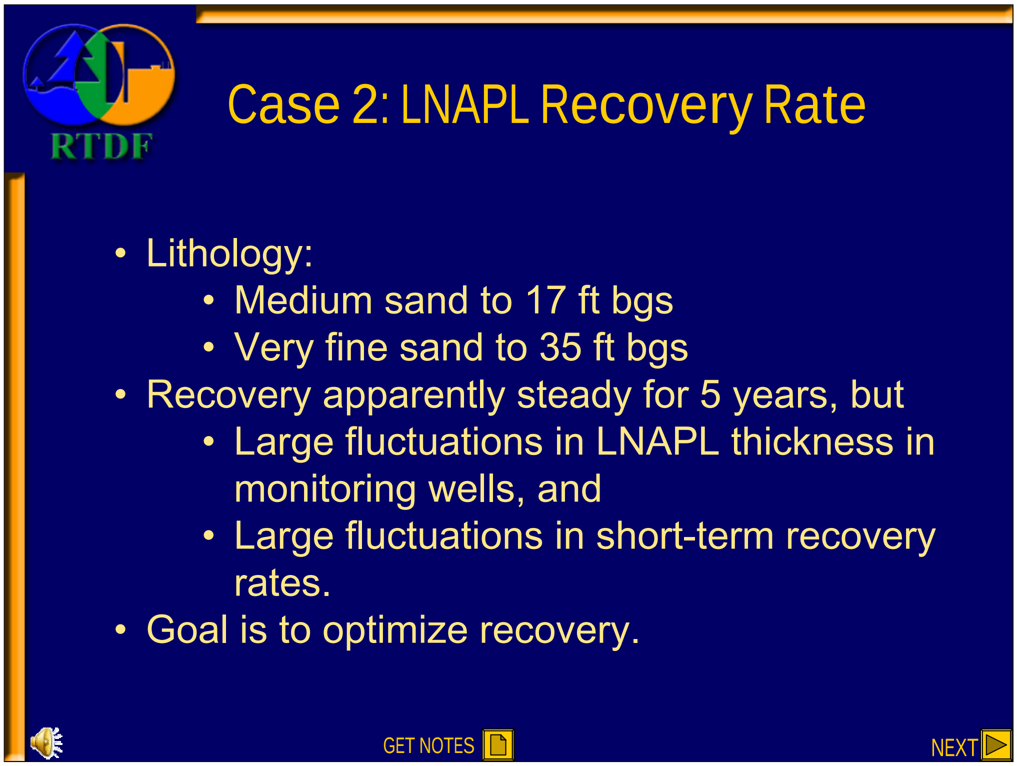

This case involves a BP refinery site. The site consists of medium sand to 17 feet below ground surface (bgs) and very fine sand to 35 feet bgs.

Although the recovery at this site apparently has been steady for five years, there have been large fluctuations in LNAPL thickness in monitoring wells and in short-term recovery rates.

The goal at this site is to optimize recovery.

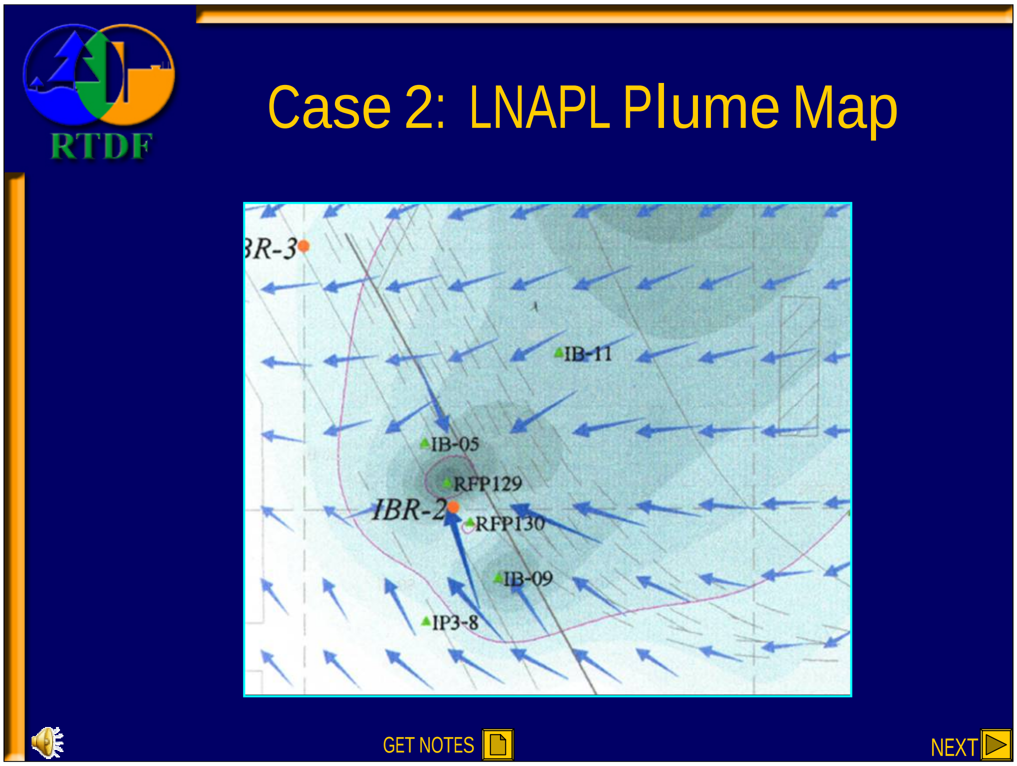

This map shows a large LNAPL plume apparently flowing primarily toward the pumping well, IBR-2. The thickest portions of the plumes are upgradient and near IBR-2, but the contouring program had difficulty showing that.

The primary purpose of the figure is to orient us and show the monitoring wells. IB-09 was the original boring, about 80 feet from IBR-2. RFP129 and RFP130 are within 15 feet of the recovery well and provide drawdown information.

Capillary pressure curves and LNAPL saturations were measured from samples from IB-09, RFP129, and RFP130.

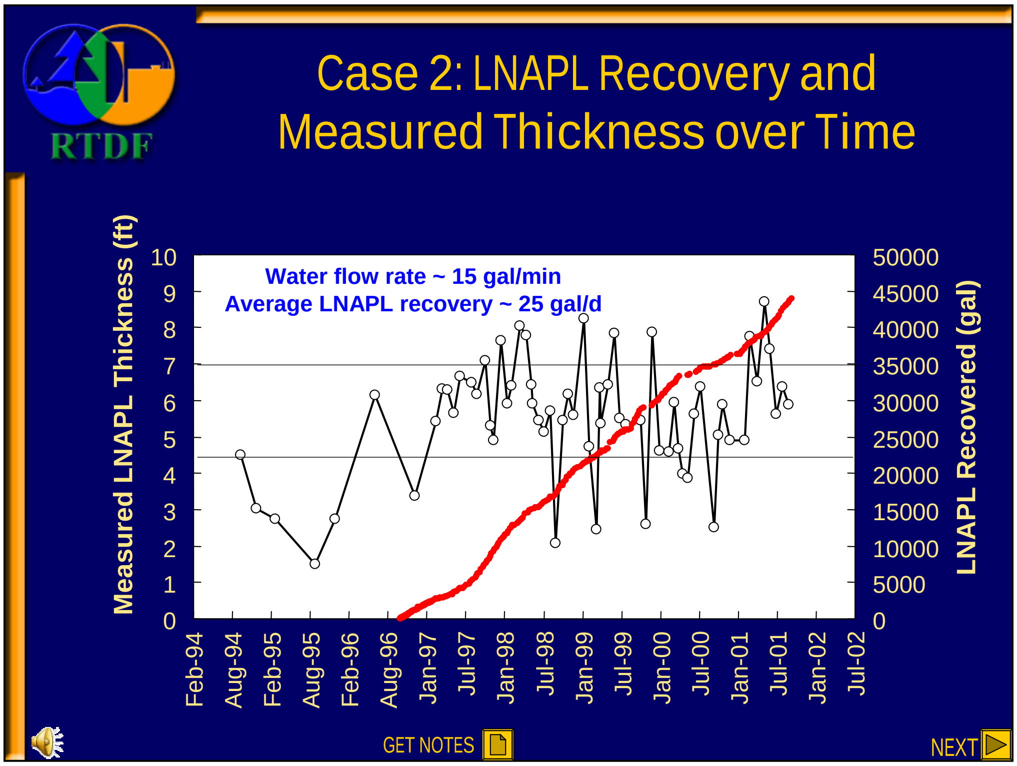

In this figure, the LNAPL thickness fluctuation in IB-09 is shown. It corresponds to a water table fluctuation that is not shown. It looks like, for the majority of the 5-year time period, the thickness was between 4.5 and 7 feet.

Note that the recovery over five years looks relatively smooth at about 25 gallons/day. As we will see later, however, there was a lot of fluctuation in the rate over short periods.

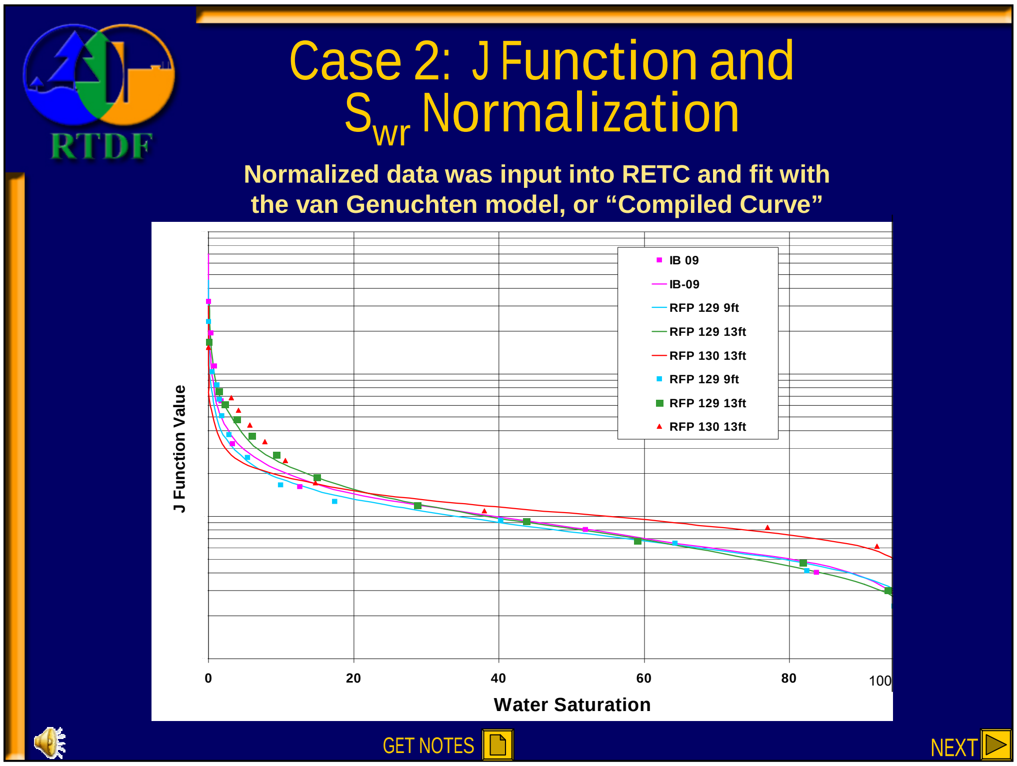

The variation in capillary pressure curves from the three monitoring wells and at various depths was somewhat similar to the variation observed in the earlier slides for Case #1.

In this case, since the media were primarily medium sands, the project team decided to normalize the curves using the Leverett J-function and, then, normalize the irreducible water saturation. The Leverett J-function is a commonly used petroleum engineering parameter which often can reduce capillary pressure data to a single curve. In this case, it worked as shown in the slide.

The normalized curves for soil samples near IBR-2 (shown on the slide before last) appear to lie upon one another.

At this point, the best fit **van Genuchten** curve was applied through all the data generated, and this curve was "un-normalized" to the average irreducible water saturation.

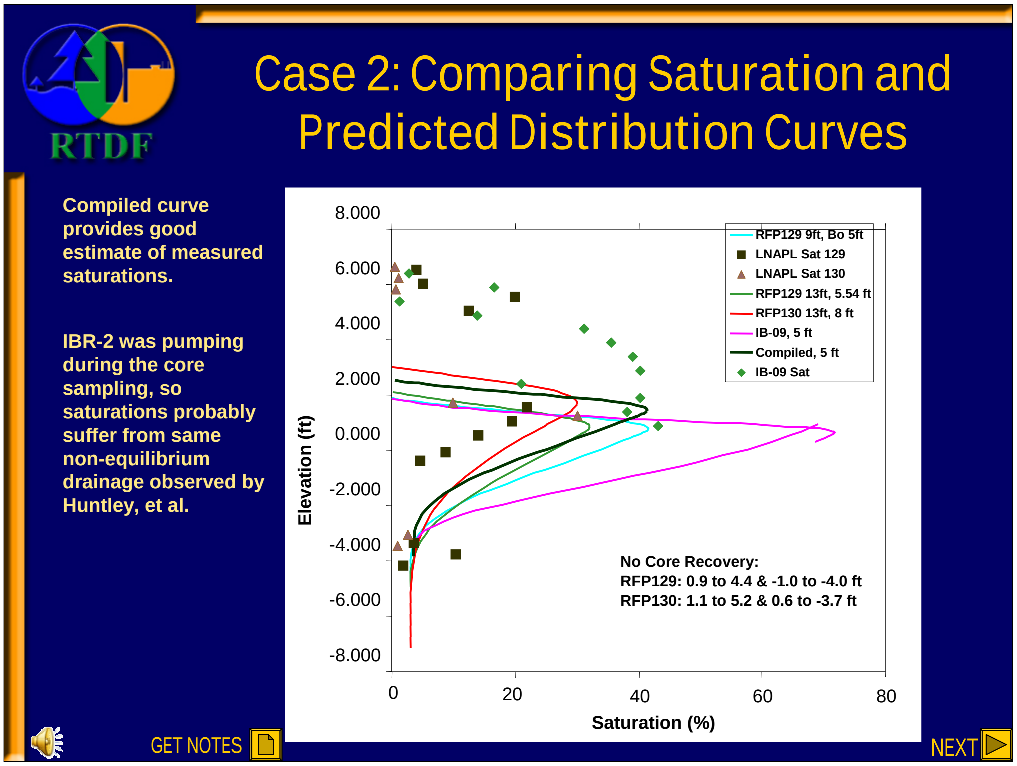

This slide compares the measured LNAPL saturations in the three monitoring wells and the predicted saturation profiles from the measured capillary pressure curves to the so-called "compiled curve" from the normalized data.

It appears that the maximum saturations and the thickness are well predicted, although some of the LNAPL saturations above 0 feet (the LNAPL-air interface) are in the vadose zone. This may be due to non-equilibrium drainage, as Huntley et al speculated, but inaccurate correction for the fluctuating water table is the more likely reason. Unfortunately, some of these data were obtained as part of the research program, and important items were not always recorded.

Also note that there was no core recovery from both RFP129 and RFP130. This is probably because some coarser materials at these depths would not stay in the core barrel.

However, it looks like a reasonable agreement, overall, between the compiled curve and the measured saturations.

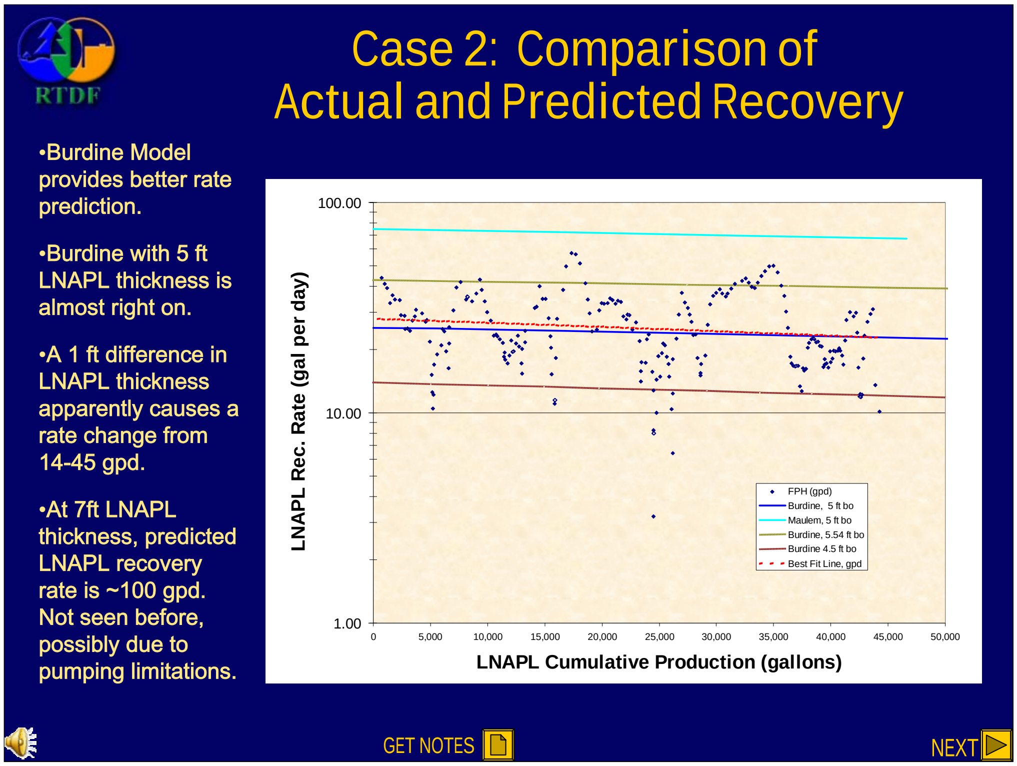

This slide shows a comparison of the actual recovery and various predicted curves using the API spreadsheets and the compiled curve capillary pressure parameters. It illustrates the types of comparisons the project team should consider. The recovery plot is gallons of LNAPL recovered/day (gpd) versus the cumulative LNAPL production. This is a decline curve analysis, which was briefly discussed earlier. It highlights a significant variation in recovery rate from about 10-40 gpd over the course of a 5-year recovery. The red dashed line is the best fit line through the recovery data. It is about 25 gpd and matches the slope of the line on the earlier plot.

The blue solid line is the rate predicted using the compiled capillary pressure parameters and the water pumping rates in the field. We can see good agreement between the overall measured rate and the predicted rate. Note that, in order to obtain a nearly constant rate over this time, a large effective drainage radius had to be set in the model to account for the constant influx of LNAPL from upgradient.

Note also that the LNAPL recovery rate predictions were made with the Burdine model for relative permeability. If the Mualem model had been used, a much higher recovery rate – the green curve at about 70 gpd – would have been predicted. The Burdine model is generally thought to be better for sands; the Mualem model for clays or silts. If possible, check the LNAPL conductivity using the baildown test described earlier.

Finally, if recovery predictions are made using monitoring well thicknesses of either 4.5 or 5.5 ft, the range of recovery rates is nearly covered. Thus, it would appear that the fluctuating water table, which cannot be controlled, is a strong factor in the fluctuating rates. In addition, because there is a large LNAPL plume upgradient that will continue to feed this recovery well, additional wells or other types of recovery systems would appear to be beneficial and are being evaluated using the models whose results are presented here.

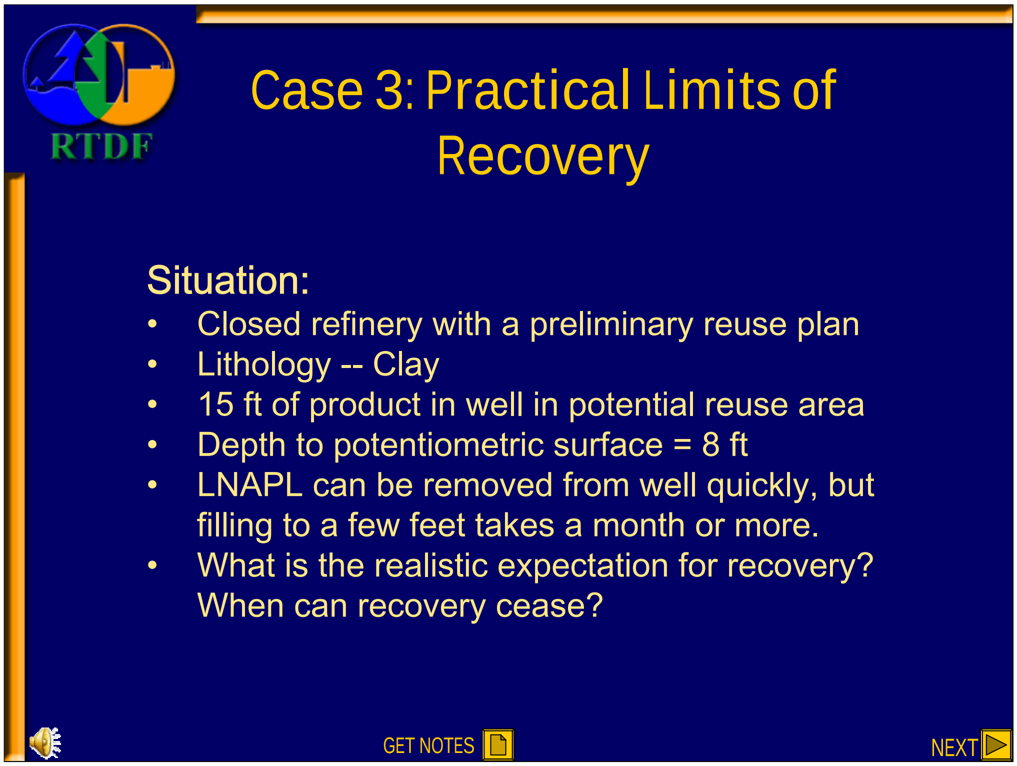

This case involves a closed BP refinery site. The soil at the site is clay.

There is 15 feet of LNAPL product in the well in the potential reuse area and about 8 feet to the potentiometric surface or water table. While LNAPL can be removed from the well quickly, filling to a few feet takes a month or more.

The questions to be resolved are: What are realistic expectations for recovery, and when can recovery cease?

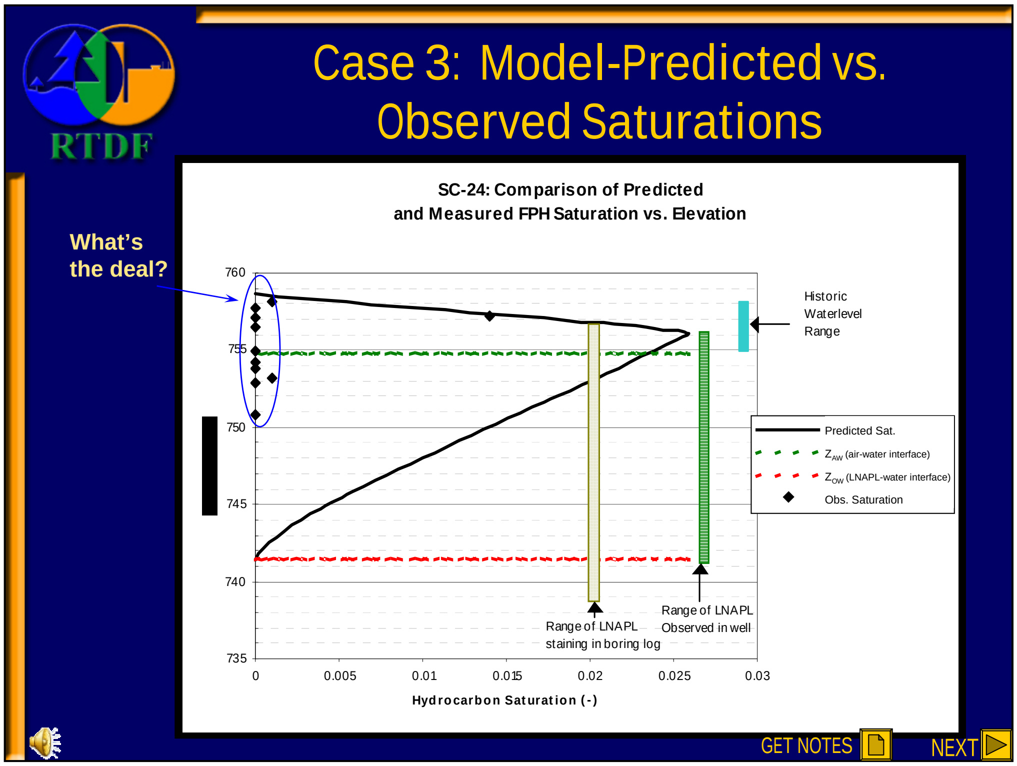

As with the previous slides, there is quite a bit of information on this one.

First, toward the right of the figure, the range of LNAPL staining in the soil boring when the well was drilled and the range of LNAPL thickness in the well are illustrated. Note that they are nearly the same.

Next, note that the historic water table (or potentiometric surface) fluctuates from about 755 to 758 feet. Thus, there is no way that the fluctuating water table drew the LNAPL staining to the depth indicated; it is due to hydrostatic pressure and capillary pressure relationships, which we discussed earlier.

Also note the predicted LNAPL saturation distribution for a 15-ft LNAPL thickness in the monitoring well. It has a maximum value of about 2.7%, which is due to the high capillary pressure of the soil.

Finally, there are only three measured LNAPL saturations above zero. Why is this? Let's move to the next slide for an explanation.

This is not a picture of the core obtained at the Case #3 site, but it is very close.

You can see the LNAPL staining from very large pores; the LNAPL is flowing through these pores. In the remainder of the core, water is held very tightly, and there is no LNAPL.

When soil samples of about 1 inch are taken for saturation analysis, it is very easy to miss the pore or pores containing LNAPL. This probably explains why the majority of LNAPL saturation measurements in the previous slide are zero.

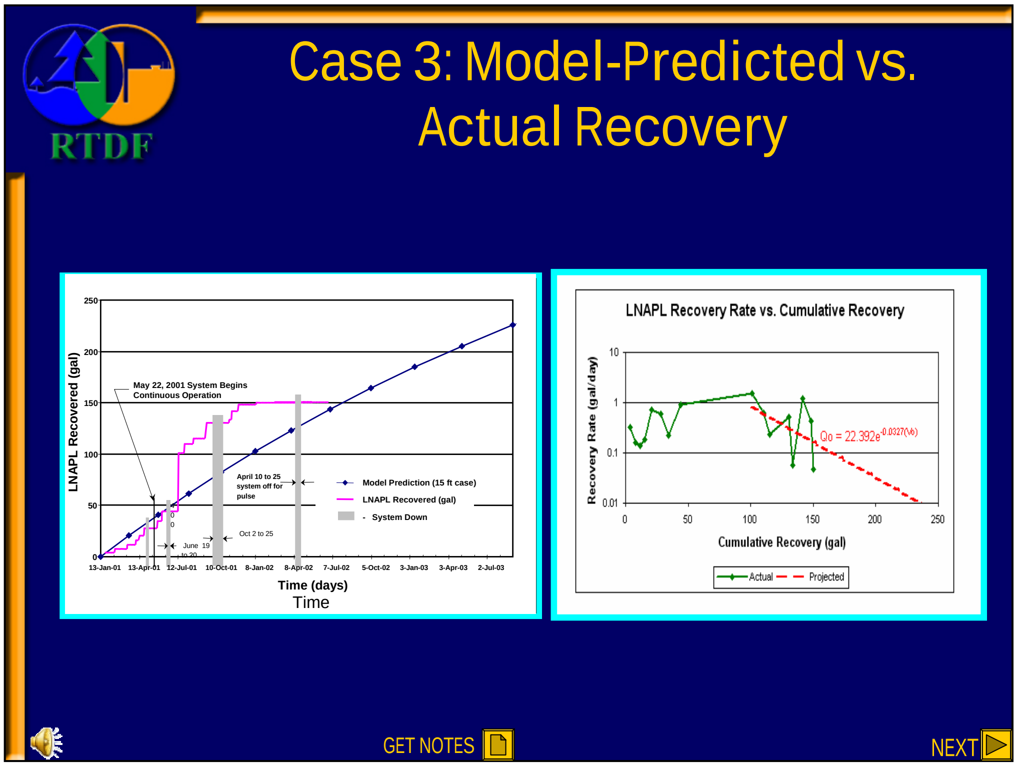

This slide shows a comparison of the predicted recovery of LNAPL with the actual recovery data. The prediction was made prior to system start-up and demonstrates the degree of reliability that modeling predictions can attain.

The actual recovery data also have been plotted in semilog decline curve format to evaluate whether the system had reached a practical endpoint. Even using aggressive vacuum-enhanced pumping technology and applied vacuum pressure of 26 inches of mercury, only 150 gallons of LNAPL were recovered over a year. The actual recovery rate at the end of one year was approximately 0.05 gallons/day.

Due to system operational changes, the recovery rate did not begin to demonstrate a decline until approximately 100 gallons of cumulative recovery. To estimate continued recovery performance, the figure includes a curve fit through the decline portion of the data that projects remaining recovery down to a hypothetical endpoint of 0.01 gallons/day (i.e., 1.3 fluid ounces/day). Operations would have had to be maintained for over four more years in order to recover an additional 86 gallons. Thus, by all reasonable standards, the recovery system had reached a point of diminishing returns.

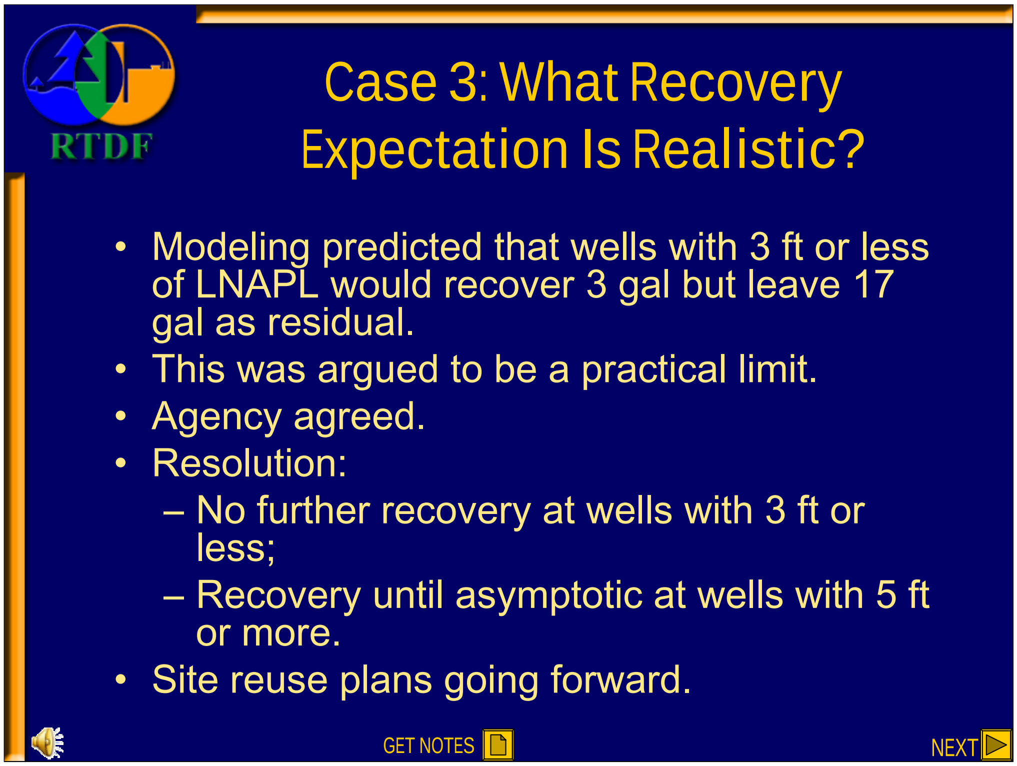

Most state regulations call for reductions to the "maximum extent practical."

At the Case #3 site, modeling predicted that wells with 3 feet or less of LNAPL would recover 3 gallons, but leave 17 gallons as residual.

This was argued to be a practical limit, and the regulating agency agreed.

The final decision was to cease recovery at locations with 3 feet or less of LNAPL and to continue recovery until asymptotic at locations with 5 feet or more.

Site reuse plans are going forward.

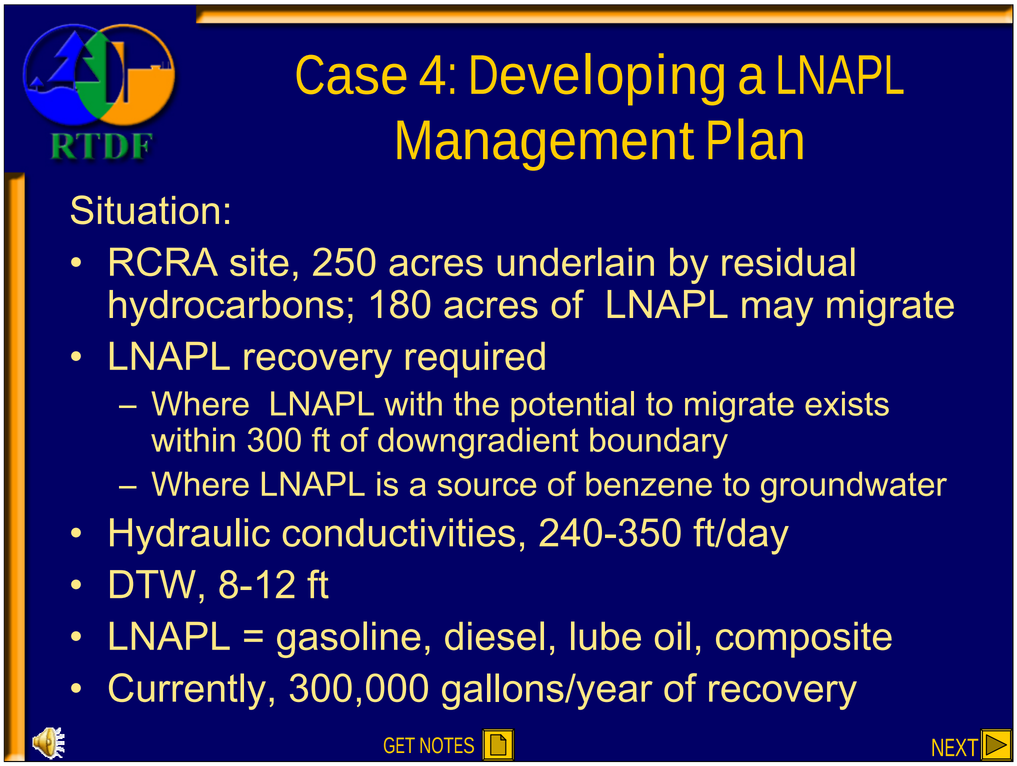

Case #4, reported by Brubaker et al, involves the development of a recovery plan for LNAPL at a closed refinery that has reuse potential. It is a 250-acre RCRA site, underlain by LNAPL. Some of the LNAPL has a very low conductivity, and some is at residual saturation. There are about 180 acres of LNAPL that have the potential to migrate.

The Remedy Decision for the site calls for LNAPL recovery when LNAPL with the potential to migrate exists within 300 feet of the downgradient boundary. The question is how to define "potential to migrate." This will be explored using what you have learned in this course. The Remedy Decision also calls for recovery when LNAPL is a source of benzene to groundwater. This will not be explored here, because the subject is beyond this training.

The site characteristics include hydraulic conductivities of 240-350 feet/day, depth to water of 8-12 feet, and LNAPL consisting of gasoline, diesel, lube oil, and composite.

Currently, recovery runs about 300,000 gallons/year. A total of 10 million gallons has been recovered so far at this site.

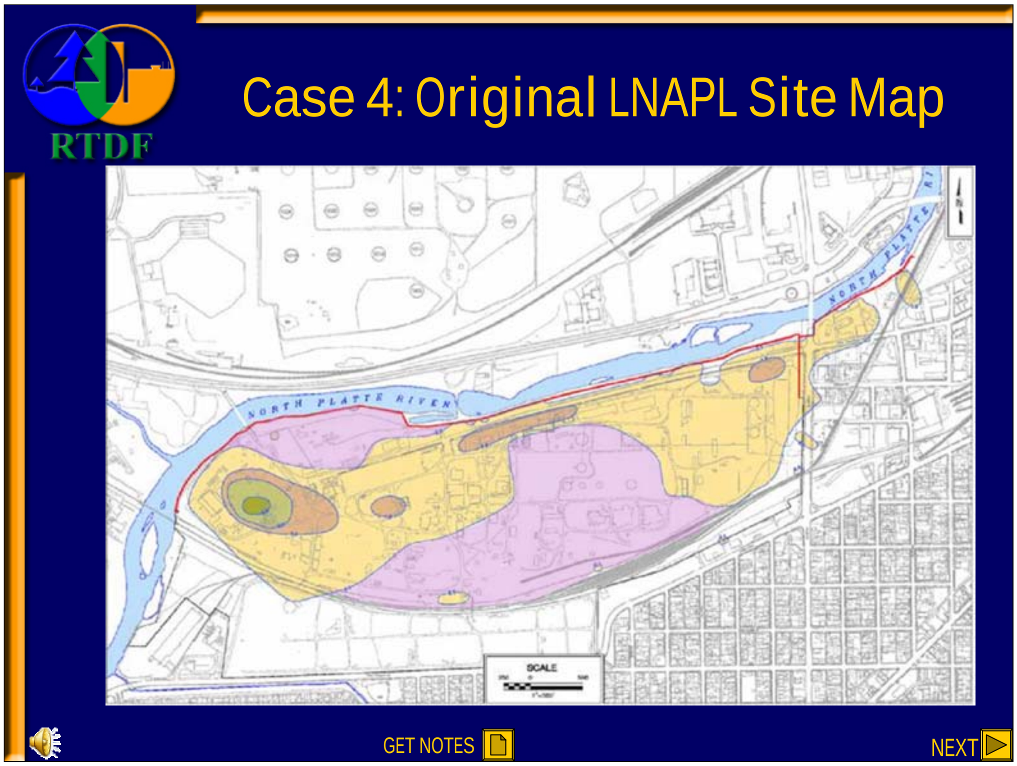

This figure depicts the areas of the site that were suspected of containing the LNAPL that had an ability to migrate. The different colors (yellowish and pinkish) are from different investigations and do not mean anything for this training. The receptor is the North Platte River.

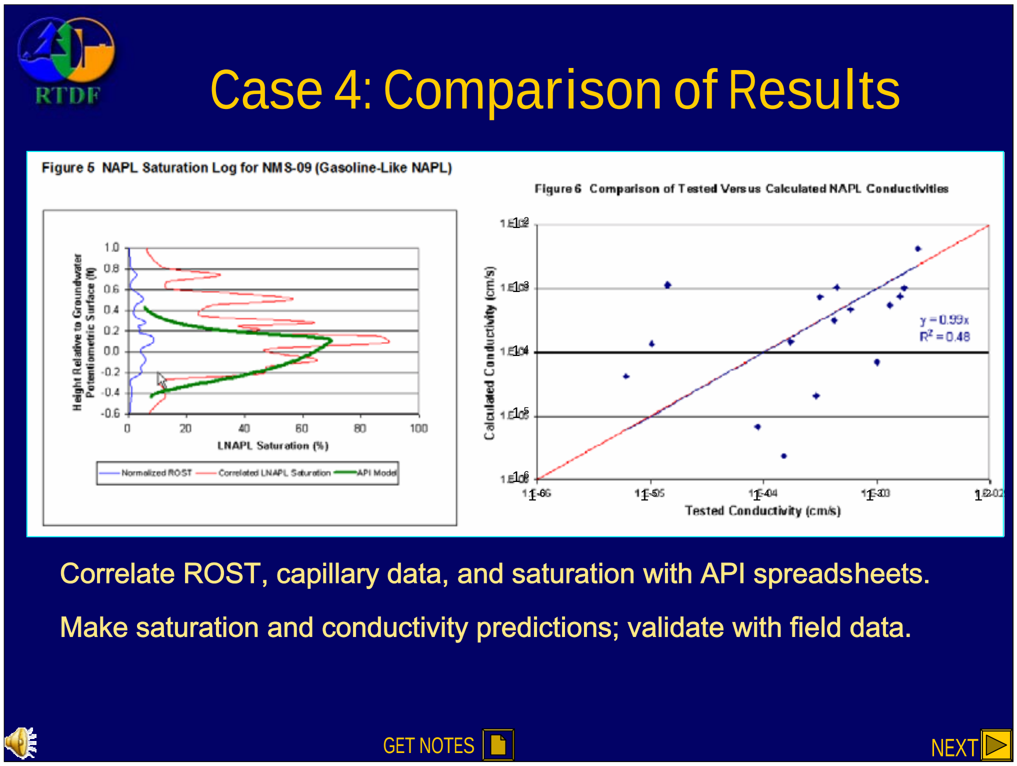

This analysis method used by Brubaker, et al is different from the one used by Huntley, et al or the method used in Case #2. It is another method for dealing with heterogeneity.

Brubaker, et al correlated **Rapid Optical Screening Tool (ROST)** intensity data with saturation measurements from borings from the site to develop a corrected LNAPL saturation profile with depth. The corrected profile then was correlated with the saturation curve from the API spreadsheets. This is shown in the left figure. This was then used to make conductivity predictions versus depth across the site. The predictions were validated with baildown tests, as shown in the right figure.

The chart on the right was shown earlier and illustrates the agreement we can expect between calculated and baildown-determined LNAPL conductivities. The scatter in data points is due largely to the varying distance between tested wells and the corresponding borings used for the calculated conductivities. In addition, normal sampling, testing, and data evaluation factors contribute to the scatter.

Still, it illustrates that we can expect reasonable conductivity predictions.

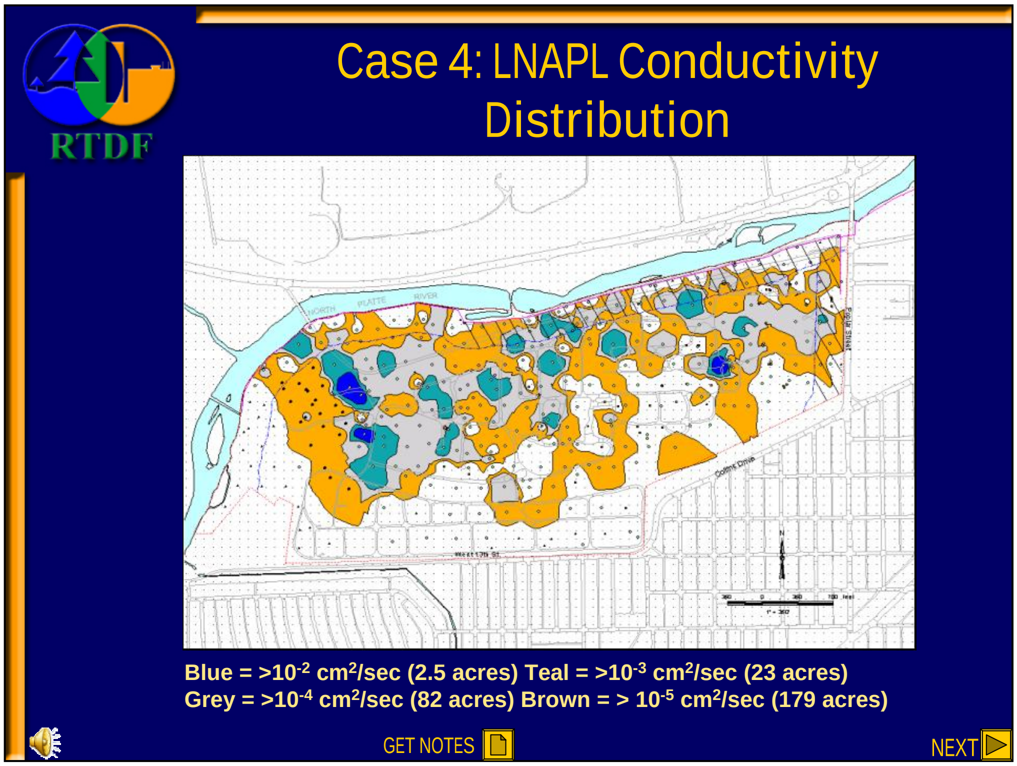

This map was generated using the API spreadsheets to predict conductivities. It shows the conductivities of LNAPL across the site.

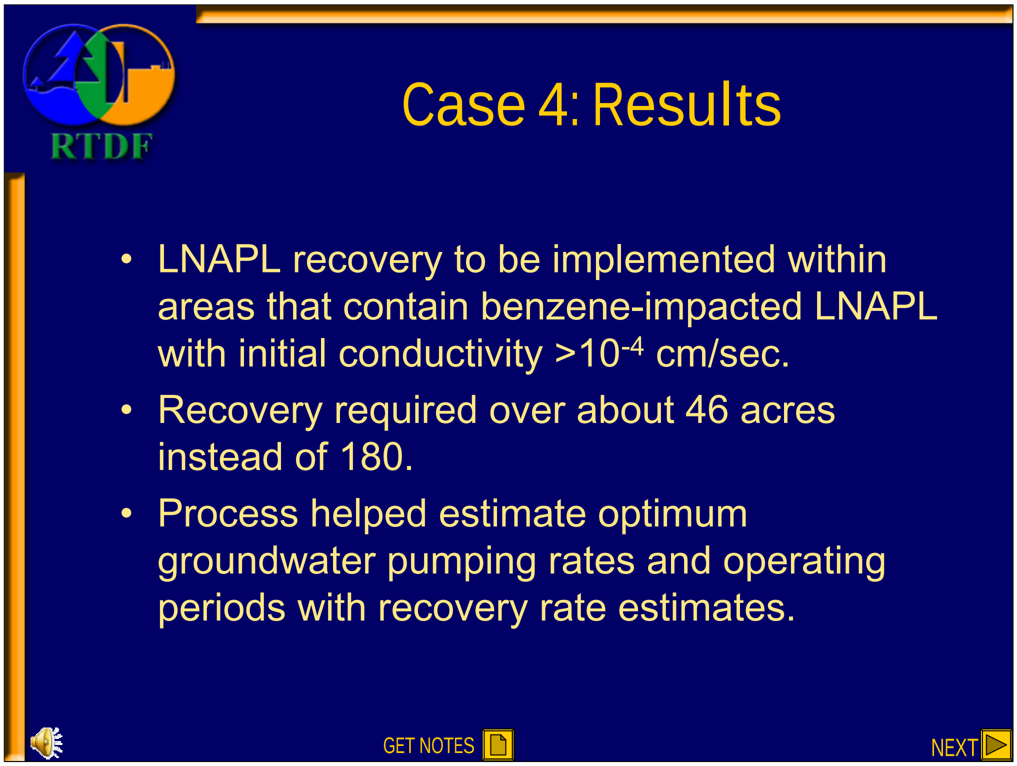

This slide shows the results of regulatory negotiation and incorporating the potential reuse of the site.

The LNAPL recovery was to be implemented only within areas that contain benzene-impacted LNAPL at an initial conductivity greater than 10^{-4} cm/sec. (You will recall from Slide 95 that the Remedy Decision calls for recovery when LNAPL is a source of benzene to groundwater.) This corresponds to a 0.15-ft thickness with a gasoline-type product and affects about 46 acres. Previously, about 180 acres were thought to require recovery. This saved a substantial amount of resources for other beneficial uses.

In addition, the process used at this site to validate predictions against field data helped estimate optimum groundwater pumping rates and operating periods with recovery rate estimates that were used to design the groundwater treatment system to remove benzene from the produced water in a wetlands.

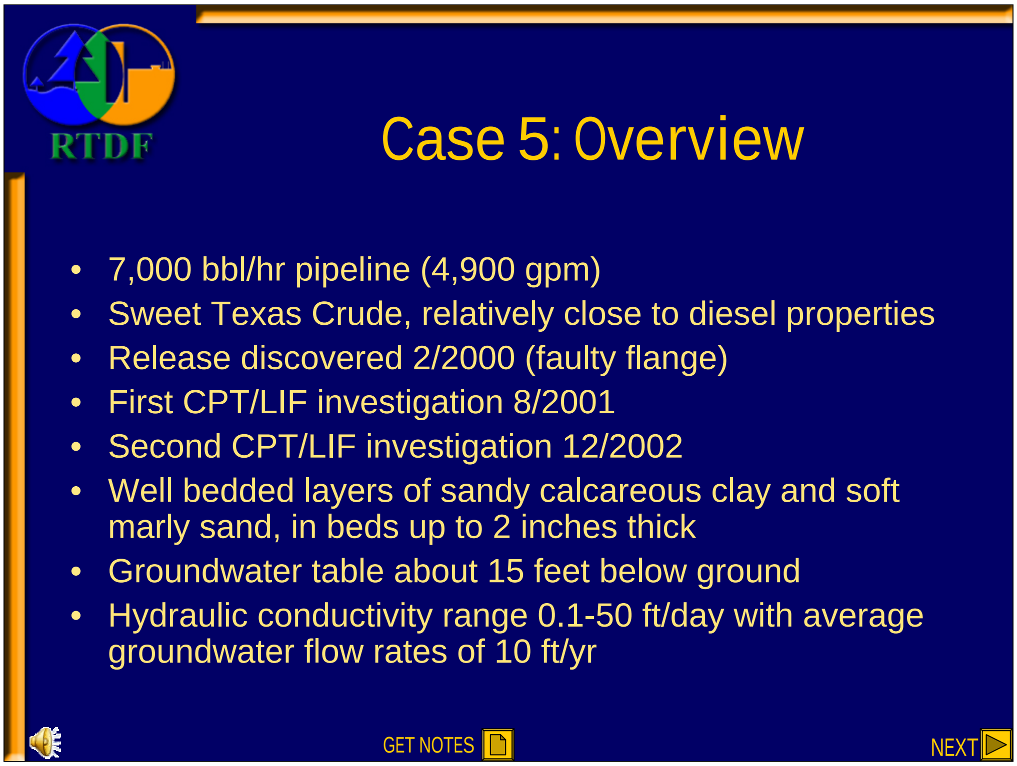

Case study #5 is from a pipeline release from a faulty flange. Pertinent site attributes are shown on this slide.

Comprehensive investigations using borehole geophysics (CPT and LIF, or ROST and LIF) followed by continuous coring and petrophysical work produced a more refined understanding of site conditions.

The case study reveals some interesting aspects of LNAPL plume genesis and mobility.

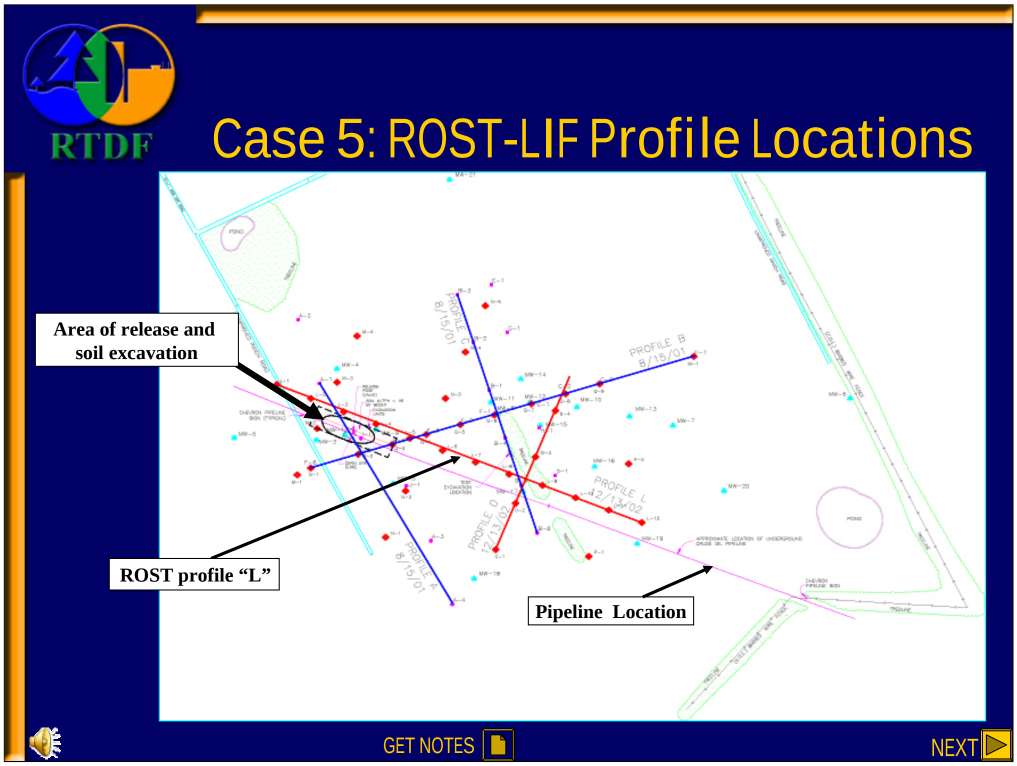

The LNAPL release was investigated twice (1½ years apart) using ROST/LIF and CPT techniques. In addition, several investigations that included soil sampling and monitoring well installation were performed throughout the course of site assessment.

Profile "L" is in the general downgradient direction for groundwater and LNAPL flow and is featured on the following slide. For scale, profile "L" is approximately 1000 feet in length. The property boundary is shown on the far right.

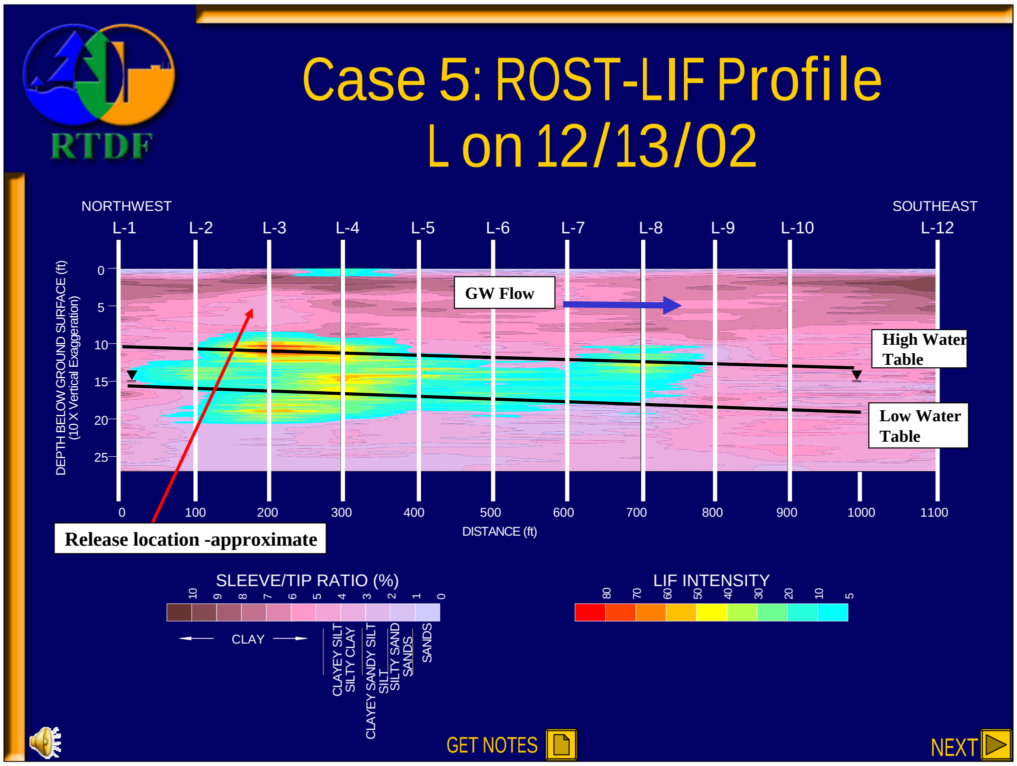

A profile of the release impacts as assessed using ROST/LIF are shown on this cross-section. It is superimposed over the geologic setting approximately two years after the release. Generally, the figure shows that higher saturations remain in the area near the release (in red and yellow) with thinner “fingering” occurring as the LNAPL migrated from the release area.

The range of groundwater fluctuation for the period of record also is shown as the black horizontal lines. It indicates a significant portion of the hydrocarbon mass settled beneath the water table, especially in the area beneath the release. This settlement probably was the result of the volume released, the density of the hydrocarbon, and LNAPL finding more permeable “stringers” in the geologic matrix.

The ROST/LIF investigation location (designated as L-1, L-2, etc.) are approximately 100 feet apart.

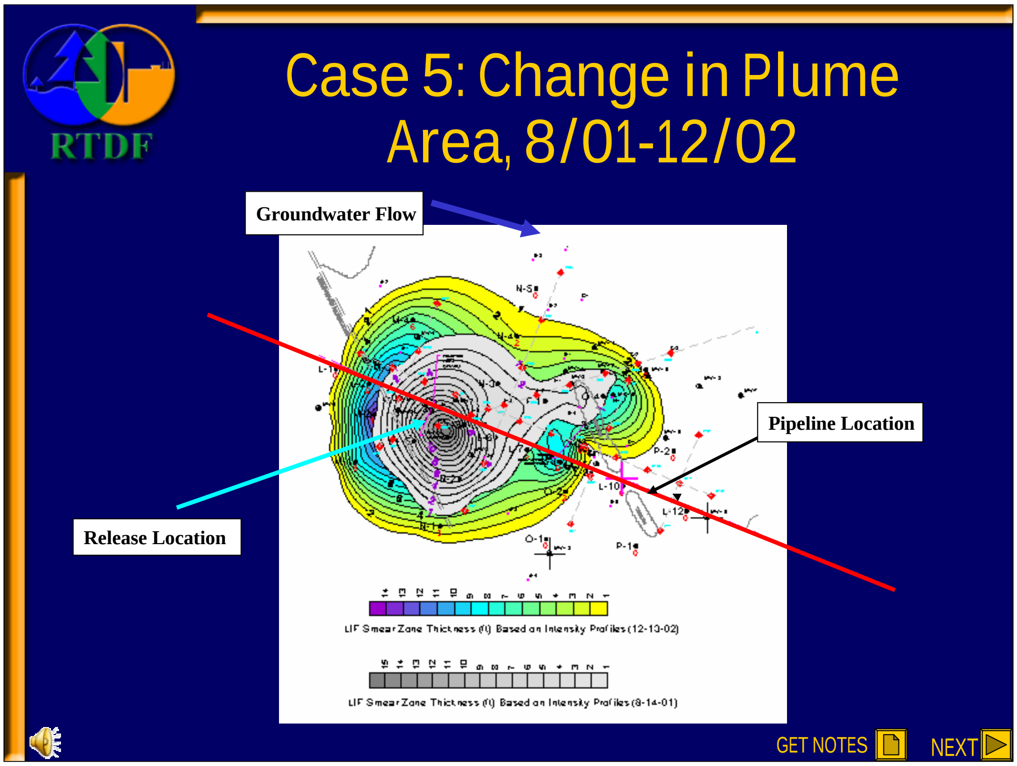

The change in the LNAPL plume footprint (i.e., smear zone) is shown at time intervals 1½ years apart (gray versus bluish yellow areas). Key findings are that LNAPL migration did not follow the groundwater gradient, but rather had a radial LNAPL gradient caused by the release.

Additionally, a portion of the plume apparently migrated upgradient before coming to a (functionally speaking) immobile condition. (Note that "functionally immobile" refers to a state or condition of the plume where some vertical and lateral redistribution of the LNAPL is acknowledged, but that additional movement is relatively minor and should not impact ongoing plume management objectives).

Unimpacted wells located around the periphery of the LNAPL footprint are monitored on a routine basis. To date, they have not shown that LNAPL expansion has occurred. Dissolved phase compounds are monitored routinely as well. They also indicate that LNAPL is reaching a stabilized footprint around the smear zone.

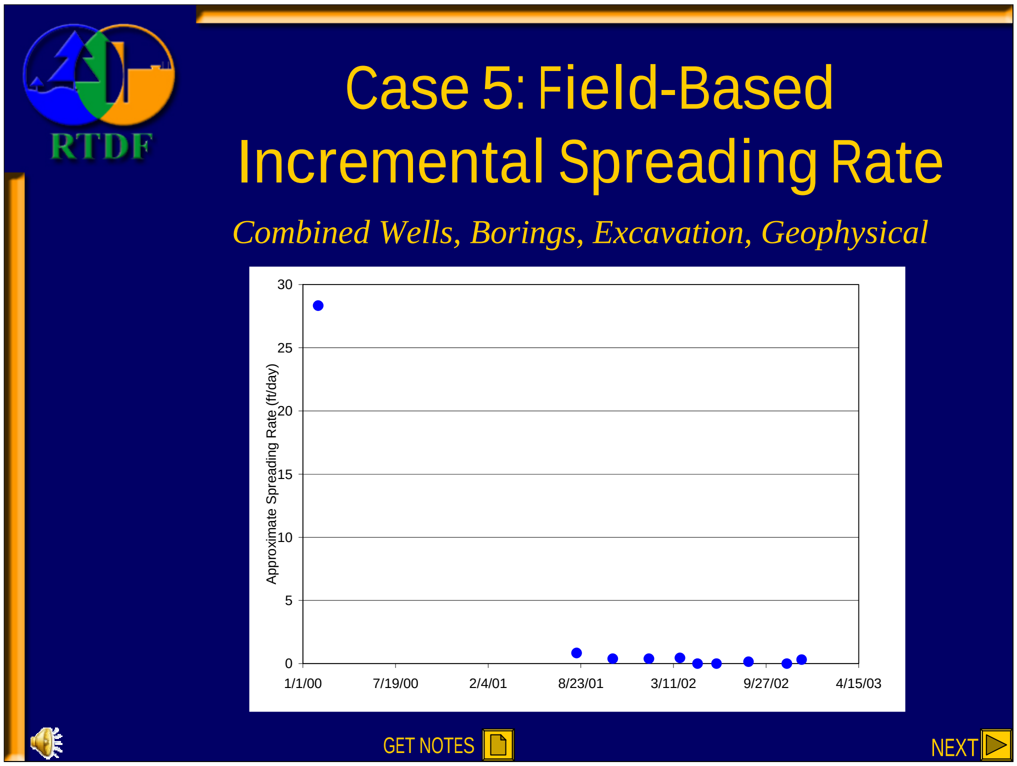

The initial rate of LNAPL movement appeared to exceed groundwater flow by 1 to 2 orders of magnitude during the initial spreading period, which was up to 25 feet/day for the LNAPL versus approximately 10 feet/year for groundwater. Spreading quickly ceased, however, as the driving forces (LNAPL gradient) dissipated and combined with other factors that resulted in the functionally immobile condition that is observed today.

Data points were determined using all available information indicating the presence of LNAPL, including soil samples, geophysical results, and well gauging/analytical history. The uncertainty in the early time range (~ 2/1/00) of estimated movement simply reflects that the date of release is known within a few weeks, but not precisely. But we do know some pipeline specifics (i.e. volume of transport etc.), and we know what the interim soil excavation sampling showed, in terms of plume distribution, following the release.

Case 5: LNAPL Gradients Using Pairs of Indicator Wells

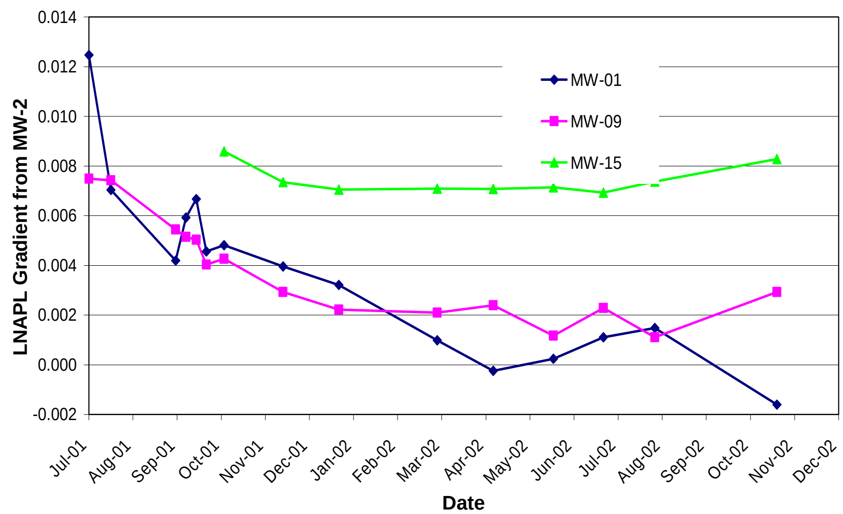

GET NOTES NEXT

This figure shows how LNAPL gradients between selected monitoring wells (MWs) generally are declining over time. MW-2 (on the vertical axis) is located near the release area. Data from MW-2 is paired with other wells (MWs 1, 9, and 15) that are located within the LNAPL smear or source zone to show how LNAPL gradients have declined over time.

LNAPL gradients were measured between these wells approximately 1 1/2 years after the release (about July 2001) and indicate that at least one order of magnitude decline (0.01 ft/ft to 0.001 ft/ft) generally occurred in less than one year (July 2001 to May 2002). In fact, the rate of gradient decline appeared to be more rapid, leading up to the initial values measured and plotted on this figure (i.e. July 2001). In this field example, MWs 1, 9, and 15 get progressively farther from MW-2. The flat or increasing gradient (as the distance between the release point near MW-2 and the other monitoring wells increases) indicates that there may be localized mounding of LNAPL as the index distance increases. Note that the rather flat-trending LNAPL gradient that exists between MW-2 and MW-15 (which are over 500 feet apart) shows that some of this expected variation will exist between points over time. These slight variations in a nearly steady profile should not be sufficient to cause further migration of the plume downgradient, as illustrated by the spreading-rate data reported in the previous slide and by more recently collected data.

Because LNAPL gradients are required to provide a driving force for the LNAPL, it appears that a decline in this parameter is one of the primary reasons this plume has reached an immobile condition.

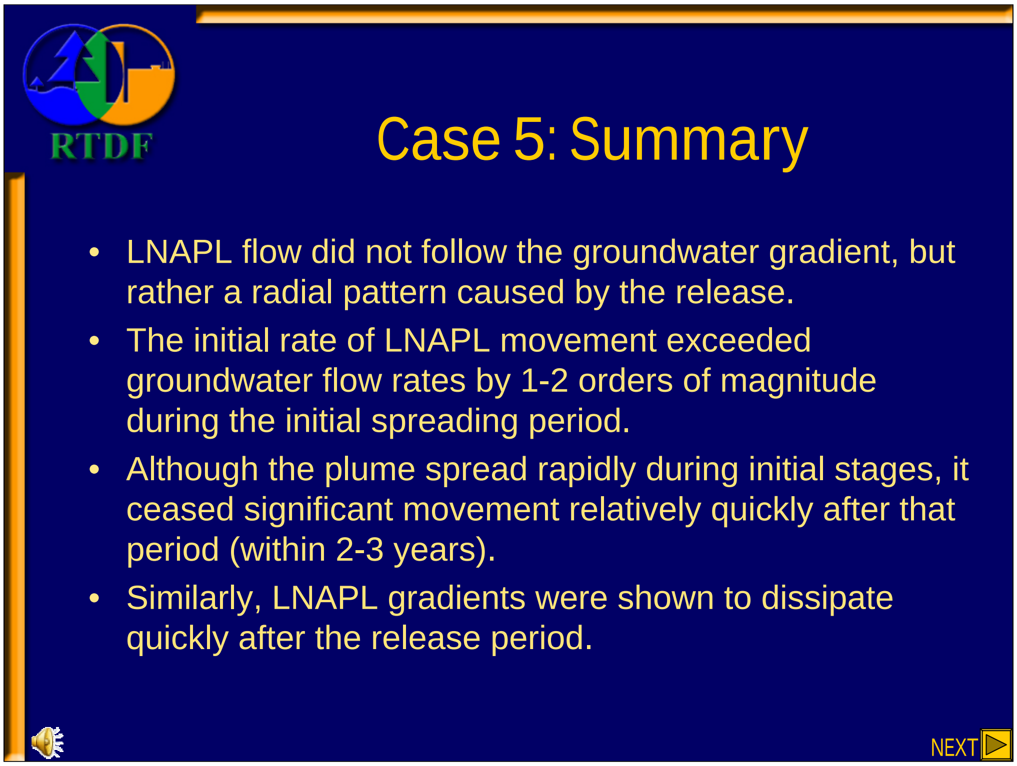
RTDF
Case 5: Summary
• LNAPL flow did not follow the groundwater gradient, but rather a radial pattern caused by the release.
• The initial rate of LNAPL movement exceeded groundwater flow rates by 1-2 orders of magnitude during the initial spreading period.
• Although the plume spread rapidly during initial stages, it ceased significant movement relatively quickly after that period (within 2-3 years).
• Similarly, LNAPL gradients were shown to dissipate quickly after the release period.
NEXT

Read slide.

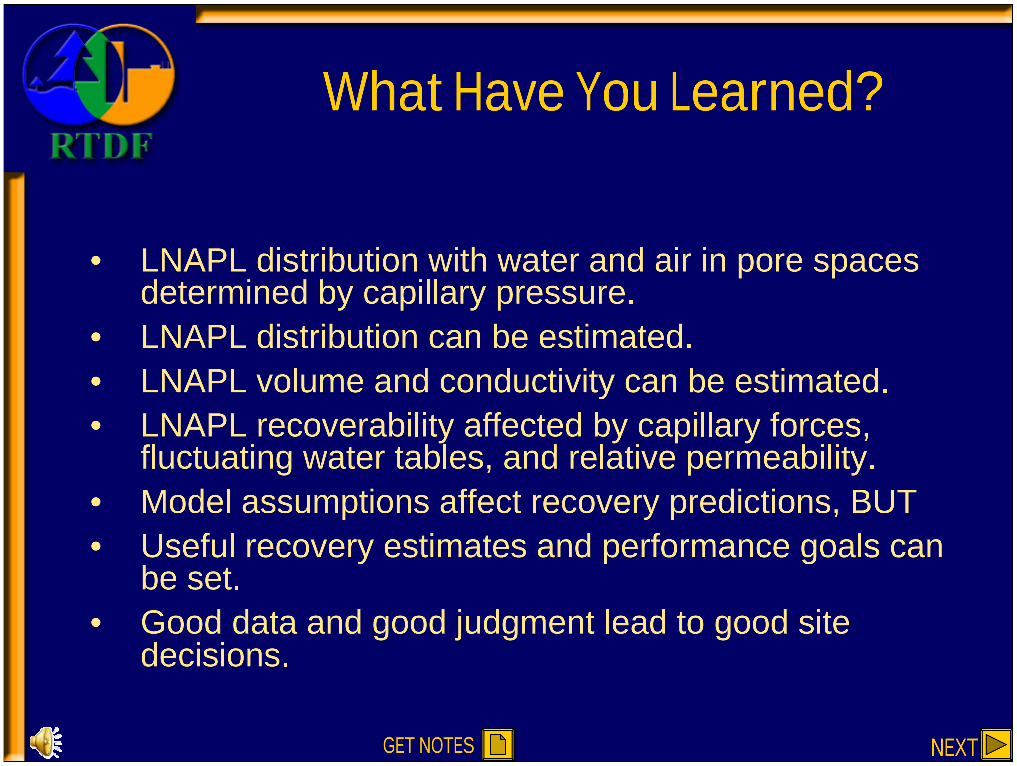

During this course, you have developed an understanding of several key points:

1. LNAPL is not a pancake in the subsurface that rests on the top of the water table. It is distributed with water and air in pore spaces, as determined by the capillary pressure.
2. LNAPL distribution can be estimated using well developed theories and methods. From this, the volume of LNAPL present in the subsurface and its conductivity also can be estimated.
3. Not all LNAPL is recoverable. Some is trapped by capillary forces, fluctuating water tables, and relative permeability effects.
4. Models used to predict LNAPL recovery are based on assumptions – like homogeneity and vertical equilibrium. While these assumptions can raise uncertainty, in general, model predictions are in the ballpark, provided that field conditions do not violate the assumptions of the model and that proper calibration is made. Comparing model predictions to field data helps increase confidence.
5. Case studies of real sites showed that investigators can use a combination of field data and good judgment to deal with issues such as heterogeneity, fluctuating water tables, etc. The case studies also demonstrated that simplified assumptions and API modeling tools can be used to produce acceptable and adequate evaluation of LNAPL mobility and recovery rates at real sites, and that these estimates have been useful in negotiations with regulators.
6. An understanding of LNAPL behavior in the subsurface – including the principles of capillary pressure, conductivity, and hydraulic recovery – and good data, combined with good professional judgment enable you to plan and execute good remedial strategies for your LNAPL sites.

This course has been prepared by the members of the Remediation Technologies Development Forum (RTDF) Non-Aqueous Phase Liquid (NAPL) Cleanup Alliance. Members include ChevronTexaco, the U.S. EPA Technology Innovation and Field Services Division, the American Petroleum Institute, Ashland, Inc., BP, ConocoPhillips, ExxonMobil, RETEC Group, Shell Oil Products US, Sierra Environmental Services, State of Wyoming Department of Environmental Quality, TriHydro Corp., the U.S. Defense Energy Support Center, U.S. EPA Regions 6 and 8, and the U.S. Naval Facilities Engineering Service Center.

Alliance members, Vic Kremesec and Barbara Padlo, BP, served as principal authors.

"The Basics" is intended to be the first of a multi-module training package. Information about follow-on modules will be provided on the NAPL Cleanup Alliance web site (www.rtdf.org/public/napl) as soon as it is available.

Notice

The NAPL Cleanup Alliance is one of the Action Teams under the Remediation Technologies Development Forum (RTDF). The RTDF was established in 1992 to foster collaboration between the public and private sectors in developing innovative solutions to mutual hazardous waste problems. The Alliance includes representatives from the petroleum industry, federal and state government, and academia who share an interest in pursuing aggressive technologies for removing large-scale non-aqueous phase liquid (NAPL) contamination

This training does not present and is not a U.S. EPA policy, guidance, or regulation. It does not create or impose any legally binding requirements or establish U.S. EPA policy or guidance. The U.S. EPA does not exercise editorial control over the information in this document and Standards of Ethical Conduct do not permit EPA to endorse any private sector product or service.

NEXT

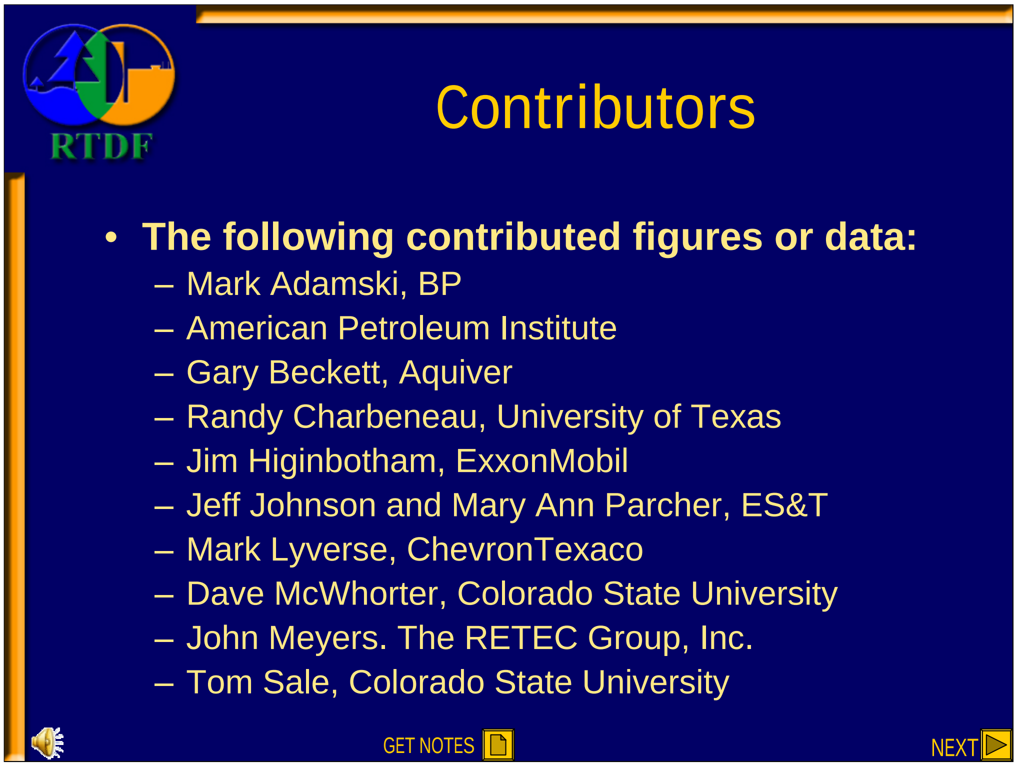

The concept and content of this course have evolved over a number of years, building upon efforts by many individuals and groups. Special thanks goes to the professionals cited in this slide and the next one, especially John Meyers of the RETEC Group, for sharing their knowledge, experience, and technical work with the Alliance during the development of the course material.

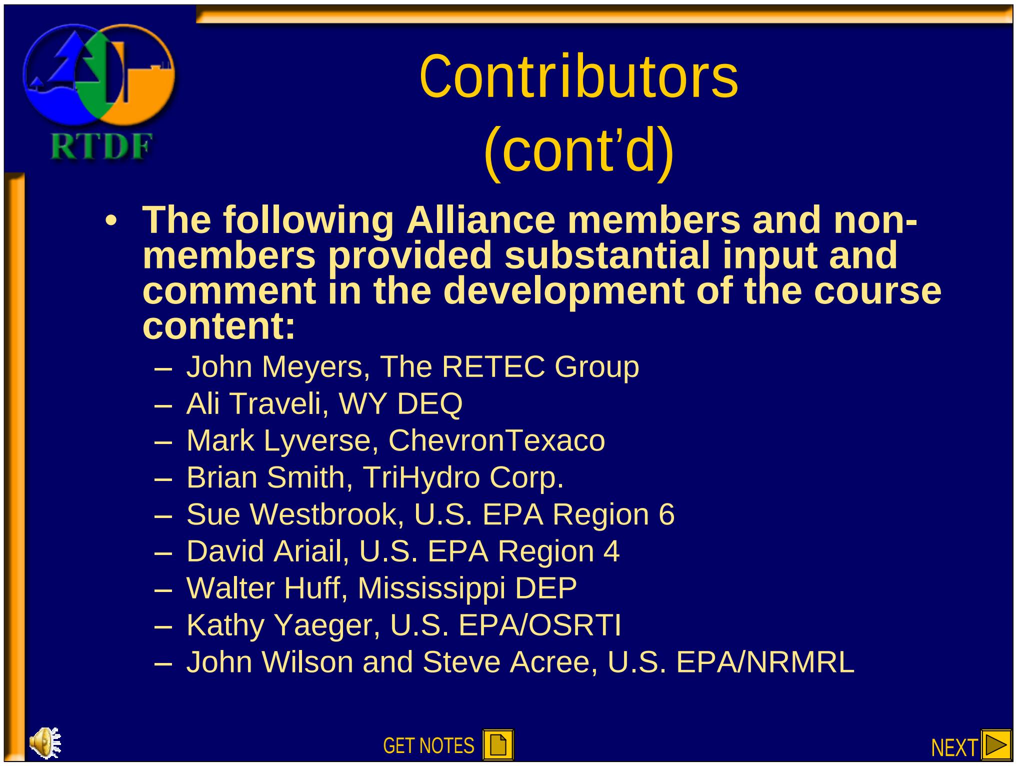

Thanks for using this training and we hope you found it helpful.